MICROCOPY RESOLUTION TEST CHART

NATIONAL BUREAU OF STANDARDS 1963 A

UNCLASS

REPORT DOCUMENTATION PAGE		READ INSTRUCTIONS BEFORE COMPLETING FORM
1. REPORT NUMBER AFIT/CI/NR 84-74D	2. GOVT ACCESSION NO.	3. RECIPIENT'S CATALOG NUMBER
4. TITLE (and Subtitle) Real-Time Estimation of Amplitude and Group Delay Distortion in a PSK Line-Of-Sight Communications Channel		5. TYPE OF REPORT & PERIOD COVERED THESIS//DISSERTATION
		6. PERFORMING ORG. REPORT NUMBER
7. AUTHOR(s) Glenn Eugene Prescott		8. CONTRACT OR GRANT NUMBER(s)
9. PERFORMING ORGANIZATION NAME AND ADDRESS AFIT STUDENT AT: Georgia Institute of Technology		10. PROGRAM ELEMENT, PROJECT, TASK AREA & WORK UNIT NUMBERS
11. CONTROLLING OFFICE NAME AND ADDRESS AFIT/NR WPAFB OH 45433		12. REPORT DATE June 1984
		13. NUMBER OF PAGES 157
14. MONITORING AGENCY NAME & ADDRESS(if different from Controlling Office)		15. SECURITY CLASS. (of this report) UNCLASS
		15a. DECLASSIFICATION/DOWNGRADING SCHEDULE

16. DISTRIBUTION STATEMENT (of this Report)

APPROVED FOR PUBLIC RELEASE; DISTRIBUTION UNLIMITED

DTIC
ELECTE
NOV 19 1984
S   D
B

17. DISTRIBUTION STATEMENT (of the abstract entered in Block 20, if different from Report)

18. SUPPLEMENTARY NOTES

APPROVED FOR PUBLIC RELEASE: IAW AFR 190-1

LYNN E. WOLAVER
Dean for Research and
Professional Development
AFIT, Wright-Patterson AFB OH

6 NOV 84

19. KEY WORDS (Continue on reverse side if necessary and identify by block number)

20. ABSTRACT (Continue on reverse side if necessary and identify by block number)

ATTACHED

84 11 14 146

DD FORM 1473   EDITION OF 1 NOV 65 IS OBSOLETE

UNCLASS

SUMMARY

Linear transmission distortion is a malady which is common to communication transmission systems of all types. Compensating for - or equalizing - this form of distortion is essential in order to realize the maximum possible error-free transmission of information. There are many established techniques for negating the effects of linear distortion with no regard to the type or severity of distortion present.

The object of the research described by this thesis is the development of an on-line technique for estimating linear transmission distortion parameters which are common to narrowband line-of-sight terrestrial microwave communication systems employing M-ary PSK modulation. The paramters of interest are represented as coefficients of a polynomial channel model in order to indicate the degree of amplitude and group delay distortion present in the channel.

This new approach employs an algorithm which first estimates the discrete channel pulse response, then determines the amount of amplitude and group delay distortion present in the estimated channel pulse response. In order to compute the distortion numerically, a finite series representation of the channel pulse response is stored at the receiver and compared to the measured (or

estimated) discrete channel pulse response. The coefficients of the channel model (representing the distortion components) are then iteratively adjusted until the difference between the computed and the measured values of the channel pulse response is minimized.

This technique differs significantly from existing methods which require off-line, frequency domain measurements in order to determine the amplitude and group delay distortion present in a communication channel. Applications for the new on-line time domain technique include characterization of digital communication channels and equipment, as well as performance monitoring of operational links.

AFIT RESEARCH ASSESSMENT

The purpose of this questionnaire is to ascertain the value and/or contribution of research accomplished by students or faculty of the Air Force Institute of Technology (AU). It would be greatly appreciated if you would complete the following questionnaire and return it to:

AFIT/NR
Wright-Patterson AFB OH 45433

RESEARCH TITLE: Real-Time Estimation of Amplitude and Group Delay Distortion in a PSK Line-of-Sight Communications Channel

AUTHOR: Glenn Eugene Prescott

RESEARCH ASSESSMENT QUESTIONS:

1. Did this research contribute to a current Air Force project?

( ) a. YES   ( ) b. NO

2. Do you believe this research topic is significant enough that it would have been researched (or contracted) by your organization or another agency if AFIT had not?

( ) a. YES   ( ) b. NO

3. The benefits of AFIT research can often be expressed by the equivalent value that your agency achieved/received by virtue of AFIT performing the research. Can you estimate what this research would have cost if it had been accomplished under contract or if it had been done in-house in terms of manpower and/or dollars?

( ) a. MAN-YEARS _____   ( ) b. $_____

4. Often it is not possible to attach equivalent dollar values to research, although the results of the research may, in fact, be important. Whether or not you were able to establish an equivalent value for this research (3. above), what is your estimate of its significance?

( ) a. HIGHLY   ( ) b. SIGNIFICANT   ( ) c. SLIGHTLY   ( ) d. OF NO
       SIGNIFICANT   SIGNIFICANT   SIGNIFICANCE

5. AFIT welcomes any further comments you may have on the above questions, or any additional details concerning the current application, future potential, or other value of this research. Please use the bottom part of this questionnaire for your statement(s).

NAME   GRADE   POSITION

ORGANIZATION   LOCATION

STATEMENT(s):

REAL-TIME ESTIMATION OF AMPLITUDE AND GROUP DELAY DISTORTION

IN A PSK LINE-OF-SIGHT COMMUNICATIONS CHANNEL

A THESIS

Presented to

The Faculty of the Division of Graduate Studies

By

Glenn Eugene Prescott

In Partial Fulfillment

of the Requirements for the Degree

Doctor of Philosophy

in the School of Electrical Engineering

Georgia Institute of Technology

June 1984

REAL-TIME ESTIMATION OF AMPLITUDE AND GROUP DELAY DISTORTION

IN A PSK LINE-OF-SIGHT COMMUNICATIONS CHANNEL

Approved:

David R. Hertling, Chairman

Joseph L. Hammond

Aubrey M. Bush

25 June 1984

Date approved by Chairman

ACKNOWLEDGMENTS

This Thesis is Dedicated

to My Wife

Jacqueline Marie

("I can fly higher than an eagle...

for you are the wind beneath my wings")

TABLE OF CONTENTS

Chapter

LIST OF TABLES

LIST OF ILLUSTRATIONS

SUMMARY

Linear transmission distortion is a malady which is common to communication transmission systems of all types. Compensating for - or equalizing - this form of distortion is essential in order to realize the maximum possible error-free transmission of information. There are many established techniques for negating the effects of linear distortion with no regard to the type or severity of distortion present.

The object of the research described by this thesis is the development of an on-line technique for estimating linear transmission distortion parameters which are common to narrowband line-of-sight terrestrial microwave communication systems employing M-ary PSK modulation. The paramters of interest are represented as coefficients of a polynomial channel model in order to indicate the degree of amplitude and group delay distortion present in the channel.

This new approach employs an algorithm which first estimates the discrete channel pulse response, then determines the amount of amplitude and group delay distortion present in the estimated channel pulse response. In order to compute the distortion numerically, a finite series representation of the channel pulse response is stored at the receiver and compared to the measured (or

estimated) discrete channel pulse response. The coefficients of the channel model (representing the distortion components) are then iteratively adjusted until the difference between the computed and the measured values of the channel pulse response is minimized.

This technique differs significantly from existing methods which require off-line, frequency domain measurements in order to determine the amplitude and group delay distortion present in a communication channel. Applications for the new on-line time domain technique include characterization of digital communication channels and equipment, as well as performance monitoring of operational links.

CHAPTER I

INTRODUCTION

Definition of the Problem

The problem is that there presently exists no effective technique for on-line, near real-time measurement of certain types of linear transmission distortion which commonly occur on a line-of-sight digital PSK channel. Current techniques are generally off-line, out of service frequency domain measurements which are normally accomplished by a microwave link analyzer (MLA) for troubleshooting, commissioning and adjustment of digital transmission systems.

An effective on-line, non-disruptive time domain technique for classifying and/or measuring certain common types of linear transmission distortion would offer a viable alternative to the MLA approach and could compete with it in both simplicity and versatility.

Background of the Problem

Practical communication channels reproduce at their output a transformed and corrupted version of the input waveform. Researchers have attempted for years to measure, classify and model the nature of the corruption (or distortion) imparted to the transmitted waveform; and to

devise methods of removing this distortion and restoring the waveform to its original structure.

There are a number of ways that distortion effects can be classified. When classified according to their statistical nature, both random and deterministic forms can be identified. Random corruption of the waveform can be additive and/or multiplicative, and generally attributable to thermal noise, impulse noise, and fades. Deterministic transformations performed by the channel can result in frequency dispersion, nonlinear or harmonic distortion, and time dispersion. For the time dispersive channel, the effect of each transmitted symbol extends beyond the time interval used to represent that symbol. The distortion caused by the resulting overlap of received symbols is called intersymbol interference (ISI), which is one of the major obstacles to reliable high speed data transmission over low noise channels with limited bandwidth.

Early Research - Transmission Distortion

Research into the problem of transmitting digital data across bandlimited media began as early as 1898 when Gulstad developed a means for increasing telegraph transmission speed on bandlimited cable systems [1]. Recognizing the need to cope with the inevitable time dispersive nature of any bandlimited transmission system, Nyquist developed the theoretical foundation for transmitting signals over such systems without intersymbol

interference [2]. Much of the early research in digital communications by Nyquist and his contemporaries was in support of telegraph transmission, which soon evolved into research supporting data transmission over many different media, including the telephone. In fact, during this era much of the digital transmission research was undertaken primarily within the context of utilizing analog voice facilities for data transmission.

On telephone line circuits, the primary cause of ISI was found to be linear distortion due to imperfect line amplitude and phase characteristics. However, early research into voice channel distortion was initially focused primarily on amplitude distortion, due to its importance to sound reproduction, especially in telephone communications, and also because it was more easily measured and studied than phase distortion. Then in 1939, Wheeler introduced paired echo theory as a simplified means of estimating the effect of both amplitude and phase distortion on a digital waveform [3].

Phase distortion has special significance for digital systems since the shape of the pulse is influenced greatly by the phase of the energy components of the pulse spectrum. The quantity used to describe this influence is called "group delay" or "envelope delay", and is defined as

$$\text{group delay} = \frac{d\psi(\omega)}{d\omega} \qquad\qquad (1\text{-}1)$$

where $\psi(\omega)$ is the channel phase characteristic. Group delay is a measure of the relative phase shift experienced by neighboring spectral components of the signal, and as indicated by (1-1), is equal to the slope of the tangent to the phase curve at any given frequency. If the phase changes linearly with frequency, the group delay is constant across the frequency band and there is no delay distortion. However, when the group delay varies with frequency, the shape of the pulse is distorted in transmission. This variational component of group delay is called delay distortion.

Erling Sunde expanded upon the work of Wheeler and others by unifying the theoretical fundamentals relating to the transmission of pulse waveforms [4]. Later, he reiated the effects of phase and amplitude distortion to the transmission of modulated pulses [5]. In this context, Sunde presents a theoretical evaluation of transmission impairments resulting from the presence of certain types of delay distortion in the channel transmission characteristic.

Early Research - Channel Models

Amplitude and group delay distortion, which manifest

themselves as ISI in the channel output waveform, can be caused either by linear distortion induced by equipment maladies, or by multipath propagation, which may be viewed as transmission through a group of channels with different delays. The important point is that, although the origin of the ISI may not be readily apparent, the nature of the problems resulting from either multipath propagation or equipment induced linear distortion are essentially equivalent [6]. In attempting to model the influence of various physical parameters on the transmitted signal, researchers have resorted to numerous mathmatical models for the transmission channel. In general, these models can be divided in two categories:

(1) Multipath channel models, which attempt to describe the corrupting effect of mutually interfering ray paths, and

(2) Linear distortion models, which attempt to describe the channel distortion in terms of mathmatical parameters.
The former is nearly always associated with radio frequency propagation, while the latter is usually associated with waveform propagation within some discrete, confined medium.

For multipath channel models, significant early achievements can be traced to the work of Zadeh [7], and Kailath [8], who sought to model a network possessing a randomly time variant impulse response. Their work served

as the foundation for the many communication channel models which were to follow. The most notable of these was developed by Bello [9], who unified the theory of characterizing randomly time-variant channels, and proposed the first useful polynomial channel model. Bello's channel model in low pass form is

$$H_c(\omega) = \sum_{n=0}^{\infty} C_n (j\omega)^n \qquad (1-2)$$

where the coefficient C_n is complex and varies slowly with time in accordance with changes in the multipath structure.

Prior to the 1970's, the emphasis in multipath propagation research was on analog radio. Only within the last ten years has the effect of fading radio channels on digital transmission started receiving attention. For example, a number of years after Bello introduced his model, it was revived and examined by Greenstein [10] who applied it to digital line-of-sight systems operating in the commercial common carrier bands. He discovered that the polynomial model was sufficiently accurate when a first order approximation was used. Hence, Greenstein's polynomial model in low pass form is

$$H_c(\omega) = (A_0 + j\omega A_1) + j(B_0 + j\omega B_1) \qquad (1\text{-}3)$$

Multipath propagation at microwave frequencies has recently been investigated in several studies and experiments [11,12,13] which were initiated when the susceptability of digitally modulated signals to selective fading appeared as a fundamental limitation to increased data rates. These studies, and subsequent experiments up until the present time, have provided sufficient evidence that the main sources of system degradation in a multipath fading channel are intersymbol interference and co-channel crosstalk due to amplitude and group delay distortion, which occurs as a result of multipath propagation.

In order to evaluate the effect of multipath fading on specific systems, Greenstein employed his model in a series of propagation tests [14]. As a result of the empirical data gathered on the multipath channel, he ammended his model slightly, as

$$H_c(\omega) = A_0 - \omega B_1 + j\omega A_1 \qquad (1\text{-}4)$$

The result of Greenstein's effort was a model that can be

used to assess multipath effects in any digital radio system [15,16].

A second important channel model which was also developed to evaluate the performance of digital radios on line-of-sight microwave paths was proposed by Rummler [17,18]. The basis for his study was a simple three-ray multipath fade, which provides a channel transfer function of the form,

$$H_c(\omega) = a\left[1 - b\, e^{j(\omega - \omega_o)\tau}\right] \qquad (1\text{-}5)$$

This model can be interpreted as the response of a channel which provides a direct transmission path with amplitude "a", and a second path providing a relative amplitude "b", at a delay of τ, and at a phase of $\omega_o\tau + \pi$ at the center frequency of the channel.

Rummler's multipath model has proven to be quite accurate and particularly useful in characterizing digital radio equipment subjected to multipath fading [19,20]. Both Greenstein's polynomial model and Rummler's multipath model are the most current channel models employed in research pertaining to multipath communication channels.

Models for deterministic, non-multipath channels containing linear distortion were introduced much earlier than the multipath models. Their primary purpose was to

account for amplitude and delay distortion encountered over telephone transmission lines. For example, Gibby and Fowler [21] determined experimentally that, for voice frequency line transmission circuits, many delay distortion characteristics have an approximate parabolic shape. Later, Gibby [22] modeled this behavior with a cosine phase characteristic.

Many useful models for time invariant channels and filters with linear distortion have been employed over the years, including sine and cosine models, Fourier series models and polygonal models [23]. The significance of these earlier linear distortion models has largely been overlooked in the current research into digital communication channel modeling. Since the fundamental limitation of digital data transmission by line-of-sight microwave systems has been shown to be intersymbol interference, it seems appropriate to employ a channel transfer function which exploits the primary influential distortion parameters which give rise to ISI - amplitude and group delay distortion. Such a model can be described in the following low pass form:

$$H(\omega) = B(\omega) \, e^{-j \, \psi(\omega)} \qquad (1-6)$$

where,

$$B(\omega) = \sum_{n=0}^{\infty} \gamma_n \, \omega^n \qquad (1\text{-}7)$$

$$\psi(\omega) = \sum_{n=0}^{\infty} \gamma_n \, \omega^n \qquad (1\text{-}8)$$

This model, with $N = 4$ and $M = 4$, has previously been employed in the study of intermodulation noise on analog FM communication systems [24]. The present research will be based upon a slight variation of this model, as explained in Chapter III.

Current Interest in the Problem

Since the research problem is to measure linear distorion on a digital communication channel according to some specified channel distortion model, the present research can be most closely associated with the field of system performance monitoring. Commercial research in this area tends to be proprietary in nature, however the U. S. Air Force conducts ongoing research in communications system performance monitoring and assessment through the Rome Air Development Center (RADC) at Griffiss AFB, New York. RADC has established a facility for the research, development and acceptance testing of performance monitoring techniques, with a current interest in real-time performance monitoring which can be incorporated into the future generation digital

radio systems.

Two real-time techniques currently under evaluation are the "template matching" approach by Halford [25] and the adaptive channel estimation (ACE) algorithm developed for the Air Force by GTE Sylvania [26]. The object of these techniques is to determine communication system performance parameters such as error rate and signal to noise ratio. In Halford's method, pattern recognition techniques are employed on the received bit stream, while the ACE algorithm assumes a nonlinear channel and employs a Volterra expansion on these nonlinearities in order to determine the system performance parameters. Although both are real-time, time domain techniques, they differ significantly from the technique proposed in the present research. Furthermore, neither technique determines explicitly the channel distortion parameters.

Introduction to the Research

The purpose of the research described in subsequent chapters is to develop a theoretical approach or technique for measuring certain types of linear transmission distortion which commonly occur on a line-of-sight digital PSK channel; and then to verify that theoretical approach using simulated data. An important criterion is that the technique employed must operate on-line with no disruption in the normal digital data traffic flow. Furthermore, it

must execute its funtion in a near real-time manner.

The contribution offered by the research described in this thesis is a systematic approach for measuring specific types of amplitude and group delay distortion in a unique and very useful manner - i. e. while the digital radio system is processing normal traffic. Several well documented concepts are employed in this system although they are modified and extended to suit the requirements of the research. The original idea for research on this technique grew out of a proposal by J. L. Hammond, et. al., for the development and implementation of an on-line instrument for testing digital radios [27,28]. The research developed, extended and verified the preliminary theoretical concepts presented by Dr. Hammond.

The ultimate usefulness of an on-line measurement technique would be for the technique to be integrated into a useful performance monitoring component of a digital radio system. It is this ultimate purpose that motivates the present research and influences certain design options which will be explained later.

In order to present the results of the research in an orderly, unified manner, several chapters of background material preceed the discussion of the research. These background chapters are intended to focus attention on the research by highlighting only the important concepts of digital communication theory which have a direct bearing on

the problem. For example, the specific communication system of interest is described completely in Chapter II, along with several signal design issues which are important to the system which estimates the channel distortion. Since a crucial ingredient in the research is the presence of transmission distortion, Chapter III summarizes the effects of various types of linear transmission distortion on a baseband signaling waveform. Also in Chapter III, a channel model is chosen in which the actual distortion within the channel is expressed as one or more parameters of the mathmatical model. Chapter IV, V and VI contain the essential details of the research in which the distortion present in the channel is estimated in terms of the channel model parameters. Chapter VII includes experimental results and performance analyses of the technique; and finally, Chapter VIII discuses conclusions to be drawn from the research as well as issues which remain to be addressed.

Chapter II

SYSTEM DESCRIPTION

The Bandpass System

In order to restrict the scope of the research to a manageable size, a specific type of digital communication system is considered. In particular, the line-of-sight MPSK communication system is chosen since systems of this kind are becoming an industry standard in both common carrier and military communications applications [29].

For a complete analysis it is necessary to develop a mathmatical model for this system which includes transmitting filters, receiving filters, and a propagation channel. Data is transmitted over the channel by modulating the phaʋe of a carrier signal as illustrated in Figure 2.1. Digital phase modulation of the carrier results when blocks of $k = \log_2 M$ binary digits of the information sequence are mapped into a set of M discrete carrier phases, as

$$\phi_n = \frac{2\pi(n-1)}{M} + \lambda \qquad n = 1,2,\ldots, M \qquad (2-1)$$

where λ is some designated offset angle to be discussed later. Therefore, for a binary information sequence

15
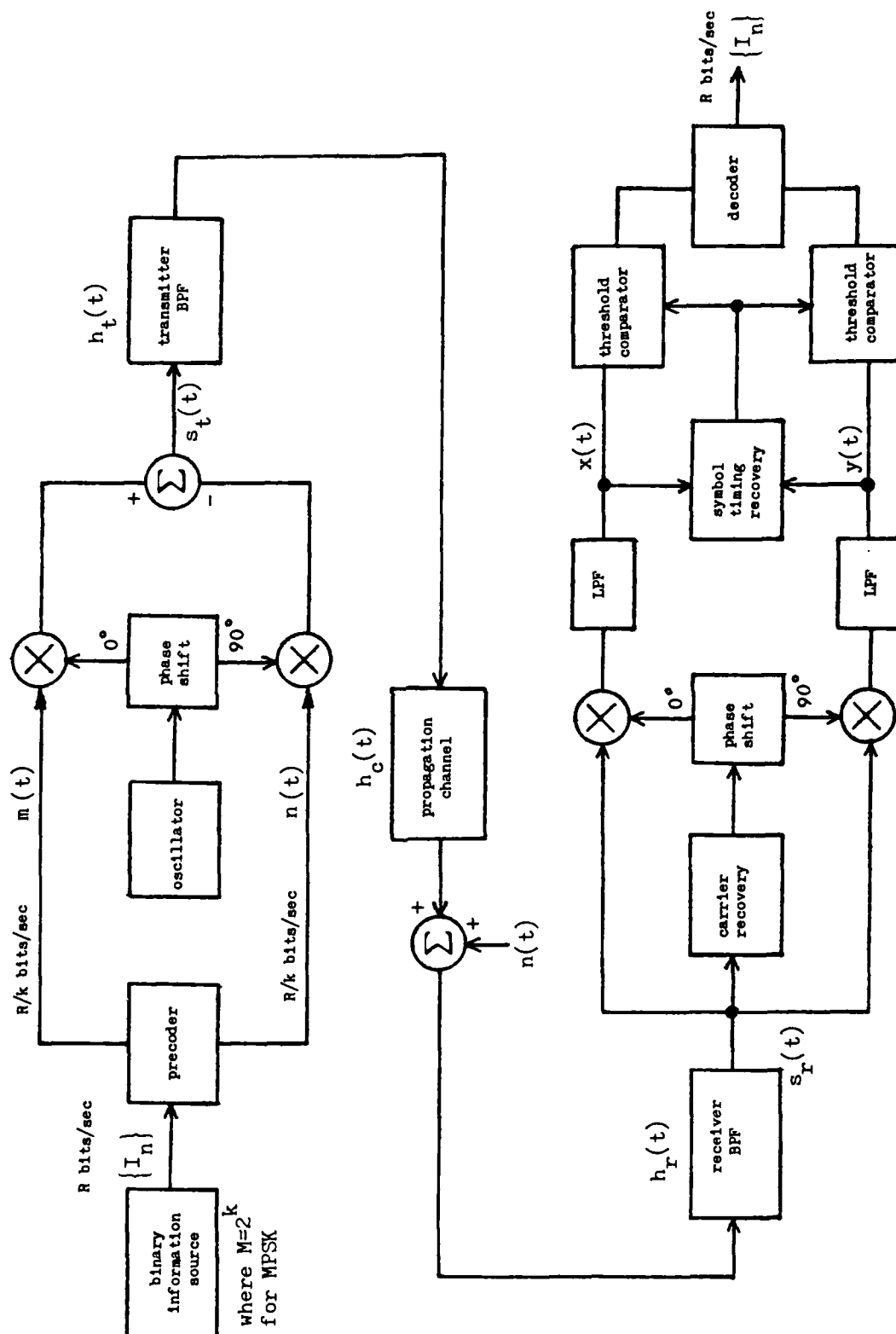
Figure 2.1 - MPSK Communication System

occuring at a rate of R bits/sec, the signaling interval over the channel is T = K/R seconds. The factor 1/T is commonly known as the channel signaling (baud) rate.

From Figure 2.1, the modulator output signal is

$$s(t) = m(t)\cos\omega_c t - n(t)\sin\omega_c t \qquad (2-2)$$

Some insight can be gained by expressing (2-2) in complex envelope notation [30] as

$$s(t) = \text{Re}\left[f(t)\ e^{j\omega_c t}\right] \qquad (2-3)$$

where

$$f(t) = \sum_{n=0}^{\infty} e^{j\phi_n}\ p(t-nT) \qquad (2-4)$$

is the baseband (complex envelope) signal, and $p(t-nT)$ is the modulator pulse function shown in Figure 2.2. Therefore it can be shown that

$$m(t) = \sum_{n=0}^{\infty} p(t-nT)\cos\phi_n \qquad (2-5)$$
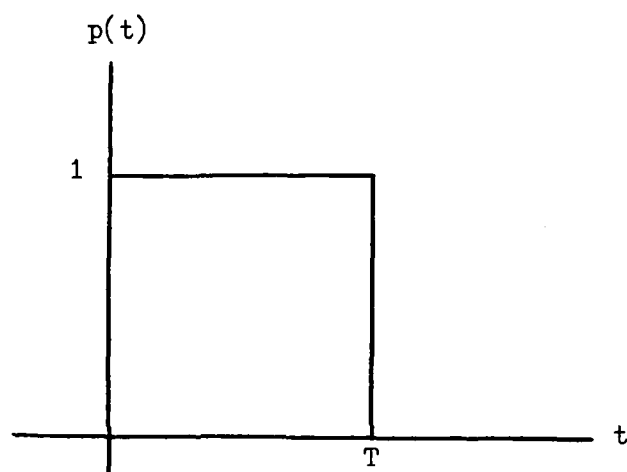
Figure 2.2 - Modulator Pulse Function for the MPSK System

$$n(t) = \sum_{n=0}^{\infty} p(t-nT)\sin\phi_n \qquad (2-6)$$

are the inphase and quadrature components of the complex baseband envelope. The amplitude of the components is dependent upon the angle ϕ_n over the interval $nT < t < (n+1)T$. After modulation, the bandpass signal is filtered, weighted or otherwise shaped by the filters and channel that follow.

The primary purpose of the transmitter filter is to shape the output RF pulse and to suppress signal energy outside the assigned channel bandwidth [31]. The transmitter filter includes not only bandpass filtering but some degree of power amplification as well. The relation between the power amplifying and filtering functions within the transmitter filter is not explicitly shown because their locations with respect to one another depend upon whether the power amplifier is linear or nonlinear. When nonlinear amplification is employed, both the input to the power amplifier and the output are constant amplitude signals. Therefore, filtering must occur after amplification. When a linear power amplifier is used, pulse shaping can be performed prior to the power amplifier, and can even be incorporated into the precoder.

The channel through which the signal is transmitted is characterized in general by a linear time-variant impulse

response of finite duration. For the line-of-sight MPSK channel a realistic assumption is that the time variations in the channel impulse response are much slower than the duration of a signaling interval. This assumption generally holds true even during fading and multipath propagation conditions on the line-of-sight channel [32]. Therefore, with a channel that is only relatively time-invariant, the adaptive signal processing to be employed will be able to track variations in the channel. The additive noise which occurs on the channel is assumed to be stationary, zero mean, white and Gaussian.

At the receiver, the receiver filter is designed to further shape the transmitted pulse and to suppress adjacent channel interference. At both the transmitter and receiver, precise frequency control and timing are required. At the receiver, time and frequency references are usually recovered from the incoming signal so that coherent detection can be performed. Timing is derived from the demodulated (baseband) signal, and is used in the final decision process to recover the information sequence. Any errors in the recovered references result in severe system performance impairments.

The Baseband System

For the purpose of mathmatical analysis it is often more convenient to represent the bandpass system in an

equivalent lowpass, or baseband form. A bandpass signal which is to be transmitted over a bandpass channel has a lowpass equivalent representation that is appropriate for transmission over a lowpass equivalent channel [33]. Therefore, all signals and filter responses can be written in complex-valued lowpass equivalent form; although in the physical system they are real-valued bandpass signals and filters. By employing complex envelope notation, the transmitted signal, $s_t(t)$; the composite channel impulse response, $h(t)$; and the received signal, $s_r(t)$, can be expressed as

$$s_t(t) = \text{Re}\left(w(t)\, e^{j\omega_c t} \right) \qquad\qquad (2\text{-}7)$$

$$h(t) = \text{Re}\ 2\left(g(t)\, e^{j\omega_c t} \right) \qquad\qquad (2\text{-}8)$$

$$s_r(t) = \text{Re}\left(z(t)\, e^{j\omega_c t} \right) \qquad\qquad (2\text{-}9)$$

The mathmatical model for the equivalent lowpass MPSK system can be determined from the baseband components of these signals as shown in Figure 2.3.

Since the system is linear and essentially time-invariant, the output signal is
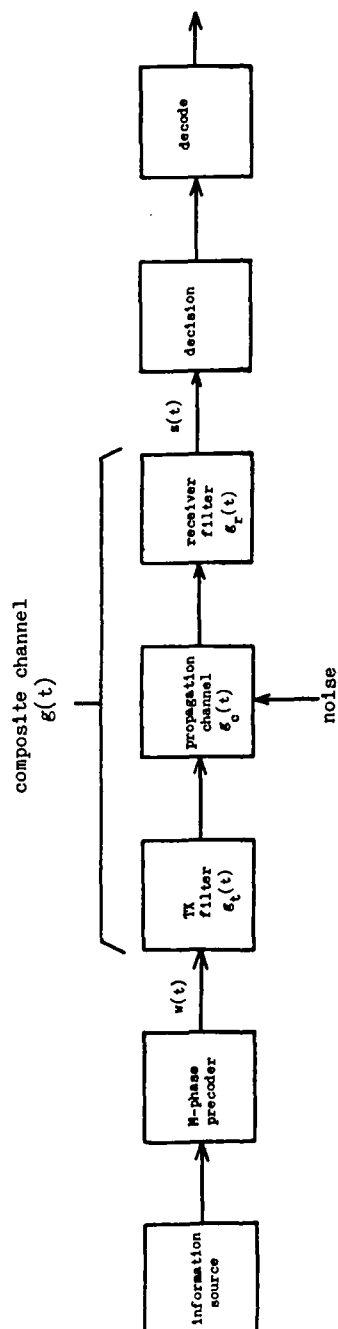
Figure 2.3 – Equivalent Lowpass MPSK Communication System

$$z(t) = \int_{-\infty}^{\infty} g(\tau) \, w(t-\tau) \, d\tau \qquad (2\text{-}10)$$

$$= g(t) * w(t) \qquad (2\text{-}11)$$

Since the signals involved in the convolution are complex, with components defined as

$$z(t) = x(t) + jy(t) \qquad (2\text{-}12)$$

$$g(t) = \text{Re}\Big(g(t)\Big) + j\text{Im}\Big(g(t)\Big) \qquad (2\text{-}13)$$

$$w(t) = u(t) + jv(t) \qquad (2\text{-}14)$$

the demodulated baseband channel received signal can be expressed as (using (2-5) and (2-6)),

$$x(t) = \sum_{n=0}^{\infty} \text{Re}\Big(g(t)\Big) * p(t-nT)\cos\phi_n - \sum_{n=0}^{\infty} \text{Im}\Big(g(t)\Big) * p(t-nT)\sin\phi_n \qquad (2\text{-}15)$$

$$y(t) = \sum_{n=0}^{\infty} \text{Re}\Big(g(t)\Big) * p(t-nT)\sin\phi_n + \sum_{n=0}^{\infty} \text{Im}\Big(g(t)\Big) * p(t-nT)\cos\phi_n \qquad (2\text{-}16)$$

Now define

$$r(t-nT) = \text{Re}\Big(g(t)\Big) * p(t-nT) \qquad (2\text{-}17)$$

$$q(t-nT) = \text{Im}\Big(g(t)\Big) * p(t-nT) \qquad (2\text{-}18)$$

as the complex channel pulse response, so that

$$x(t) = \sum_{n=0}^{\infty} r(t-nT)\cos\phi_n - \sum_{n=0}^{\infty} q(t-nT)\sin\phi_n \qquad (2\text{-}19)$$

$$y(t) = \sum_{n=0}^{\infty} r(t-nT)\sin\phi_n + \sum_{n=0}^{\infty} q(t-nT)\cos\phi_n \qquad (2\text{-}20)$$

After demodulation, the signals are sampled at the baud interval, t=kT, in order to present to the decision circuitry a set of sufficient statistics (i. e. a sequence of numbers) from which the original binary information signal can be recovered. It is therefore more convenient to remove any time dependence from the expressions in (2-19) and (2-20), so that

$$x_k = \sum_{n=0}^{\infty} r_{k-n}\cos\phi_n - q_{k-n}\sin\phi_n \qquad (2\text{-}21)$$

$$y_k = \sum_{n=0}^{\infty} r_{k-n}\sin\phi_n + q_{k-n}\cos\phi_n \qquad (2\text{-}22)$$

The inphase and quadrature pulse responses, r_k and q_k have an important influence upon the received signal. For example, it can be seen that nonzero q_k results in mutual interference (crosstalk) between the inphase and quadrature components of the received signal; while any distortion which may occur within the channel will cause r_k to corrupt the received signal and impair the detection process. Should q_k be nonzero and also contain distortion, the received signal will not only be corrupted but crosstalk will also exist. The significance of these features will be exploited in a subsequent chapter to develop a channel distortion model which can effectively represent each of these cases.

Bandlimited Signal Design

The Signaling Pulse

Since the digital MPSK system operates in an increasingly crowded spectrum environment, a very important consideration is maximizing the rate of information transfer within a restricted bandwidth allocation. The Federal Communication Commission has imposed strict limitations in the form of a spectrum envelope (FCC Rules and Regulations, Section 21.106), which limits the bandwidth of spectral emissions. An example is shown in Figure 2.4 [34].

Bandlimiting of the digital signal is normally accomplished both at the transmitter filter and the receiver
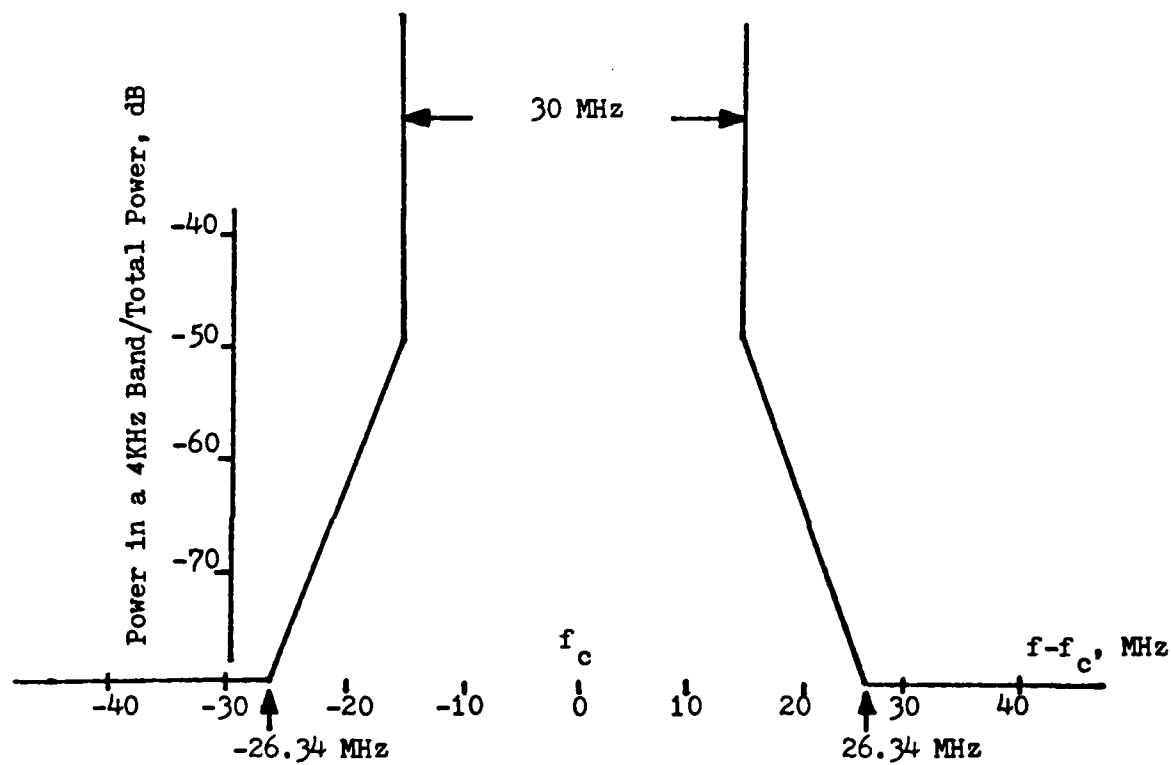
Figure 2.4 – FCC Envelope for 30 MHz Bandwidth

filter. Proper design of these filters allows out-of-band signal power to be suppressed while shaping the desired bandlimited signaling pulse. Because of the bandlimiting requirement, a certain amount of time dispersion in the signaling pulse is inevitable. However, in his landmark paper on channel characteristics, Nyquist [2] proved that, with proper design of the signaling pulse, perfect recovery of the information signal could be accomplished even at signal rates as high as 1/T, where T is the signaling interval of the baseband modulator pulse.

A popular family of pulses that satisfy the Nyquist criterion have the mathmatical form

$$p(t) = \frac{\sin \pi t/T}{t/T} \frac{\cos \alpha \pi t/T}{1-4(\alpha t/T)^2} \qquad (2-23)$$

and are called raised cosine pulses. These pulses, shown in Figure 2.5, are bandlimited with α equal to the ratio of the excess bandwidth of the composite channel to the ideal Nyquist bandwidth, 2T. For all values of α, the function is unity at sample instant t=0, and zero at all incremental sampling instants, t=nT. Therefore, using the raised cosine family of pulses, signaling can occur at a rate of 1/T without intersymbol interference.

After the desired signaling pulse has been selected, the transmitter and receiver filters must be specified.

(a)

(b)
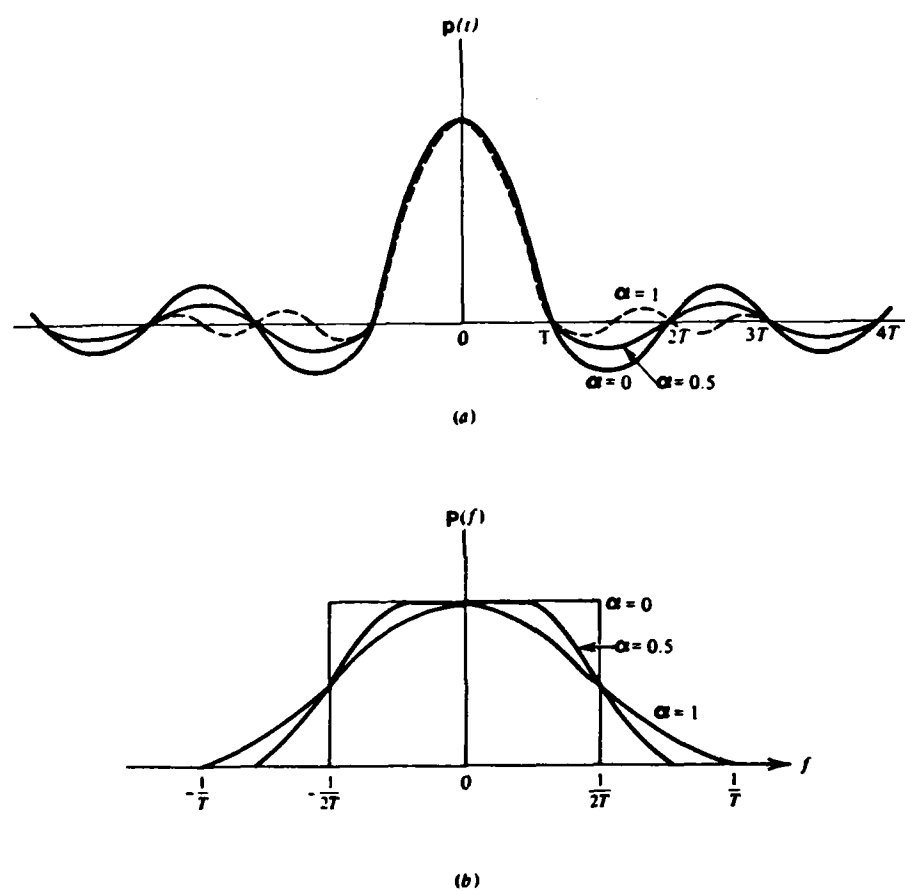
Figure 2.5 - Raised Cosine Signaling Pulse and Spectrum

Often, the receiver filter is matched to the signaling pulse on the channel and the following partitioning is used when designing the transmitter and receiver filters:

$$H_r(\omega) = \sqrt{P(\omega)} \qquad (2\text{-}24)$$

$$H_t(\omega) = \frac{\sqrt{P(\omega)}}{P(\omega)} \qquad (2\text{-}25)$$

where $H_r(\omega)$ and $H_t(\omega)$ are the responses of the receiver and transmitter filter, respectively; and $P(\omega)$ is the Fourier transform of (2-23). This partitioning has been shown to be optimum under some special circumstances [35].

Signal Constellation

In (2-1), an offset phase angle, λ, was employed when mapping the information sequence into M discrete phases. The purpose of this offset is to prevent discrete lines in the signaling pulse spectrum from appearing and possibly exceeding the FCC limitations. These spectral lines vanish when the information symbols are equally likely, zero mean, and symmetrically positioned in the complex plane [36]. Figure 2.6 illustrates 4PSK and 8PSK signal constellations with both $\lambda = 0$ and λ equal to the appropriate offset value.
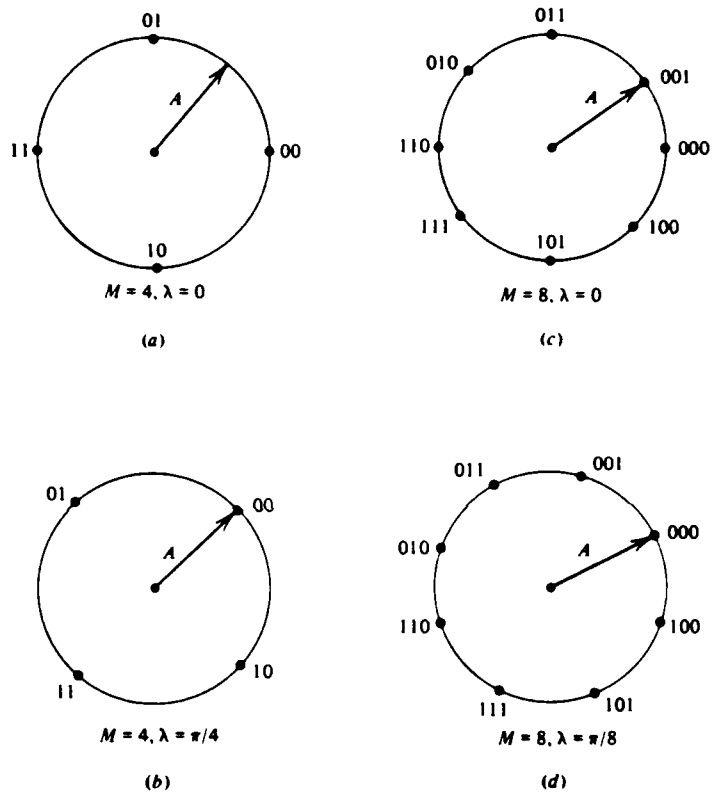
Figure 2.6 - PSK Signal Constellation for M = 4 and M = 8
(from [30])

Information Scrambling

A digital communication system must be "bit sequence transparent" in order to be effective. This means that the system can convey any given sequence of information bits. Since symbol timing recovery at the receiver is dependent upon baud interval transitions in the demodulated signal, an extremely long series of 1's or 0's could cause loss of timing, resulting in a large burst of data errors. This problem is solved by the use of data scramblers, which restrict the occurance of periodic sequences, and sequences containing long strings of 1's or 0's.

An equally important function of the data scrambler is to help keep the transmitted power spectrum within FCC limits. When the information sequence is random, the energy of the baseband signal and of the corresponding bandpass signal is sufficiently dispersed to reduce the peaks of the power spectral density. If, however, the baseband pulse sequence includes a periodic pattern, discrete line components will appear in the transmitted spectrum. In this case, some of these peaks may exceed the permissable level. Therefore, scrambling is used to substantially increase the period of the input data sequence by converting it into a random-like sequence known as a pseudo-random binary sequence (PRBS). PRBS generators are easily implemented from maximal length binary shift registers [37], and incorporated into digital communications equipment.

CHAPTER III

LINEAR TRANSMISSION DISTORTION

The Significance of Linear Transmission Distortion

High bit-rate digital radio systems have only recently been integrated into nearly every modern telecommunications network. Considerable effort has gone into the research, design and development of these systems to make them as efficient in their use of the available channel bandwidth as possible. However, the push to achieve even higher data rates within a limited band will continue in order to accomodate denser channel populations within any given network. The maximum bit-rate that can be processed by a digital radio is determined by the minimum possible length of each signaling interval and the number of information bits which can be transmitted by each discrete signal. The former is limited by intersymbol interference, and the latter by intersymbol interference and random noise.

An inherent property of all physical channels is time dispersion, whether due to bandlimiting or linear distortion. In the absence of distortion, intersymbol interference occurs as a result of time dispersion suffered by the signal when transmitted over a bandlimited network. By carefully designing the signaling pulse to satisfy the

Nyquist criterion, much of the difficulty caused by intersymbol interference due to bandlimiting can be overcome. However, when some form of linear transmission distortion is introduced into the communications network, this distortion (which may also be time dispersive), combined with the time dispersion induced by bandlimiting, can cause a significant amount of degradation in the signaling waveform. This degradation cannot normally be overcome by altering the shape of the signaling pulse. It results in an increase in the transmission system error rate which can only be overcome to a limited degree by increasing the received signal-to-noise ratio [38]. Therefore, any form of linear distortion imparted to either the amplitude or phase of a signaling pulse will be observable as an increase in intersymbol interference in the received waveform.

Sources of Linear Distortion

When time dispersive effects are present in a communication system, received signal levels can be greatly depressed at some frequencies while signals remain nominally undisturbed at neighboring frequencies. Time dispersive effects can result from both amplitude selectivitly and dynamic changes in envelope delay distortion within the transmission system. Together, these variations corrupt the desired linear amplitude and phase (flat delay)

characteristics of the channel and produce intersymbol interference; which, in turn, raises the bit error rate over the channel to unacceptable levels. Modest in-band amplitude dispersion, a linear 0.2 dB/MHz, for example, has been shown to be sufficient to cause the bit error rate to exceed operational limits [39]. Other research has shown that envelope delay distortion comparable to the symbol length of a digital signal could be intolerable [40].

In the present study, two types of time dispersive channels containing linear transmission distortion are defined - system distortion channels and multipath distortion channels. Both introduce intersymbol interference into the signaling pulse, although the mechanism by which it is caused is very different.

System Distortion Channel

The system distortion channel is best represented by the telephone channel, where time dispersion is attributed to imperfect frequency response characteristics of the filters, components and hardware comprising the channel. For example, low frequency cutoff is encountered in actual systems where transformers are required; and in most channels, the amplifiers unavoidably introduce some distortion which cannot be completely compensated. Also, lumped networks employed for equalization introduce a sinusoidal ripple into the phase characteristics of the received signal. A linear phase characteristic, if it could

actually be realized, would imply either incomplete channel cutoff or infinite transmission delay.

Distortion characteristics are normally expressed in terms of attenuation and group delay as a function of frequency. An ideal channel has a constant amplitude and group delay across its frequency band. Since the amplitude and group delay characteristics of a telephone channel are generally not constant, a signal transmitted through such a channel undergoes amplitude distortion and delay distortion respectively [41].

Multipath Distortion Channel

Although most of the delay distortion observed on line-of-sight radio links is introduced by the radio and not the propagation path [42], a primary source of intersymbol interference in digital communications is amplitude and group delay distortion induced by multipath propagation. The significant difference is that for the multipath channel, the amplitude and group delay distortion are time-variant channel parameters, whereas in the system distortion channel, they are time-invariant.

Multipath propagation, which can be both time dispersive and frequency dispersive in nature, occurs when signals originating from a common source arrive at the receiver out of phase with each other. Although the multipath induced degradation of digital systems depends upon the fade depth and time delay between multipath

signals, the frequency dependent amplitude and group delay variations caused by multipath propagation are linear with frequency during a large percentage of the time [43].

Time dispersive fading due to multipath propagation has been tolerated on microwave paths for many years. This has been possible since virtually all systems employed analog frequency modulation. In analog FM, the distortion effects of multipath propagation are less important, since the degradation caused by linear distortion manifests itself only as an increase in thermal noise due to a received signal level drop. Fades of this nature were found to generally behave gracefully, and furthermore, loading conditions on the analog system were light during multipath propagation.

Recently, the conversion of microwave transmission systems to digital modulation has required closer consideration of the effects of multipath induced in-band distortion. In digital systems, the distortion mechanisms are more critical because of the randomized nature of the transmitted data stream, which essentially means that loading is constant at all times. Under these conditions, the transmit spectrum is well defined and therefore, distortion induced by multipath conditions is more readily observed and measured than in analog systems.

The Channel Distortion Model

In order to develop a model which incorporates amplitude and group delay distortion as parameters, the system shown in Figure 3.1 represents the communication system, with $P(\omega)$ the response of the composite channel to the signaling pulse, and $T(\omega)$ the portion of the system which introduces distortion. Therefore,

$$P(\omega) = A(\omega)\ e^{-j\omega t_d} \qquad (3\text{-}1)$$

where t_d is the undistorted channel delay, and $A(\omega)$ the composite channel amplitude response. Also,

$$T(\omega) = B(\omega)\ e^{-j\psi(\omega)} \qquad (3\text{-}2)$$

where $B(\omega)$ represents some form of amplitude distortion and $\psi(\omega)$ contains the channel phase distortion. In the absence of distortion, $B(\omega) = 1$ and $\psi(\omega) = 0$.

The performance of pulse transmission under various forms and amounts of delay distortion can be related to a basic function known as the channel pulse response. This function gives the shape of a single carrier pulse at the channel output under ideal conditions or in the presence of a particular kind of transmission distortion under

$G(\omega)$

W(ω) ——— | $P(\omega)$ | ——— | $T(\omega)$ | ——— Z(ω)
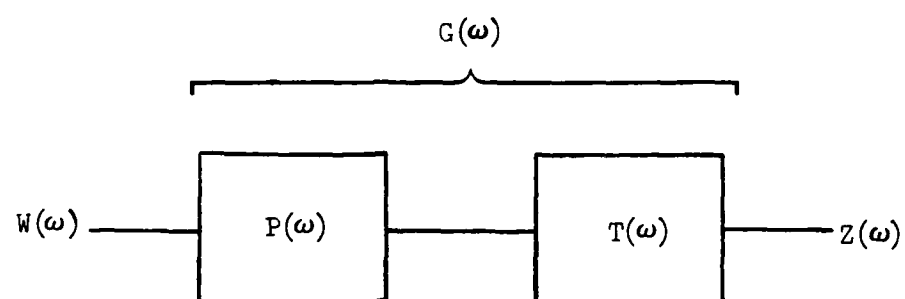
Figure 3.1 - Lowpass Channel Distortion Model

consideration. If the composite channel, $G(\omega)$, is assured to be complex, and $P(\omega)$ is the raised cosine pulse spectrum as shown in Figure 2.5, then the inphase and quadrature components of the baseband channel pulse response are

$$r(t) = \frac{1}{\pi} \int_{-\infty}^{\infty} P(\omega)B(\omega)\cos\Big(\omega t - \psi(\omega)\Big)d\omega \qquad (3-3)$$

$$q(t) = \frac{1}{\pi} \int_{-\infty}^{\infty} P(\omega)B(\omega)\sin\Big(\omega t - \psi(\omega)\Big)d\omega \qquad (3-4)$$

where an appropriate analytical representation of $B(\omega)$ and $\psi(\omega)$ now need to be selected.

The task of mathmatically representing amplitude and group delay distortion has been given considerable attention in the literature (a brief summary is given by Papoulis [23]). A polynomial representation has been selected for the research. In this approach, the distortion components are

$$B(\omega) = 1 + \gamma\omega \qquad (3-5)$$

$$\psi(\omega) = \beta_2\omega^2 + \beta_3\omega^3 \qquad (3-6)$$

These components are illustrated in Figure 3.2. Note that $\gamma\omega$ represents a linear amplitude slope, while $\beta_3\omega^3$ represents a phase distortion component varying as the third power of frequency from midband, which corresponds to group delay distortion increasing as the second power of frequency from the midband. The phase distortion component varying as the square of frequency from midband, $\beta_2\omega^2$, corresponds to a linear delay distortion slope about the midband frequency. Lower order polynomial phase terms ($\beta_0 + \beta_1\omega$) are not included as part of the distortion model, since these components do not impart distortion to the waveform.

Fortunately, this simple representation of amplitude and group delay distortion parameters can adequately represent the shapes of many forms of distortion actually encountered in practice. For example, linear delay distortion is approximated when a bandpass channel with gradual cutoffs is established to one side of midband of a flat bandpass channel with sharp cuttoffs. This often occurs on loaded cable systems. Quadratic delay distortion is approached near midband of a flat bandpass channel with sharp cutoffs, such as a carrier system voice channel [44].

Also, recent studies [39] on the effect of multipath induced amplitude and delay distortion indicate that the predominate forms of distortion encountered on multipath channels are linear amplitude slope, linear delay slope and quadratic delay distortion.
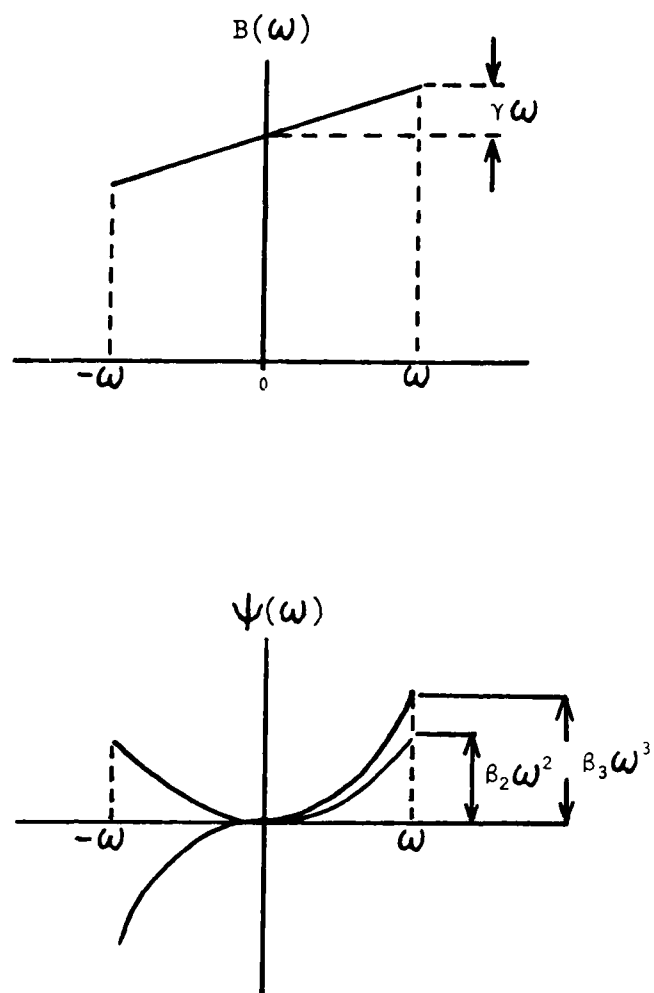
Figure 3.2 – Transmission Gain and Phase Shapes
for the Distortion Model

Amplitude or delay distortion can be expressed in terms of the difference in transmission delay between any two reference frequencies in the channel band. The standard adopted here is the difference in delay (or amplitude) between the midband frequency and the maximum (band edge) frequency, as shown in Figure 3.2.

The choice of distortion components in (3-5) and (3-6) is further justified in that these three components are the minimum combination required to represent the following three important situations:

(1) Intersymbol interference present in the received complex signal with no mutual interference (crosstalk) between the received components (i. e. $q(t) = 0$). In this case, the pulse spectrum at the detector input will have even symmetry about the midband frequency, and the phase characteristic will have a component of odd symmetry. This occurs when β_3 is the only nonzero distortion component.

(2) No intersymbol interference present in the received complex signal, but some degree of mutual interference between the received quadrature components. In this case, both the pulse spectrum at the detector input and the phase characteristics have odd symmetry about the midband frequency. This occurs whenever γ is nonzero.

(3) Both intersymbol interference and mutual interference between the quadrature components of the received complex signal are present. In this case, both the

pulse spectrum at the detector input and the phase characteristic have even symmetry about the midband frequency. This occurs when β_2 is nonzero.

These three cases are illustrated in Figure 3.3 with a raised cosine signaling pulse with $\alpha = 1.0$. These figures each represent the complex channel pulse response resulting from a particular type of linear distortion (i. e. linear amplitude distortion, linear delay distortion, or quadratic delay distortion).

The Discrete Channel Pulse Response

Since the transmitter sends discrete-time symbols at a rate of 1/T symbols per second and the sampled received baseband signal is also a discrete signal with samples occuring at a rate of 1/T per second, it is obvious that the cascade of analog filters $g_t(t)$, $g_c(t)$, $g_r(t)$ and the sampler can be represented in this case by an equivalent discrete-time transversal filter as shown in Figure 3.4 [45]. W_k is the input information sequence, and the tap gains, p_{-N}, p_{-N+1}, ..., p_0, ..., p_{N-1}, p_N represent the discrete-time channel pulse response. Also, white Gaussian noise samples are added to the channel output to complete the lowpass model. The ideal, undistorted discrete channel pulse response will be
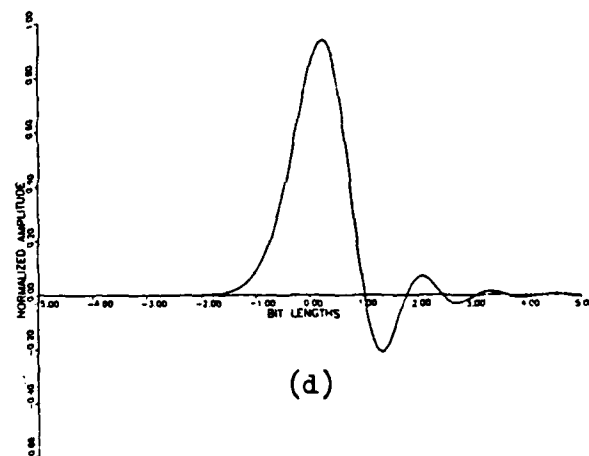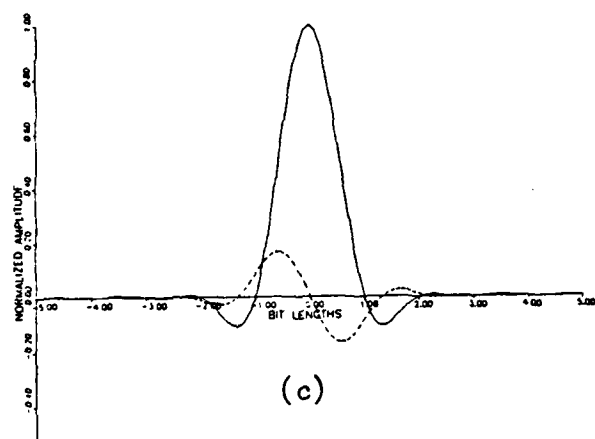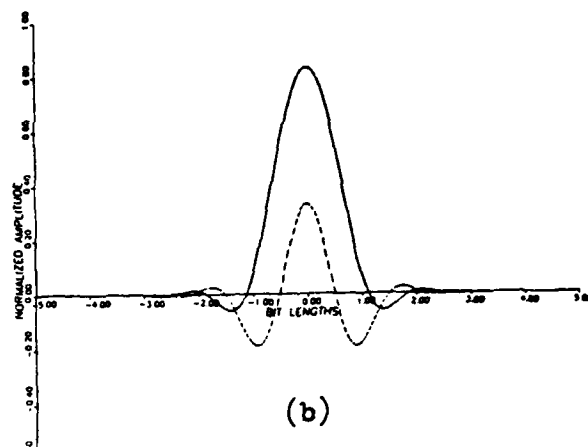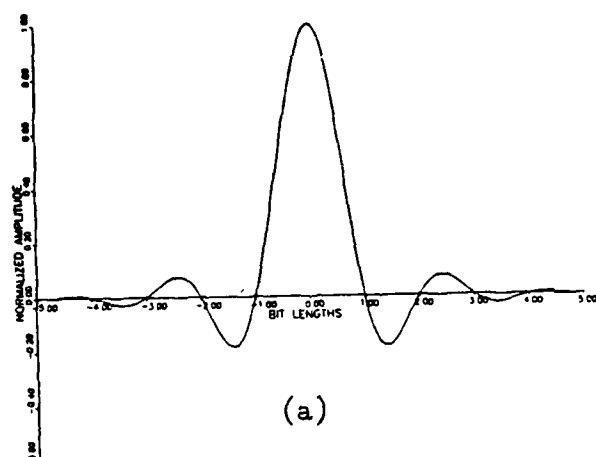
Figure 3.3- Examples of a single signaling pulse after being subjected
to a) zero distortion, b) linear amplitude distortion,
c) linear group delay distortion and d) parabolic group
delay distortion. (Note: quadrature component shown as
dotted line)

44
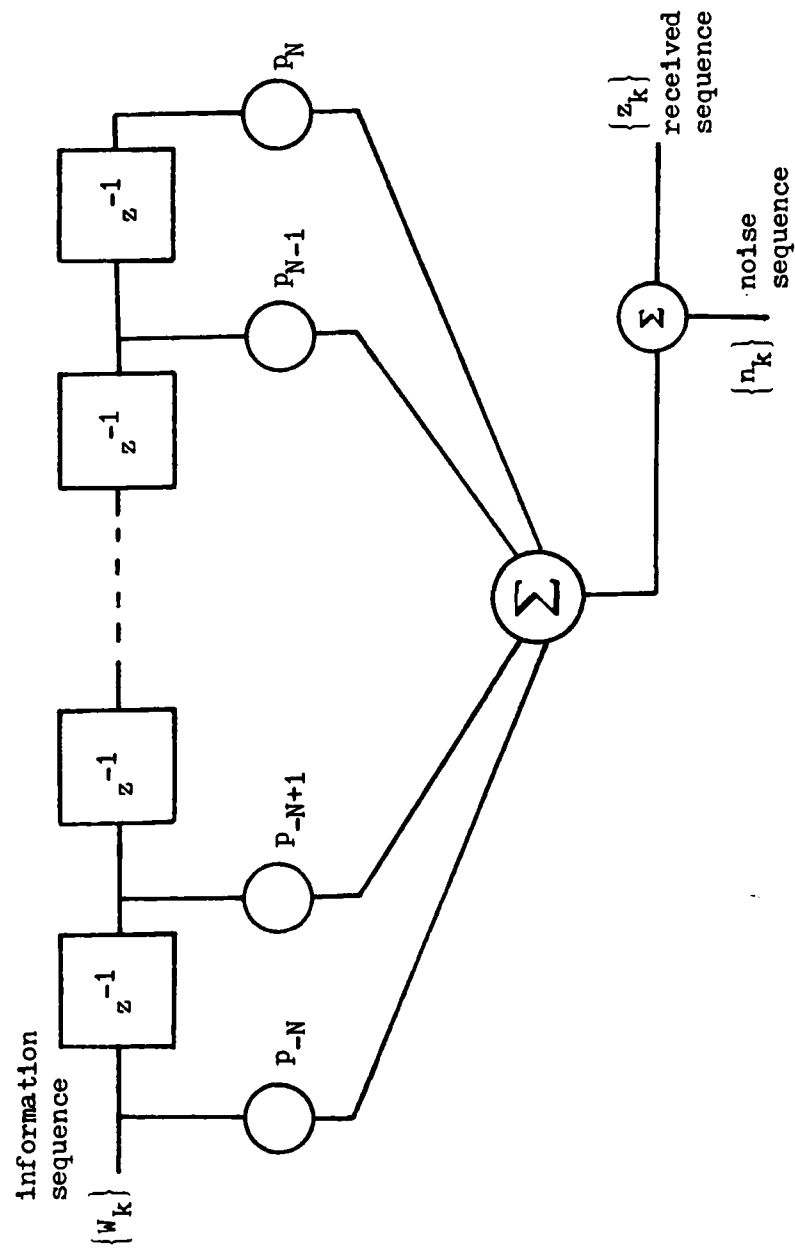
Figure 3.4 - The Lowpass Discrete-Channel Model

$$p(t) = \begin{cases} 1, & N = 0 \\ 0, & \forall N \neq 0 \end{cases} \qquad (3\text{-}7)$$

so that, in the case where no amplitude or delay distortion is present in the channel, only the $N = 0$ component of the discrete channel pulse response will have a nonzero value. When distortion is present in the channel, the discrete channel pulse response will have more than one nonzero sample, indicating the presence of intersymbol interference.

Therefore, the discrete channel pulse response is nothing more than a sequence of regularly spaced samples of the channel pulse response, with the samples taken at baud intervals. For the multilevel, or MPSK channel, all of the tap gain values, as well as the input information signal and output baseband signal are complex. Therefore Figure 3.4 can be represented in an equivalent form for the multilevel channel as shown in Figure 3.5. Here, the inphase and quadrature components of the discrete channel pulse response are explicitly represented.

In the presence of amplitude or group delay distortion, the inphase and quadrature discrete channel pulse responses will contain certain levels of intersymbol interference and crosstalk. By observing the characteristics of the intersymbol interference and
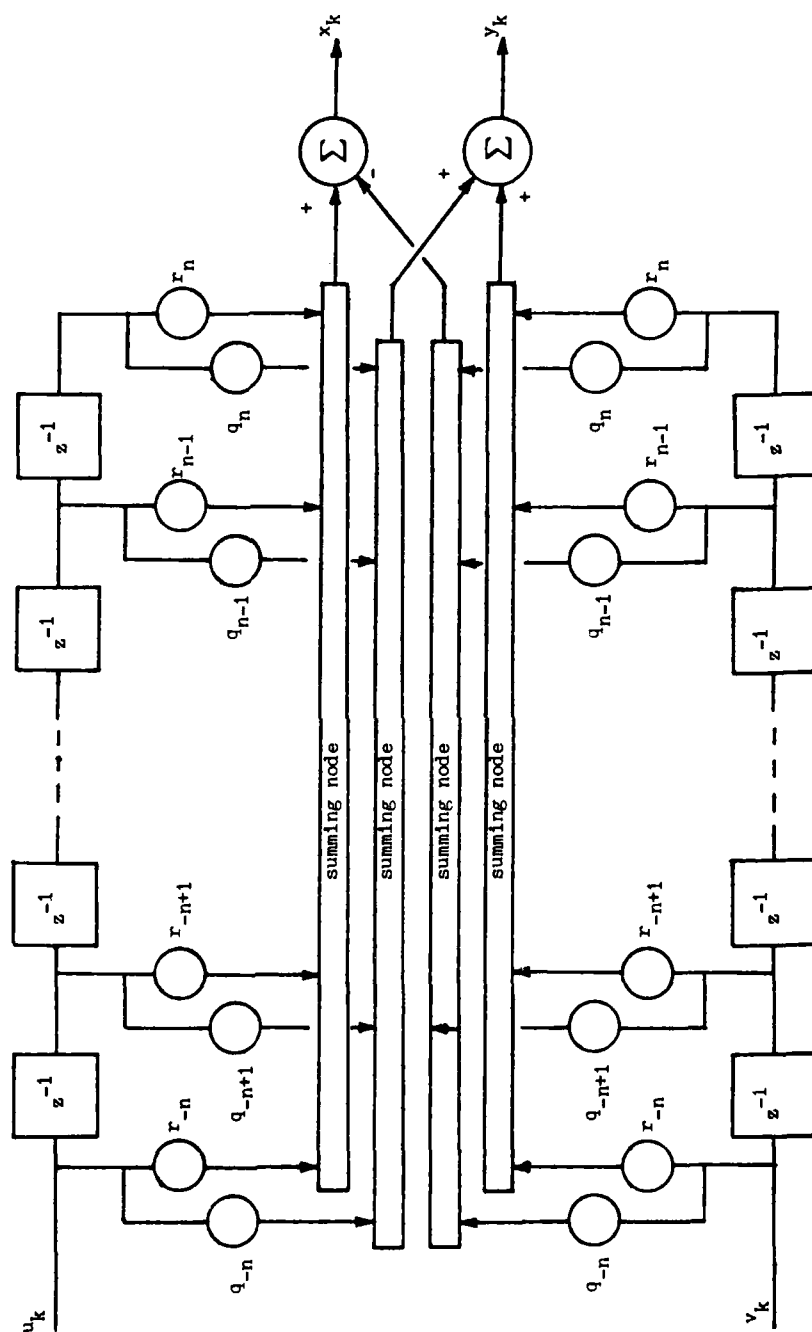
Figure 3.5 – The Lowpass Complex Discrete-Channel Model

crosstalk in the complex channel pulse response, the system for estimating channel distortion (described in the next chapter) will recover the exact analytical representation of the distortion present in the received waveform.

CHAPTER IV

THE SYSTEM FOR ESTIMATING CHANNEL DISTORTION

System Description

The system employed in the research for estimating channel distortion is illustrated in Figure 4.1. The system is essentially an add-on processor which requires only the baseband and detected data sequences as inputs. It consists of three primary subsystems which will be described at length in later chapters. They are:

(1) The channel estimator - determines the complex channel pulse response.

(2) The channel simulator - attempts to emulate the output of the channel estimator at a specific number of discrete points.

(3) The system algorithm - adjusts and optimizes the distortion components within the channel simulator until the channel simulator output matches the channel estimator output (i. e. minimizes the error signal).

The system for estimating channel distortion is based upon a class of well known adaptive systems known to automatic control theorists as the model reference adaptive system (MRAS) [46]. The basic MRAS structure is shown in Figure 4.2. The reference model gives the desired response

49
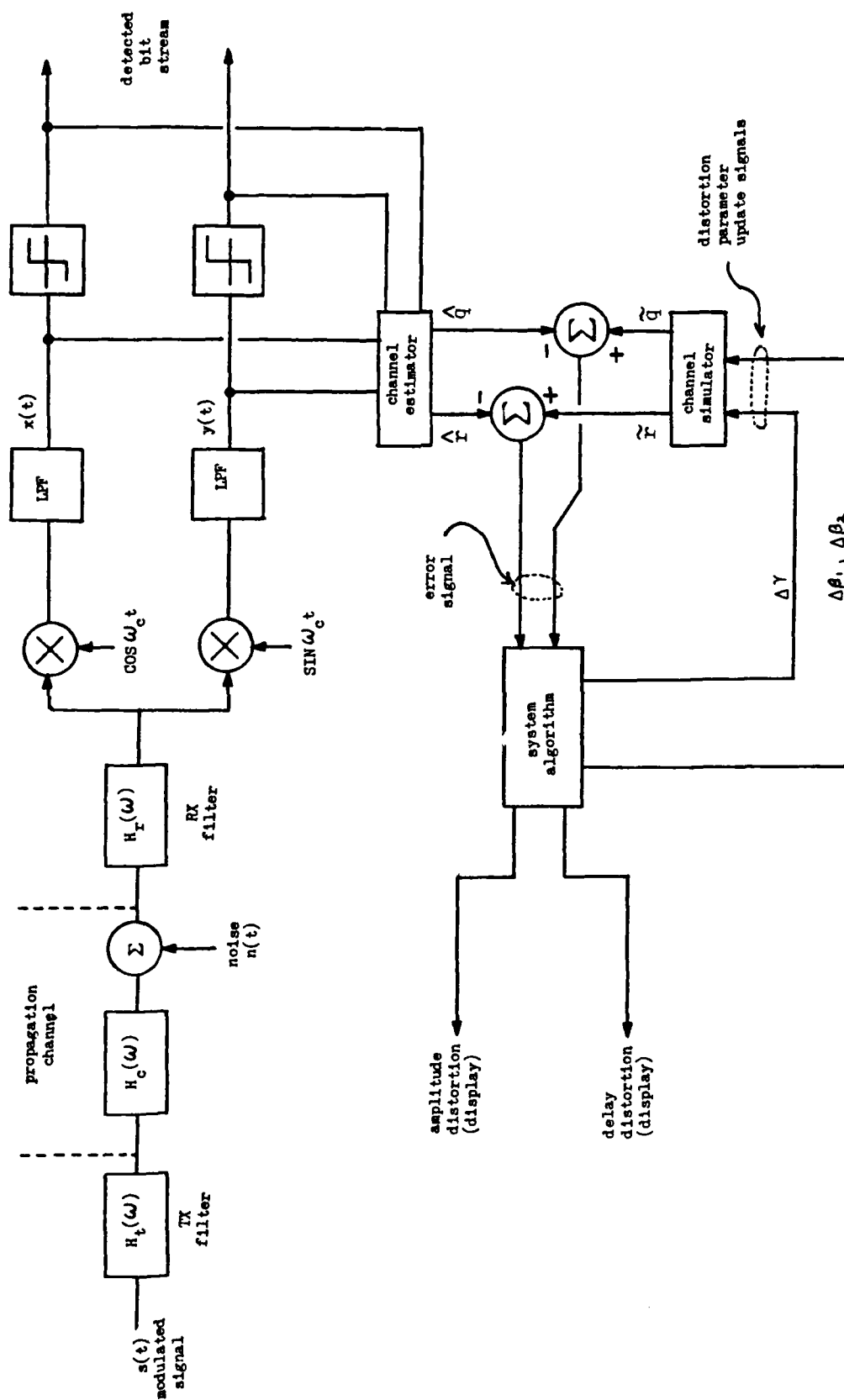
Figure 4.1 - Overall System Diagram of the Distortion Estimator
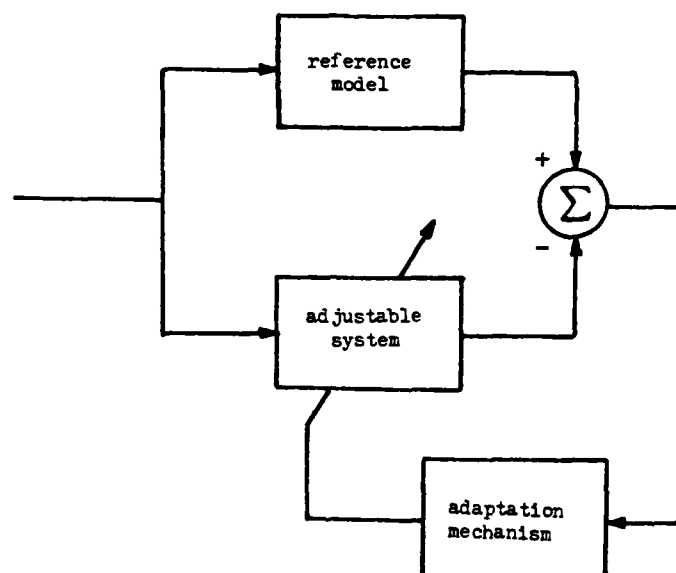
Figure 4.2 - Basic Configuration of a Model Reference
Adaptive System (MRAS)

of the adjustable system, while the task of the adjustable system is to adaptively minimize a function derived from the difference between the outputs of the adjustable system and those of the reference model. This is accomplished through an adaptation mechanism that modifies the parameters of the adjustable system. In order to successfully implement this system, some prior knowledge of either the model or the adaptive system is normally required. The important advantage of this type of system is its relatively high speed of adaptation [47], which is due to the direct comparison of the reference model output with the output of the adjustable system. The result of that comparison becomes the error signal which modifies the parameters of the adjustable system. The MRAS concept is adapted for use in the research as shown in Figure 4.1, which illustrates the manner in which the distortion estimation process is interfaced with the communication system.

As previously noted in Chapter I, the primary contribution of the research is the systematic manner in which several subsystems are brought together in order to measure or estimate the amount and type of linear distortion on a specific MPSK communication channel. It is appropriate at this point to indicate the specific contribution of the research with respect to each of the subsystems which comprise the overall technique.

Subsystem Description

The channel estimator is a self-contained system identification processor which employs sampled outputs from the receiver demodulator and the recovered information sequence in order to estimate the discrete complex channel pulse response,

$$\hat{p}(t) = \hat{r}(t) + j\hat{q}(t) \qquad (4-1)$$

The channel estimator corresponds to the reference model in the MRAS. The channel estimator very closely resembles an adaptive equalizer in both structure and operation. Use of this approach to estimate the pulse response of a simple binary (real) channel was first proposed by Magee and Proakis [45]. The estimator employed in the present research is unique in that it extends the real channel estimator to the complex case, so that channel identification can be accomplished when multilevel signaling is employed on the channel.

The channel simulator computes the discrete complex channel pulse response,

$$\tilde{p}(t) = \tilde{r}(t) + j\tilde{q}(t) \qquad (4-2)$$

based upon a prior knowledge of the mathmatical specification of the undistorted transmitted waveform. The channel simulator corresponds to the adjustable system in the MRAS. Its adjustable parameters are the channel amplitude and group delay distortion components, γ, β_2, and β_3 which were defined in Chapter III. These components are incorporated into the mathmatical specification of the channel pulse response, and are constantly updated by the system algorithm until the channel simulator output corresponds to the channel estimator output. The mathmatical foundation for the channel simulator is taken from Sunde's [5] early investigations on the effects of transmission distortion on digital waveforms. Sunde's formulation for expressing the inphase and quadrature baseband waveforms was aimed at graphically and numerically evaluating distortion. The channel simulator employes Sunde's general approach by using the analytical expressions for the received baseband waveforms tailored to the specific types of distortion of interest (described in Chapter III), and also to the specific timing intervals of interest. In this manner, continuous rapid updating of the simulator is possible through the system algorithm. Additionally, a novel alternative method is developed for representing the discrete complex channel pulse response as a numerical series in terms of the ideal undistorted channel pulse response.

The system algorithm functions as the MRAS adaptation mechanism by adjusting the distortion components within the channel simulator so that the error between the estimated and simulated channel pulse responses is minimized. When some predefined minimum error value is reached, the resulting distortion components can be displayed in some useful form. This entire procedure operates in an iterative manner, so that the system adapts to changes in channel distortion as multipath variations occur. The system algorithm, as employed in the research, is a straightforward steepest descent optimization system in which the convergence speed is adjusted after every iteration. Since fast operation is a desirable characteristic, adjustment of the algorithm's convergence parameter allows the system to zero in on the optimum values of the channel distortion parameters in relatively few steps. Algorithms of this type are well documented in the literature, and have been in use for quite some time.

Sampling the Channel Pulse Response

The discrete channel pulse response, as explained in Chapter III, consists of a series of N discrete values which represent the channel pulse response sampled at N different times. Any errors occuring in the estimated pulse response cannot be overcome by the adaptive system. Therefore, a primary concern in the research is representing the channel

pulse response in a form which can be determined with the greatest degree of accuracy. This requires judicious selection of the number and spacing of samples of the estimated channel pulse response. Several possible choices are illustrated in Figure 4.3.

While observing the overall system performance, no distinct advantage was realized by fractional baud interval spacing (such as shown in Figure 4.3b) over full baud interval spacing (as shown in Figure 4.3a). Accuracy of the distortion estimation system was more dependent upon the number of samples than upon their location. Since the physical form of the channel pulse response is mathmatically constrained, it is obvious that a widely dispersed set of samples will yield more accurate curve fitting results than a set of narrowly dispersed samples.

Baud interval sampling was selected as the best overall approach for the distortion estimation process. The primary motivation for this selection lies in the simplicity it affords. With baud interval sampling the entire distortion estimation system can operate as a "clip-on" instrument which can attach to any digital radio and make the necessary measurements using only the signals provided by the radio itself. Furthermore, it can attach at points which are normally accessible for measurement or observation (i. e. the baseband signal and the detected bit stream).

If fractional sampling were employed, a separate

56
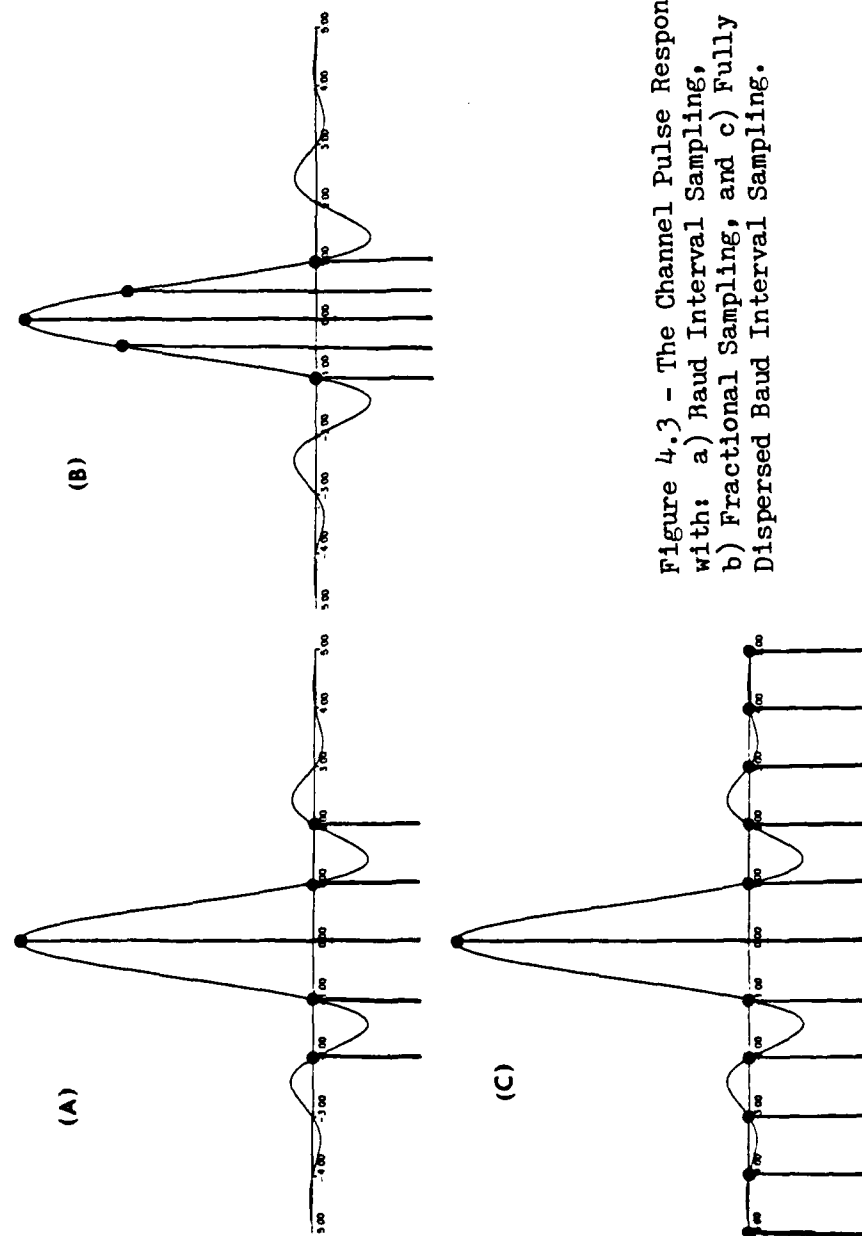
Figure 4.3 - The Channel Pulse Response with: a) Baud Interval Sampling, b) Fractional Sampling, and c) Fully Dispersed Baud Interval Sampling.

baseband receiver would need to be incorporated into the distortion estimation process so that sampling at an increased rate could be accomplished. This greatly increases the cost and complexity of the system. Since the channel estimator operates as a decision-directed device and is dependent upon the correct recovery of the information sequence, fractional sampling would require threshold detection of the received baseband signal at numerous intermediate levels. This would greatly increase the susceptability of the distortion estimation process to noise induced error and needlessly complicate the system.

With baud interval sampling, the only remaining sampling concern is the number of samples to be employed in representing the discrete channel pulse response. Obviously, the goal is to use as few foints as necessary to obtain reasonably accurate results. Since the channel has a finite pulse response, only enough samples are needed so that any time dispersion induced by amplitude or group delay distortion will be sufficiently represented. For most reasonable values of amplitude and group delay distortion (i. e. distortion not severe enough to completely close the aperture in the eye diagram) no more than 11 sample values will ever be needed, as shown in Figure 4.3c.

Since the digital radio employs baud-interval sampling in its normal operation, a convenient property of the received pulse (due to the Nyquist criterion) can be

used to advantage, where

$$r(t) = \begin{cases} 1, & t = 0 \\ 0, & t = \pm T, \pm 2T, \ldots \end{cases} \qquad (4-3)$$

when no distortion is present. Therefore, if the inphase (or quadrature) pulse response is sampled at nonzero integral values of T (i. e. $t = \pm T, \pm 2T, \pm 3T$, etc.). Any nonzero signal values detected at these points represents the presence of some form of distortion. The sample at t=0, which ideally is unity, can be used as a normalizing factor for the other sample values.

CHAPTER V

ESTIMATION OF THE CHANNEL PULSE RESPONSE

Introduction

In order to characterize or measure the amplitude or group delay distortion present in a communication channel, the response of the channel to a single isolated signaling pulse must be determined. This basic function, previously defined as the "channel pulse response", gives the shape of a single baseband signaling pulse at the detector output under ideal conditions or in the presence of a particular kind of transmission distortion. Later sections will be concerned with the specific approach used to determine the distortion present in the channel pulse response. This chapter is concerned primarily with the real-time estimation of the unknown channel pulse response under normal traffic conditions.

Specific techniques employed to estimate the pulse response of a communication channel are derived from generalized principles commonly associated with the broad discipline of system identification. Fortunately, communications channels have certain unique characteristics which can be used to advantage in the identification process. For example, a communication channel can normally

be characterized as an unknown system with a distorted output signal from which parameters or properties of the system must be estimated. Usually, a number of assumptions can be made which hold true for most communication channels of interest. These are as follows:

(1) Some property of the input signal, and usually the input signal itself, is known. In the present study, the input signal is assumed to belong to the class of Nyquist pulses with a sinusoidal-rolloff spectrum.

(2) The general structure of the system is known. The system is linear and may be slowly time varying. However, the variation in the channel is assumed to be slow in time with respect to the length of a single signaling interval.

(3) Properties of the interference are known. Multiplicative interferences are assumed to be linear in nature, while additive interferences are restricted to the assumption of zero mean, additive white Gaussian noise.

For the channel identification problem, the sources of interference and the characterization of the interference are generally unimportant.

Two significant characteristics of a line-of-sight communication channel which will greatly simplify and facilitate the channel identification process are:

(1) The data stream is assumed to be randomized. That is, the transmitted symbols can be considered to be

identically distributed independent random variables. The validity of this assumption was established earlier.

(2) The recovered information sequence is assumed to be correct. That is, the received data symbols are detected and quantized with zero probability of error.

Using these important assumptions, the singular goal of the communication channel identification problem is to obtain an equivalent discrete-time representation of the actual channel pulse response.

The need for determining the communication channel pulse response is found in several important communications signal processing applications. These are adaptive equalization, echo cancellation, and maximum-liklihood sequence estimation (MLSE).

Adaptive equalizers for digital communication channels are normally implemented as finite impulse response tapped delay line filters, as shown in Figure 5.1. The purpose of the linear adaptive equalizer is to invert or undo the time dispersive influence of the channel. The equalizing filter should have a frequency response, $H_c(\omega)$, such that the actual channel response multiplied by $H_c(\omega)$ yields the assumed (i. e. distortionless) channel response. In this manner, the channel is compensated for amplitude and phase distortion. However, with the proper choice of signaling pulse (e. g. a Nyquist pulse), the equalizer coefficients, C_n, will indicate the inverse of the channel
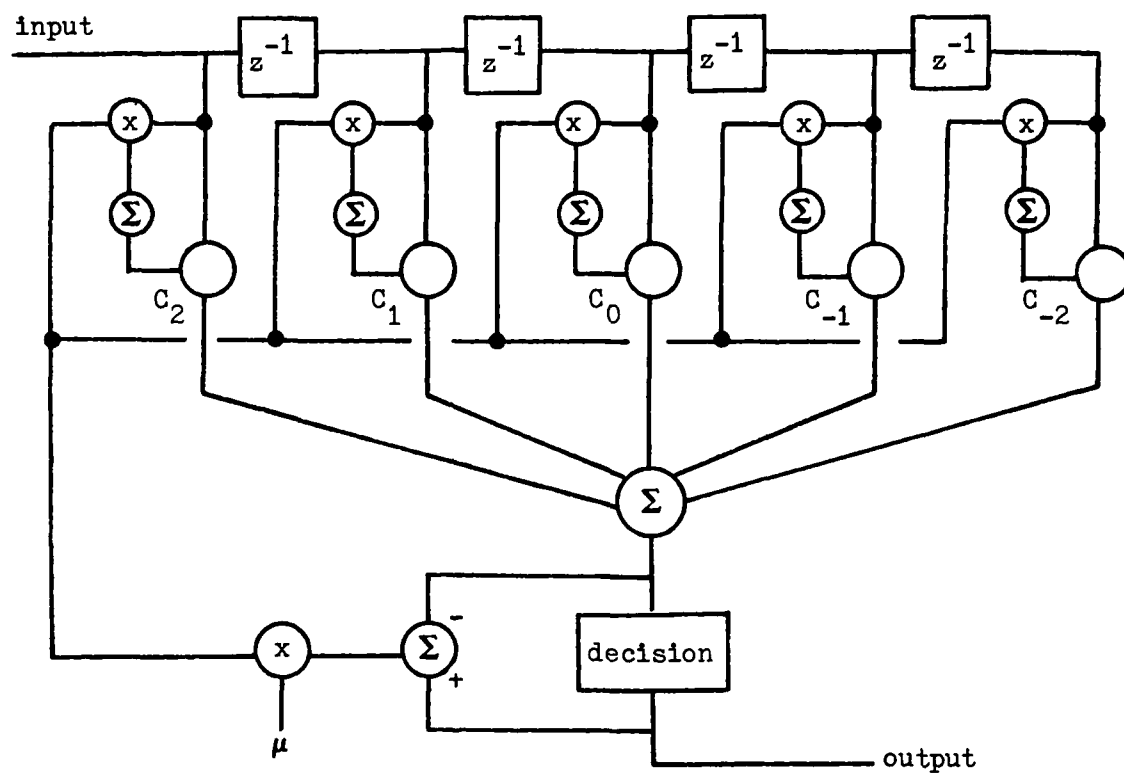
Figure 5.1 - Adaptive Linear Equalizer

pulse response at the sampling intervals when equalization is complete. Although it is not the purpose of the adaptive equalizer to identify the channel (in fact, the actual values of the tap coefficients are usually not of interest), an implicit channel identification process is performed during normal operation of the equalizer.

A more direct requirement for obtaining the channel impulse response can be found in the design of echo cancellers [48]. The basic function of the echo canceller is to synthesize a replica of the echo and subtract it from the returned signal, as shown in Figure 5.2. This assumes the echo path is linear and therefore completely specified by its impulse response. Most practical echo cancellers use transversal tapped delay line filters in which the tap weights are adjusted in a manner very similar to that of the adaptive equalizer. The transversal filter simulates the impulse response of the echo channel so that the convolution of the filter tap weights with the input signal yields an exact replica of the echo signal. This replica is then subtracted from the actual echo signal, thus effectively cancelling it. Echo cancellers can be used for speech or data. The primary difference is that echo cancellers employed for speech applications require sampling at the Nyquist rate, while data echo cancellers need only sample at the signaling rate. Therefore, many more tap delays are required for a speech echo canceller than for the data echo
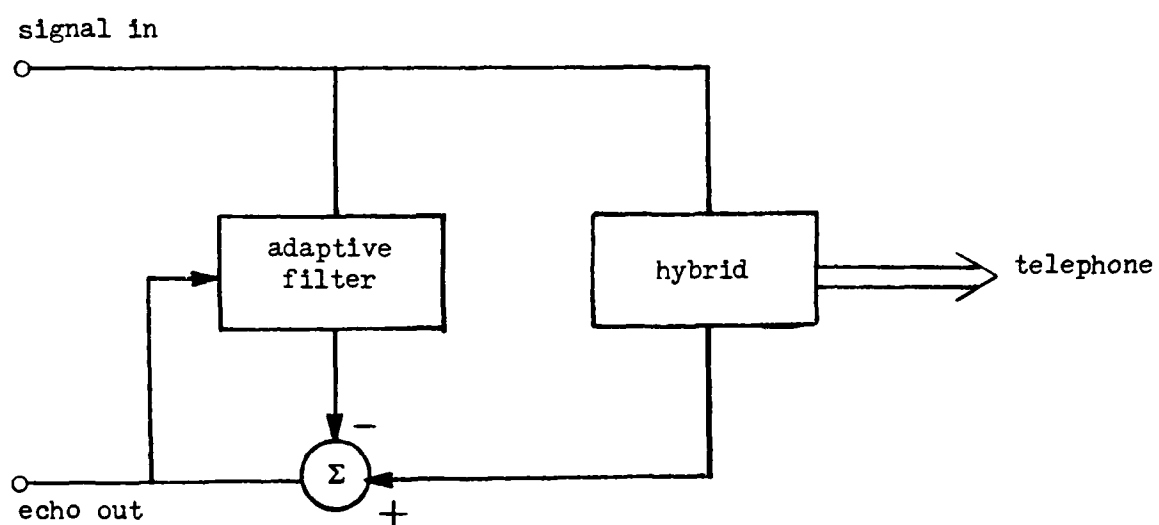
Figure 5 .2 - Echo Canceler

canceller.

A final important application which requires explicit knowledge of the channel pulse response occurs in the maximum-liklihood sequence estimation scheme originally proposed by Forney [49]. A probabilistic detection algorithm forms the main portion of the receiver structure shown in Figure 5.3. This algorithm requires knowledge of the channel pulse response for proper operation. Therefore, an adaptive estimator is provided which operates on both the recovered information sequence and the received signal sequence to provide a measurement of the channel pulse response.

There are a number of system identification techniques which have been tailored to the specific problem of estimating the pulse response of a communication channel [50]. The remainder of this chapter will concentrate on adapting and extending one of these techniques to the MPSK line-of-sight communication channel. The approach chosen is called the adaptive channel estimator, which was first proposed by Proakis [51]. The advantage of this approach is that it is less expensive to implement than many other approaches; and also it can tolerate some degree of correlation in the input signaling states. Furthermore, it can operate on the normal traffic flow without need for a training period.
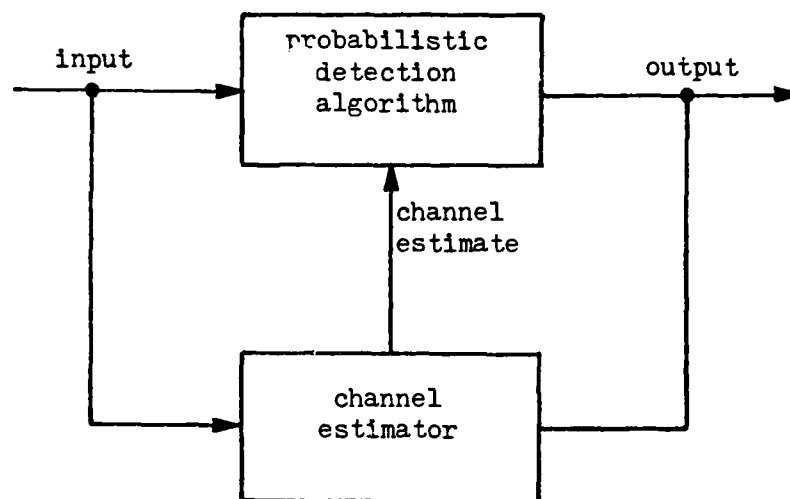
Figure 5.3 - Adaptive Probabilistic Detector

Adaptive Channel Estimation

The Real (Binary) Channel Estimator

The channel estimator employed in the research is based upon an adaptive linear filter which seeks to minimize the mean-square error between the actual received sequence and a signal formed by filtering the transmitted information sequence. The general structure of the adaptive channel estimator is shown in Figure 5.4.

The transmitted information sequence is filtered by a finite impulse response (FIR) filter, which consists of a tapped delay line connected to an adaptive linear combiner. The combiner sums the weighted signal samples and subtracts this output signal from the desired filter output. The error signal thus formed is used to drive an adaptive algorithm to adjust the tap gains so that the error signal is minimized according to some criterion.

The adaptive linear filter has been employed in a number of important applications including adaptive antenna arrays, noise canceling, pattern recognition, and system identification. Perhaps the most pervasive application of these filters in the communications field to date is in the adaptive channel equalizer, which seeks to reduce the effect of intersymbol interference in a received signal. When the adaptive filter is employed in a system identification scheme for a communication channel it becomes an adaptive channel estimator. The purpose of the channel estimator is
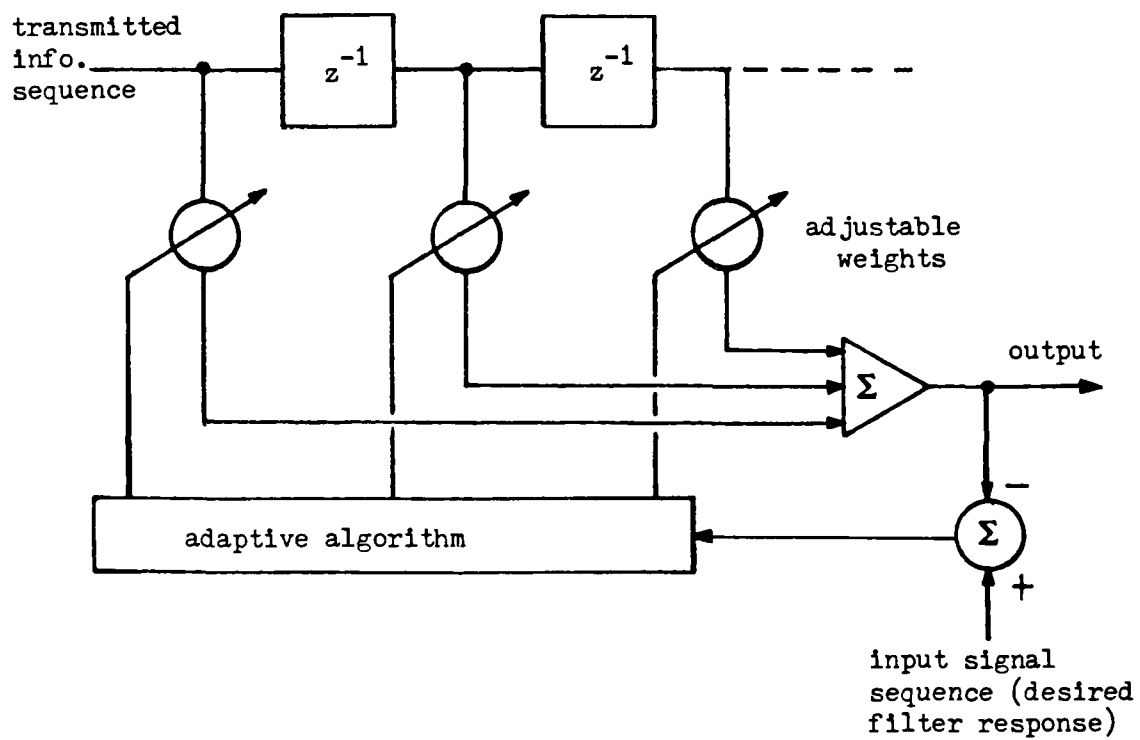
Figure 5.4 - Adaptive Linear Filter

to identify the presence of intersymbol interference in the received signal by actually extracting the channel pulse response from the received data signal. One notable application for the adaptive channel estimator in the literature was proposed by Proakis for a binary channel [52]. In this application, the channel estimator was one of the primary components of a maximum-liklihood receiver which employed a Viterbi Algorithm in a nonlinear equalization and detection scheme. This estimator, in combination with the Viterbi algorithm proved to be effective in communicating over slowly time-varying channels having significant amounts of intersymbol interference.

The adaptive channel estimator for the binary channel is shown in Figure 5.5. The similarity of the estimator to an adaptive equalizer is obvious, in that both are essentially linear transversal filters whose parameters are adjusted according to some minimization algorithm. In both cases, the parameters of adjustment are the tap gain coefficients. The most obvious difference between the equalizer and the estimator is that the input to the equalizer tapped delay line is the received baseband data sequence; while the input to the estimator tapped delay line is the detected information sequence. The coefficients of the equalizer are adjusted so that the output sequence closely resembles the detected information sequence; while the coefficients of the estimator are adjusted so that the
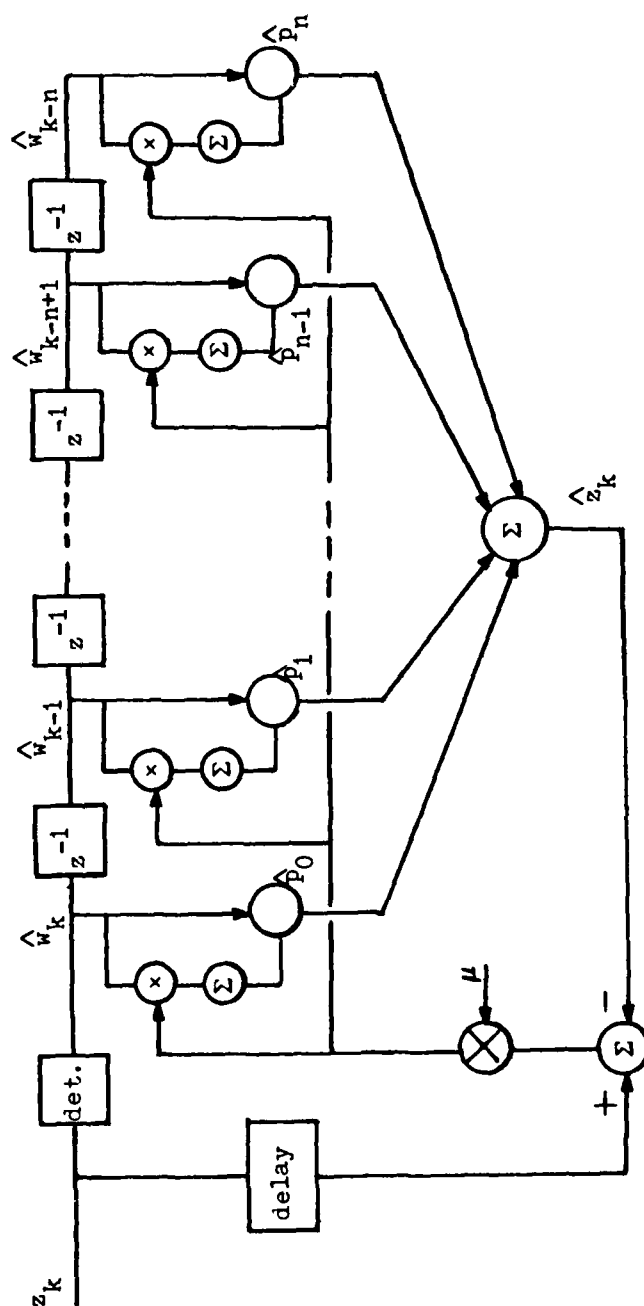
Figure 5.5 - Adaptive Binary Channel Estimator

output sequence closely resembles the received baseband data sequence.

The essential purpose of the real channel estimator is to approximate the sampled channel pulse response of the equivalent discrete-time channel model developed in Chapter III. To accomplish this, the received baseband data signal is sampled at each baud interval, T, and input to the filter as the sequence z_k. This sequence is passed through a decision device (threshold detector) which makes a determination on a bit-by-bit basis of the original transmitted information sequence. An important assumption in the proper operation of this system is that all decisions are correct. This is a reasonable assumption for line-of-sight microwave systems operating in a low probability of error environment. After detection, the information sequence, $\hat{w}_k$, is input to the filter where an estimate of the received data, $\hat{z}_k$, is formed by multiplying the sequence of symbols stored in the tapped delay line by the corresponding tap gains and summing the products. The estimate of the received signal is,

$$\hat{z}_k = \sum_{j=0}^{M} \hat{p}_j \, \hat{w}_{k-j} = \hat{\underline{p}}^T \, \hat{\underline{w}}_k \tag{5-1}$$

which can be recognized as a convolution sum for a tapped delay line filter. An error signal is formed by taking the

difference between the estimated sequence $\hat{z}_k$ and the actual received sequence, z_k ,

$$\epsilon = (z_k - \hat{z}_k) \qquad (5\text{-}2)$$

Then the mean-square error is just the expected value of the squared error,

$$E\left(\epsilon^2\right) = E\left[(z_k - \hat{z}_k)^2\right] = \xi \qquad (5\text{-}3)$$

Note that,

$$z_k = \sum_{j=-N}^{N} p_j w_{k-j} + n_k \qquad (5\text{-}4)$$

is the output of the discrete-channel model discussed earlier.

It has been shown that when the mean square error between z_k and $\hat{z}_k$ is minimized, the resulting values of the tap gain coefficients of the channel estimator are the values of the equivalent discrete-channel model which was discussed in Chapter III. The tap gains that minimize the mean-square error must satisfy the following set of linear equations,

$$\sum_{k=-N}^{N} p_k \, E\left(w_j w_k\right) = \sum_{k=0}^{M} \hat{p}_k \, E\left(\hat{w}_j \hat{w}_k\right) \tag{5-5}$$

The tap gains are adjusted recursively via a steepest descent algorithm, such as,

$$p_{k+1} = p_k + \mu \epsilon_k \, \hat{w}_k \tag{5-6}$$

where μ controls the speed of convergence and accuracy of the algorithm. As long as the information sequence is uncorrelated, the optimum tap gain coefficients are exactly equal to the respective values of the equivalent discrete-channel model. In fact, as long as the number of taps in the estimator is greater than or equal to the number of significant values in the discrete-channel model (M>2N+1), the input sequence need not be uncorrelated for the estimator to provide accurate results. Under all of these conditions, the minimum mean-square error is equal to the noise variance.

The Complex Channel Estimator

Since the research concentrates on M-ary PSK systems, it is necessary to extend the capabilities of the adaptive binary channel estimator so that the pulse response of a complex channel can be accurately determined. Unfortunately, the complex discrete-channel model of Figure

3.5 (and illustrated in Figure 5.6 in block diagram form) introduces potentially troublesome cross terms which significantly complicate the problem of estimating the discrete channel pulse response.

A mathmatical solution for using an adaptive filter to estimate the pulse response of a complex communication channel was achieved by using the same general structure as the real channel estimator, and then allowing all the signals to be complex. Therefore,

$$z_k = x_k + j \, y_k \qquad (5\text{-}7)$$

$$w_k = u_k + j \, v_k \qquad (5\text{-}8)$$

$$p_k = r_k + j \, q_k \qquad (5\text{-}9)$$

where r_k and q_k are the inphase and quadrature components of the channel pulse response, respectively. x_k and y_k are the sampled baseband data sequences, while u_k and v_k are the transmitted information sequences (assuming no decision errors occur). The filter output sequence is,

$$\hat{z}_k = \sum_{i=0}^{N} p_i \, w_{i-k} = P^T W_k = W_k^T \, P \qquad (5\text{-}10)$$
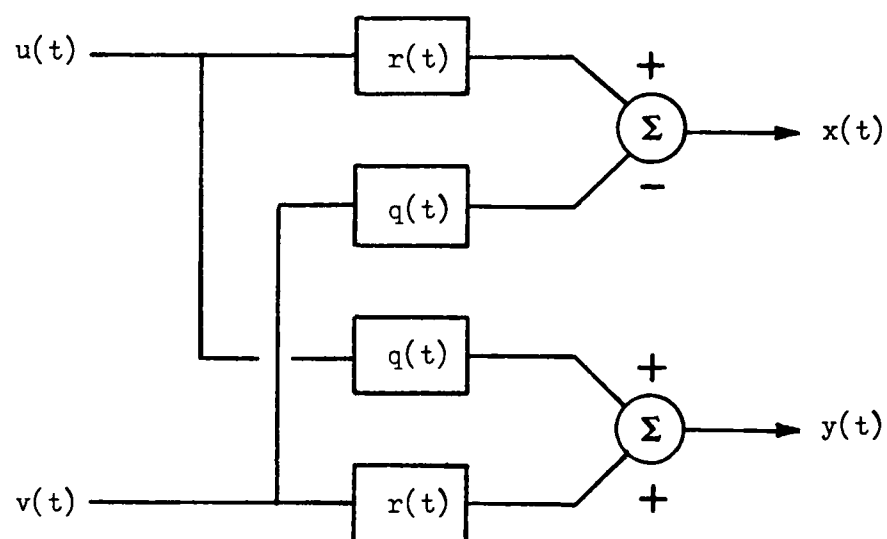
Figure 5.6 - Model of the Complex Channel

The error signal at any time, k, is defined as the difference between the actual output and desired output,

$$\epsilon_k = (z_k - \hat{z}_k) = z_k - W_k^T P = z_k - P^T W_k \qquad (5-11)$$

As before, the criterion which will be minimized will be the mean-square of the difference signal, ϵ_k . However, now all values are complex, so it is the average total error power that is minimized,

$$\xi_k = E\left\{\epsilon_k \epsilon_k^*\right\} \qquad (5-12)$$

Note that since the two components of the error are in quadrature relationship to one another, they cannot be minimized independently. This can be seen clearer by expanding the expression for ξ_k,

$$\xi_k = E\left\{(z_k - P^T W_k)(z_k^* - P^{T*} W_k^*)\right\} \qquad (5-13)$$

Carrying out the complex operations yields,

$$\xi_k = E\left\{z_k z_k^*\right\} - E\left\{z_k W_k^{T*} P^* + z_k^* W_k^T P\right\} + E\left\{P^T W_k^* W_k^T P^*\right\} \qquad (5-14)$$

which reduces to,

$$\xi_k = E\left\{z_k z_k^*\right\} - 2\mathrm{Re}\left[E\left\{z_k^* \ W_k^{\mathsf{T}}\right\} P\right] + P^{\mathsf{T}} \ E\left\{W_k^* \ W_k^{\mathsf{T}}\right\}P^* \qquad (5-15)$$

Defining the vector, A, as the cross correlation between the complex conjugate of the desired response (a scalar) and the W vector gives,

$$A = E\left\{z_k^* \ W_k^{\mathsf{T}}\right\} = E \begin{bmatrix} z_k^* \ W_{1-k} \\ z_k^* \ W_{2-k} \\ \vdots \\ z_k^* \ W_{n-k} \end{bmatrix} \qquad (5-16)$$

The input autocorrelation matrix, B, is defined as,

$$B = E\left\{W_k^* \ W_k^{\mathsf{T}}\right\} = E \begin{bmatrix} W_{1-k}^* \ W_{1-k} & W_{1-k}^* \ W_{2-k} & \cdots \cdots \\ W_{2-k}^* \ W_{1-k} & W_{2-k}^* \ W_{2-k} & \cdots \cdots \\ \vdots & \vdots & \ddots \\ \vdots & \vdots & W_{n-k}^* \ W_{n-k} \end{bmatrix} \qquad (5-17)$$

This matrix is real, symmetric and positive definite [53]. The mean-square error can now be expressed as,

$$\xi_k = E\left\{z_k z_k^*\right\} - 2\mathrm{Re}\left\{A^{\mathsf{T}} \ P\right\} + P^{\mathsf{T}} \ BP^* \qquad (5-18)$$

Note that the mean-square error is now a quadratic function of the tap gains. ξ_k can be viewed as a concave hyperbolic surface with a unique minimum. Adjusting the tap gains to minimize ξ_k is accomplished by an algorithm which descends along this surface until the minimum is reached.

ξ_k can be solved exactly, and the optimum tap gain vector determined by taking the gradient of the mean-square error function with respect to the tap gains,

$$\nabla_k = \begin{bmatrix} \dfrac{\delta E\left\{\epsilon_k \epsilon_k^*\right\}}{\delta P_1} \\ \vdots \\ \dfrac{\delta E\left\{\epsilon_k \epsilon_k^*\right\}}{\delta P_n} \end{bmatrix} \qquad (5\text{-}19)$$

Now by exchanging the expectation operator with the partial derivative operator, the gradient becomes,

$$\nabla_k = E \begin{bmatrix} \dfrac{\epsilon_k^* \delta\epsilon_k + \epsilon_k \delta\epsilon_k^*}{\delta P_1} \\ \vdots \\ \dfrac{\epsilon_k^* \delta\epsilon_k + \epsilon_k \delta\epsilon_k^*}{\delta P_n} \end{bmatrix} = -2\text{Re}\left\{A - BP\right\} \qquad (5\text{-}20)$$

The optimal tap gain vector, $\widetilde{P}$, called the Weiner weight vector can be obtained by setting the gradient equal to zero, so that,

$$\widetilde{P} = B^{-1} A \qquad (5\text{-}21)$$

This equation is a matrix version of the Weirer-Hopf equation in complex form. The minimum mean-square error then becomes,

$$\xi_{k(\text{min})} = E\left\{z_k z_k^*\right\} - 2\text{Re}\left\{A^\mathsf{T} \widetilde{P}\right\} + A^\mathsf{T} \widetilde{P}^* \qquad (5\text{-}22)$$

The objective of the adaptive process is to achieve a solution which approaches the optimal solution, $\widetilde{P}$. An exact solution requires prior knowledge of the correlation matrices A and B. Although these matrices could be computed empirically, doing so would present serious computational difficulties if the number of tap gains is large or the input data rate high. Since the objective is to develop a technique that can function on-line and track dynamic changes in the channel, it is more practical to employ a recursive statistical estimation algorithm, such as the method of steepest descent.

The method of steepest descent depends upon a measurement of the gradient of the mean square error function, ξ_k. Each estimate of the tap gain vector, P, is successively updated in proportion to the negative of the gradient vector as follows,

$$P_{k+1} = P_k + \mu(-\nabla_k) \qquad (5\text{-}23)$$

However, since computation of the gradient vector still requires knowledge of the correlation matrices, no advantage can be gained by this technique over a direct numerical solution for minimizing the mean square error.

Fortunately, a simple procedure for finding an approximation to the optimal tap gain vector has been devised by Widrow and Hoff [54], and is called the least mean-square (LMS) algorithm. This algorithm does not require explicit measurement of correlation functions, nor does it involve matrix inversion. Accuracy is limited by statistical sample size, however, since the tap gain values are based on real-time measurement of the input signal. The LMS algorithm is an implementation of the steepest descent technique employing an estimation of the actual gradient. The algorithm is,

$$P_{k+1} = P_k + \mu(-\hat{\nabla}_k) \qquad (5\text{-}24)$$

where $\hat{\nabla}_k$ is an estimate of the true gradient. This estimate is obtained by taking a single value of the error signal ϵ_k, and its conjugate ϵ_k^* ; and differentiating it as if it were the true mean-square error,
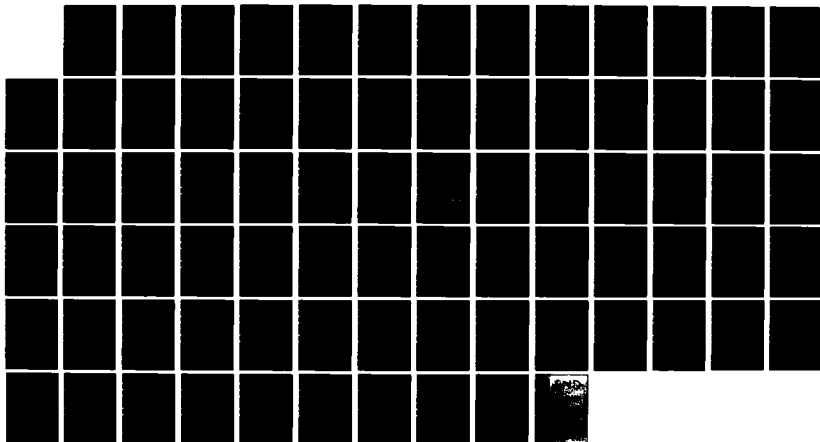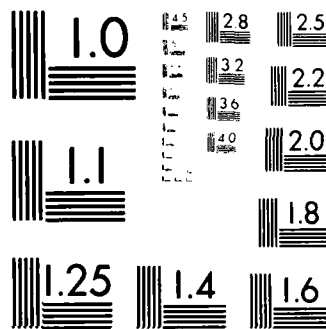
MICROCOPY RESOLUTION TEST CHART
NATIONAL BUREAU OF STANDARDS 1963-A

$$\hat{\nabla}_k = \begin{bmatrix} \dfrac{\delta \epsilon_k \, \epsilon_k^*}{\delta p_1} \\ \vdots \\ \dfrac{\delta \epsilon_k \, \epsilon_k^*}{\delta p_n} \end{bmatrix} = \epsilon_k \, \nabla(\epsilon_k^*) + \epsilon_k^* \, \nabla(\epsilon_k) \qquad (5\text{-}25)$$

Taking the gradient of the error signal with respect to both the real and imaginary components of the tap gain matrix, P, yields,

$$\hat{\nabla}_k = -2 \epsilon_k \, W_k^* \qquad (5\text{-}26)$$

Therefore, the LMS algorithm in complex form can be expressed as,

$$p_{k+1} = p_k + 2 \mu \epsilon_k \, W_k^* \qquad (5\text{-}27)$$

where, as usual, μ is a constant parameter that controls stability and rate of convergence. The advantage of this algorithm is that it is updated on every received data sample, so that the adaptive process is continuously seeking the optimum value of the tap gain coefficients. Since each increment the algorithm makes is based on a rough estimate

of the actual gradient, some amount of measurement noise is present in the algorithm at all times. However, it has been shown that this noise is attenuated by the adaptive process, which acts as a low pass filter [55]. Proof of convergence of the LMS algorithm and its behavior under various signal conditions are well documented in the literature [56] and will not be repeated here. It should be noted that algorithms other than the LMS approach have been developed for use in adaptive processes. Widrow [52] compared the LMS approach to the differential steepest descent (DSD) technique and to the linear random search (LRS) technique. The LMS algorithm was found to be faster and generally more efficient than the other two. Proakis [30] also discusses a number of alternatives, including the Kalman algorithm and various lattice algorithms. Each have their own specialized advantages. However, for overall combined performance, including speed of operation, efficiency, and simplicity, the popular LMS algorithm was judged to be the best approach to employ in the channel estimator.

The final step is to express the LMS algorithm in terms of a MPSK lowpass system so that it can be implemented and its operation verified under a variety of signal distortion conditions. The system used to implement the LMS algorithm is shown in Figure 5.7.

Several important design considerations for the channel estimator remain to be discussed. These are:
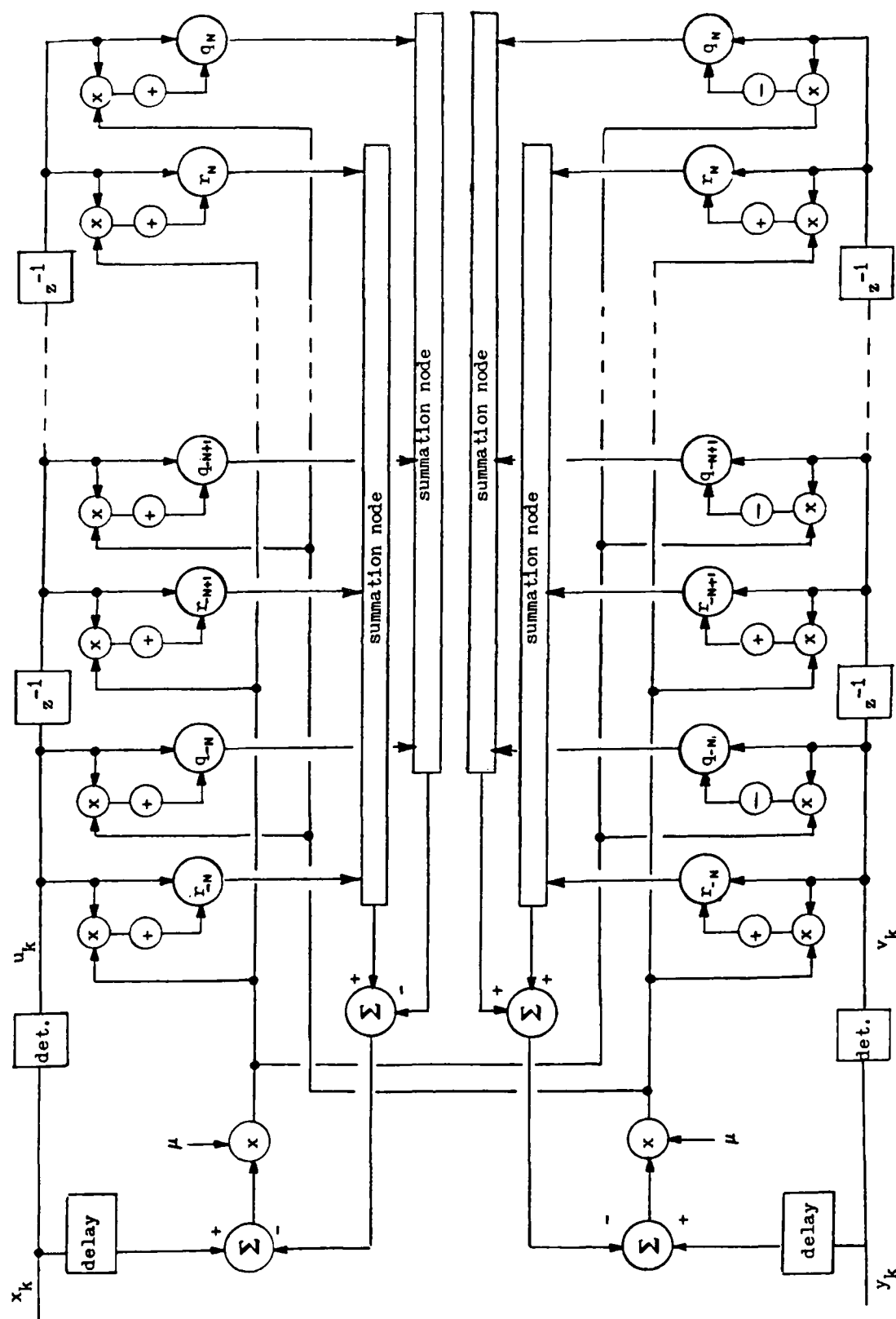
Figure 5.7 - The Complex Channel Estimator

83

(1) Selection of the number of taps

(2) Selection of the convergence parameter,

(3) Investigation of convergence properties under noise conditions

The number of taps to be employed in the channel estimator is primarily a function of the dispersion of the channel pulse response. Under severe amplitude or delay distortion, a greater amount of time dispersion occurs and hence, a larger number of taps are required. One of the results of the research was the determination of the maximum time dispersion imparted to the channel pulse response under the entire range of expected conditions. It was determined that the maximum possible ranges of amplitude and delay distortion requires no more than 11 taps in the channel estimator. The number of taps selected has an important impact on the convergence properties of the estimator. However, in the current application, the overriding consideration is the use of as few taps as necessary (to minimize convergence time) to represent a channel pulse response resulting from a variety of possible distortion conditions.

As previously mentioned, the gradient estimate used in the LMS algorithm is unbiased, and the expected value of the weight vector converges to the Weiner weight vector when the input sequence is uncorrelated. Widrow [55] showed that by starting with an arbitrary initial weight vector, the

algorithm will converge in the mean and remain stable as long as the parameter, μ, is greater than zero but less than the reciprocal of the maximum eigenvalue, λ_{max}, of the input autocorrelation matrix (5-17),

$$\frac{1}{\lambda_{max}} > \mu > 0 \qquad (5\text{-}28)$$

Furthermore, since λ_{max} must be less than the trace of the autocorrelation matrix (which is equal to the total power of the input signal components), the algorithm is unconditionally stable when,

$$\left[\sum_{i=1}^{N} E\left\{W_i W_i^*\right\} \right]^{-1} > \mu > 0 \qquad (5\text{-}29)$$

where N is the number of taps.

An understanding of estimator convergence under noise conditions is essential for an accurate evaluation of the system. An important characteristic of the LMS algorithm is that the gradient estimation process introduces noise into the tap gains which is proportional to the number of taps and the speed of adaptation. Gradient noise affects the adaptive process both during initial transients and during

steady state, and results in an excess mean squared error. This is known in the literature as "misadjustment" [54], and is a measurement of the ratio of the average excess mean squared error to the minimum mean squared error,

$$M = \frac{\text{average excess MSE}}{\text{minimum MSE}} \qquad (5-30)$$

Another noise consideration is the effect of the additive Gaussian noise present on the input signal. It has been shown [45] that as long as the input sequence is uncorrelated, and the number of taps is sufficient to represent the estimated channel pulse response, the minimum mean square error will be equal to the noise variance. These concepts will be investigated in Chapter VII and measurements will be made to verify expected performance.

CHAPTER VI

THE CHANNEL SIMULATOR AND SYSTEM ALGORITHM

The channel simulator, together with the system algorithm comprise the two essential components of an optimization scheme which seeks to match an analytical description of the channel pulse response with the actual measured, or estimated value of the pulse response. While linear distortion induced by both the radio system components and the propagation medium alters the amplitude and phase characteristics of a digital bandpass signal, the channel simulator and system algorithm will observe the estimated channel pulse response, and from a knowledge of the transmitted pulse, determine the amplitude and phase (group delay) distortion parameters of the channel.

Simulating the Channel Pulse Response

The Full Accuracy Simulator

The complex channel pulse response can be expressed analytically in terms of the inverse Fourier transform of the product of the signaling pulse spectrum and the channel distortion transmission characteristic as previously illustrated in Figure 3.1, to yield,

$$r(t) + jq(t) = \frac{1}{2\pi} \int_{-\infty}^{\infty} P(\omega)B(\omega)\, e^{-j\psi(\omega)} e^{j\omega t}\, d\omega \qquad (6\text{-}1)$$

which can be expressed in terms of the inphase and quadrature components of the channel pulse response,

$$r(t) = \frac{1}{2\pi} \int_{-\infty}^{\infty} P(\omega)B(\omega)\, \cos\{\omega t - \psi(\omega)\}\, d\omega \qquad (6\text{-}2)$$

$$q(t) = \frac{1}{2\pi} \int_{-\infty}^{\infty} P(\omega)B(\omega)\, \sin\{\omega t - \psi(\omega)\}\, d\omega \qquad (6\text{-}3)$$

where $P(\omega)$ is the Fourier transform of the real-valued, undistorted transmitted signaling waveform shown in Figure 2.5. $B(\omega)$ and $\psi(\omega)$ are the distortion polynomials, as previously defined,

$$B(\omega) = 1 + \gamma\omega \qquad (6\text{-}4)$$

$$\psi(\omega) = \beta_2 \omega^2 + \beta_3 \omega^3 \qquad (6\text{-}5)$$

Therefore, (6-2) and (6-3) represent the mathmatical basis for the channel simulator, in which the only unknown variables are the distortion parameters γ, β_2, and β_3. As the system algorithm attempts to minimize the error between

the estimated and simulated pulse responses, only the distortion parameters need to be adjusted.

An upper bound on the performance of the distortion estimation system can be obtained by employing (6-2) and (6-3) along with an 11 point sampling scheme (i. e. sampling at T = -5, -4, ..., 0, 1, ..., 5) as the so called "full accuracy" version of the channel simulator. In this case, the integral expressions for r(t) and q(t) can be evaluated to the full accuracy of any available processor. As the precision provided in the evaluation of (6-2) and (6-3) increases, the time required for the distortion estimation system to provide a useable output increases as well. Therefore, the method of evaluating r(t) and q(t) represent an important hardware consideration in the construction of the distortion estimation system. Since this system may be invisioned as a built-in test component (as opposed to an add-on processor), it may be necessary to approximate r(t) and q(t) to some lesser degree of accuracy in some applications.

Although all research has been conducted with the full accuracy simulator using the Georgia Tech Cyber computer, it is worthwhile to describe a theoretical approach which uses a limited accuracy simulator, since the eventual implementation of the system for estimating channel distortion may require such an approach.

The Limited Accuracy Simulator

The limited accuracy simulator employes a truncated Taylor series approximation of r(t) and q(t). The object is to speed up the operation of the distortion estimation process and reduce the cost of its hardware implementation at the cost of sacrificed accuracy.

In the absence of any distortion within the channel, the inphase component of the channel pulse response can be defined as,

$$r(t) = \frac{1}{\pi} \int_{-\infty}^{\infty} P(u) \cos(ut) \, du = r_o(t) \qquad (6-6)$$

that is, $r_o(t)$ represents the special case,

$$B(u) = 1 \qquad (6-7)$$

$$\psi(u) = 0 \qquad (6-8)$$

where "u" is now the frequency variable. If p(t) is assumed to be a real valued signal with even symmetry, it follows that $q_o(t)=0$.

Employing the following trigonometric identities:

$$\sin\{ut - \psi(u)\} = \sin(ut)\cos\psi(u) - \cos(ut)\sin\psi(u) \qquad (6\text{-}9)$$

$$\cos\{ut - \psi(u)\} = \cos(ut)\cos\psi(u) + \sin(ut)\sin\psi(u) \qquad (6\text{-}10)$$

(6-2) and (6-3) can be expressed as,

$$r(t) = \frac{1}{\pi}\int_{-\infty}^{\infty} P(u)\{B(u)\cos\psi(u)\}\cos(ut)du$$

$$+ \frac{1}{\pi}\int_{-\infty}^{\infty} P(u)\{B(u)\sin\psi(u)\}\sin(ut)du \qquad (6\text{-}11)$$

$$q(t) = \frac{-1}{\pi}\int_{-\infty}^{\infty} P(u)\{B(u)\cos\psi(u)\}\sin(ut)du$$

$$+ \frac{1}{\pi}\int_{-\infty}^{\infty} P(u)\{B(u)\sin\psi(u)\}\cos(ut)du \qquad (6\text{-}12)$$

where the terms in brackets are distortion terms. Now it is convenient to express the distortion components in polynomial form to facilitate later calculations. Therefore, the Taylor series for the elementary forms above is,

$$\cos\psi(u) = \sum_{n=0}^{\infty} \frac{(-1)^n \, \psi(u)^{2n}}{(2n)!} \qquad (6\text{-}13)$$

$$\sin\psi(u) = \sum_{n=0}^{\infty} \frac{(-1)^n \, \psi(u)^{2n+1}}{(2n+1)!} \qquad (6\text{-}14)$$

Now the distortion terms present in (6-11) and (6-12) can be defined as,

$$\zeta(u) = B(u) \sum_{n=0}^{\infty} \frac{(-1)^n \psi(u)^{2n}}{(2n)!} \qquad (6-15)$$

$$\eta(u) = B(u) \sum_{n=0}^{\infty} \frac{(-1)^n \psi(u)^{2n+1}}{(2n+1)!} \qquad (6-16)$$

where $\zeta(u)$ and $\eta(u)$ are polynomials in the frequency variable, with γ, β_2, and β_3 as coefficients. The inphase and quadrature signals are, therefore,

$$r(t) = \frac{1}{\pi} \int_{-\infty}^{\infty} P(u)\zeta(u)\cos(ut)du + \frac{1}{\pi} \int_{-\infty}^{\infty} P(u)\eta(u)\sin(ut)du \qquad (6-17)$$

$$q(t) = \frac{-1}{\pi} \int_{-\infty}^{\infty} P(u)\zeta(u)\sin(ut)du + \frac{1}{\pi} \int_{-\infty}^{\infty} P(u)\eta(u)\cos(ut)du \qquad (6-18)$$

By considering progressively higher orders of the derivative of $r_o(t)$, the generalized result is,

$$r_o^{(n)}(t) = \frac{1}{\pi} \int_{-\infty}^{\infty} (-1)^{n/2} u^n P(u)\cos(ut)du, \quad \text{(for n even)} \qquad (6-19)$$

$$\overset{(n)}{r_o}(t) = \frac{1}{\pi} \int_{-\infty}^{\infty} (-1)^{n/2} u^n P(u) \sin(ut) du, \quad (\text{for } n \text{ odd}) \qquad (6\text{-}20)$$

where $\overset{(n)}{r_o}(t) = d^n r_o(t)/dt$. Since $\zeta(u)$ and $\eta(u)$ are polynomials, (6-17) and (6-18) can be expanded into a polynomial which includes integrals of progressively higher orders of the frequency variable:

$$
\begin{aligned}
r(t) = \frac{1}{\pi} \sum_n \frac{(-1)^n}{(2n)!} \int_{-\infty}^{\infty} P(u)B(u)\, \psi(u)^{2n} \cos(ut) du \\
+ \frac{1}{\pi} \sum_n \frac{(-1)^n}{(2n+1)!} \int_{-\infty}^{\infty} P(u)B(u)\, \psi(u)^{2n+1} \sin(ut) du \qquad (6\text{-}21)
\end{aligned}
$$

with a similar expression for $q(t)$. Note that the product $B(u)\,\psi(u)$ is itself a polynomial. By expanding this polynomial, (6-19) and (6-20) can be used to eliminate all integral expressions. Therefore, the final result is an expression for the inphase and quadrature signal components in terms of higher orders of the derivative of the undistorted pulse $r_o(t)$:

$$
\begin{aligned}
r(t) = \sum_{m=0}^{M} \sum_{n=0}^{N} \frac{(-1)^n}{(2n)!\,(m!)} \beta_2^{2n} \beta_3^{m} \overset{(4n+3m)}{r_o}(t) \\
+ \sum_{m=0}^{M} \sum_{n=1}^{N} \frac{(-1)^{n+1}}{(2n-1)!\,(m!)} \gamma\beta_2^{2n-1} \beta_3^{m} \overset{(4n+3m-1)}{r_o}(t) \qquad (6\text{-}22)
\end{aligned}
$$

$$q(t) = \sum_{m=0}^{M} \sum_{n=1}^{N} \frac{(-1)^n}{(2n-1)!(m!)} \beta_2^{2n-1} \, \beta_3^m \, r_o^{(4n+3m-2)}(t)$$

$$+ \sum_{m=0}^{M} \sum_{n=0}^{N} \frac{(-1)^{n+1}}{(2n)!(m!)} \gamma \beta_2^{2n} \, \beta_3^m \, r_o^{(4n+3m+1)}(t) \qquad (6\text{-}23)$$

where the only unknown quantities are γ, β_2 and β_3 ; and both M and N must be equal to infinity in order for (6-22) and (6-23) to be equivalent to (6-11) and (6-12). Obviously, the number of terms used in any computation must be finite. Therefore, an important consideration in the implementation of this approach is to determine M and N so that sufficiently accurate results can be obtained.

Although it is beyond the scope of the present research to evaluate the accuracy of (6-22) and (6-23), preliminary indications are that M and N need be no larger than 2 to accurately describe a received signal that has been subjected to typical levels of channel distortion.

The System Algorithm

The system algorithm is a multidimensional optimization processor which seeks to minimize the difference between the estimated channel pulse response and the simulated channel pulse response (reference Figure 4.2). The analytical expressions for the channel pulse response given by (6-2) and (6-3) are employed in a recursive scheme to determine γ, β_2, and β_3. This is accomplished by first estimating the channel pulse response at the desired

sampling instants as described in the previous chapter. The next step is to formulate some "objective" function to be minimized. The objective function (also called the error function) is normally a unimodal function of the variables which are to be optimized. One of the most common objective functions is the sum of the squares of the difference between the solution having present parameter values, and the desired solution. Therefore, the objective, or error, function to be minimized is,

$$E = \sum_{k=-N}^{N} \left\{ \left[\widetilde{r}(kT) - \widehat{r}(kT) \right]^2 + \left[\widetilde{q}(kT) - \widehat{q}(kT) \right]^2 \right\} \qquad (6\text{-}24)$$

where $2N+1$ is the number of sample points at which the simulated pulse response will attempt to match the estimated pulse response. Now define the error components of (6-24) to be,

$$\epsilon_{r,k} = \widetilde{r}(kT) - \widehat{r}(kT) \qquad (6\text{-}25)$$

$$\epsilon_{q,k} = \widetilde{q}(kT) - \widehat{q}(kT) \qquad (6\text{-}26)$$

so that,

$$E = \sum_{k=-N}^{N} \left\{ \epsilon_{r,k}^2 + \epsilon_{q,k}^2 \right\} \qquad (6\text{-}27)$$

Since E represents a unimodal function in the γ, β_2, β_3 parameter space, the solution is formed by taking the gradient of E with respect to each distortion parameter and setting the result equal to zero:

$$\nabla E = \begin{bmatrix} \dfrac{\delta E}{\delta \gamma} \\[2ex] \dfrac{\delta E}{\delta \beta_2} \\[2ex] \dfrac{\delta E}{\delta \beta_3} \end{bmatrix} = \begin{bmatrix} 2 \displaystyle\sum_{k=0}^{N} \epsilon_{r,k} \dfrac{\delta \epsilon_{r,k}}{\delta \gamma} + \epsilon_{q,k} \dfrac{\delta \epsilon_{q,k}}{\delta \gamma} \\[2ex] 2 \displaystyle\sum_{k=0}^{N} \epsilon_{r,k} \dfrac{\delta \epsilon_{r,k}}{\delta \beta_2} + \epsilon_{q,k} \dfrac{\delta \epsilon_{q,k}}{\delta \beta_2} \\[2ex] 2 \displaystyle\sum_{k=0}^{N} \epsilon_{r,k} \dfrac{\delta \epsilon_{r,k}}{\delta \beta_3} + \epsilon_{q,k} \dfrac{\delta \epsilon_{q,k}}{\delta \beta_3} \end{bmatrix} \qquad (6\text{-}28)$$

The matrix on the right can be expressed as the sum of two Jacobian matrices. The Jacobian is defined in this case as,

$$J(\gamma, \beta_2, \beta_3) = \begin{bmatrix} \dfrac{\delta \epsilon_{-N}}{\gamma} & \dfrac{\delta \epsilon_{-N}}{\delta \beta_2} & \dfrac{\delta \epsilon_{-N}}{\delta \beta_3} \\[2ex] \dfrac{\delta \epsilon_{-N+1}}{\delta \gamma} & \dfrac{\delta \epsilon_{-N+1}}{\delta \beta_2} & \dfrac{\delta \epsilon_{-N+1}}{\delta \beta_3} \\[1ex] \vdots & \vdots & \vdots \\[1ex] \dfrac{\delta \epsilon_{N}}{\delta \gamma} & \dfrac{\delta \epsilon_{N}}{\delta \beta_2} & \dfrac{\delta \epsilon_{N}}{\delta \beta_3} \end{bmatrix} \qquad (6\text{-}29)$$

Therefore, (6-28) becomes,

$$\nabla E = 2\left\{ \underline{J}_r^T \underline{\epsilon}_r + \underline{J}_q^T \underline{\epsilon}_q \right\} \tag{6-30}$$

Where $\underline{J}_r$ and $\underline{J}_q$ are Jacobian matrices for the inphase and quadrature error components, respectively; and $\underline{\epsilon}_r$, $\underline{\epsilon}_q$ are the vectors which contain the individual errors, $\epsilon_{r,k}$, $\epsilon_{q,k}$. To simplify notation, (6-30) can be further generalized to the following expression:

$$\nabla E = 2 \, \underline{J}^T \underline{\epsilon} \tag{6-31}$$

where,

$$\underline{\epsilon} = \begin{bmatrix} \epsilon_r \\ \epsilon_q \end{bmatrix} \tag{6-32}$$

$$\underline{J} = \begin{bmatrix} \underline{J}_r^T \\ \underline{J}_q^T \end{bmatrix} \tag{6-33}$$

and by allowing $\underline{x}$ to represent a vector containing the distortion components,

$$\underline{x} = \begin{bmatrix} \gamma \\ \beta_2 \\ \beta_3 \end{bmatrix} \qquad (6\text{-}34)$$

then (6-31) becomes,

$$\nabla E(\underline{x}) = 2\underline{J}^T(\underline{x}) \, \in(\underline{x}) \qquad (6\text{-}35)$$

Now (6-35) can be used to obtain a change, $\delta\underline{x}$, such that the magnitude can be reduced in some systematic iterative fashion. The increment, $\delta\underline{x}$, can be incorporated into (6-35) as follows,

$$\nabla E(\underline{x} + \delta\underline{x}) = 2\underline{J}^T(\underline{x} + \delta\underline{x}) \, \in(\underline{x} + \delta\underline{x}) \qquad (6\text{-}36)$$

It often happens that the Jacobian does not vary much as the parameters are changed. Even if this is not true at the start of an iterative search for the minimum, it will be true as the minimum is approached [56]. Thus the approximation,

$$\nabla E(\underline{x} + \delta \underline{x}) \approx 2\underline{J}^{\mathsf{T}}(\underline{x}) \in (\underline{x} + \delta \underline{x}) \qquad (6\text{-}37)$$

In order to choose the parameter change, $\delta \underline{x}$, so that the gradient becomes zero, an approximation for $\in (\underline{x} + \delta \underline{x})$ must be found. Expanding this function in a Taylor series and retaining the first order terms yields,

$$\in (\underline{x} + \delta \underline{x}) \approx \in (\underline{x}) + \sum_{k=-N}^{N} \frac{\delta \in (\underline{x})}{\delta x_k} \delta x_k \qquad (6\text{-}38)$$

where $x_1 = \gamma$, $x_2 = \beta_2$, $x_3 = \beta_3$. Employing the Jacobian once again yields,

$$\in (\underline{x} + \delta \underline{x}) \approx \in (\underline{x}) + \underline{J}(\underline{x}) \delta \underline{x} \qquad (6\text{-}39)$$

This approximation can be used to estimate the parameter changes $\delta \underline{x}$ that will produce a zero gradient at $\underline{x} + \delta \underline{x}$. Substituting (6-39) into (6-36) yields,

$$\underline{J}^{\mathsf{T}}\underline{J} \, \delta \underline{x} \approx -\underline{J}^{\mathsf{T}} \in (\underline{x}) \qquad (6\text{-}40)$$

Therefore, the following algorithm can be used to minimize the least squared error:

$$\underline{x}_n = \underline{x}_{n-1} + \delta \underline{x}_n \qquad (6\text{-}41)$$

$$\delta \underline{x}_n = -(\underline{J}^T \underline{J})^{-1} \underline{J}^T \in (\underline{x}_n) \qquad (6\text{-}42)$$

Unfortunately, the inversion of the Jacobian matrix is a costly procedure which should be avoided. This can be done by resorting to an approximation of the function $\delta \underline{x}$ in (6-42). By using the straightforward steepest descent optimization technique defined by (6-41), $\delta \underline{x}$ need only be proportional to the negative gradient of the objective function [57], such as,

$$\delta \underline{x} = -\alpha \underline{J}(\underline{x}) \qquad (6\text{-}43)$$

where α is a positive constant that controls the convergence characteristics of the steepest-descent technique. If α is small, convergence is slow and expensive. However, a large α may jump $\underline{x}$ beyond the minimum error function [58]. The approach chosen is to make α variable upon each iteration of (6-41). Therefore, if

$$E_n(\underline{x}) < E_{n-1}(\underline{x}) \qquad (6\text{-}44)$$

then α is increased by a factor of 2 for the next iteration. When α is too large, so that $E(\underline{x})$ is not decreasing as desired, α is decreased by a factor of 0.1, and the iteration continues. The algorithm is terminated when the error function is sufficiently close to some minimum value, δ_{min}.

The overall system algorithm is shown iin Figure 6.1. The system algorithm incorporates the optimization features just described to determine the values of amplitude and group delay distortion present in the estimated channel pulse response. The behavior of the algorithm and the accuracy of the overall operation will be further discussed in the following chapter.
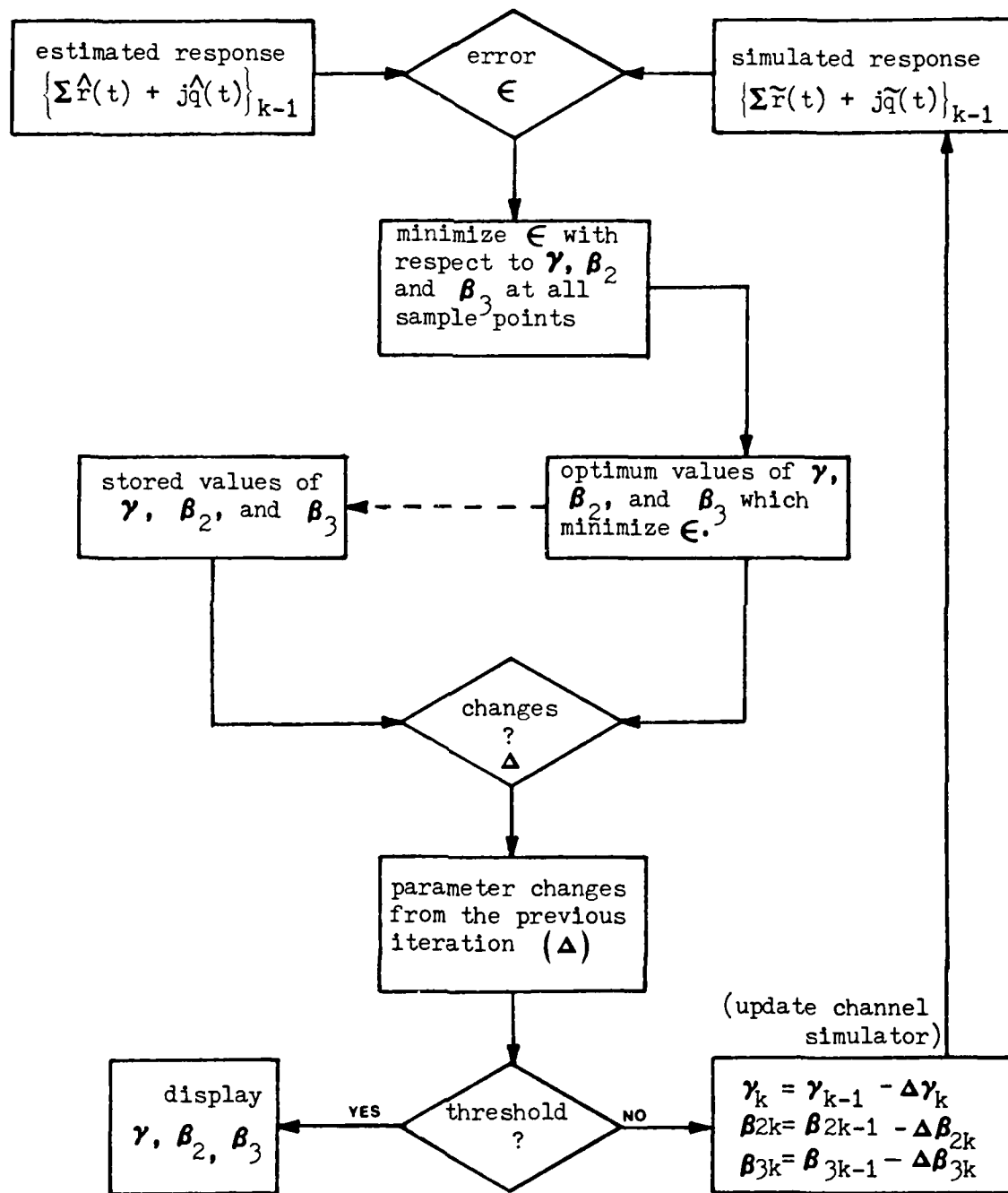
Figure 6.1 - System Algorithm for the Distortion Estimator

CHAPTER VII

EXPERIMENTAL RESULTS

Introduction

Verifying the expected performance of the system for estimating channel distortion is one of the most important aspects of the research. This chapter describes that performance by examining the behavior of each of the subsystems of the distortion estimation process under a variety of noise levels and transmission distortion values. Error analyses are then performed on each critical phase of the process. Results are generally presented in a graphical format which serves to provide insight into the expected performance of the system in a realistic operating environment.

Before the performance of each subsystem is considered in detail, the process of simulating the digital communication system is discussed and several important simulation tools are presented. The importance of the simulation cannot be overemphasized. Since the distortion estimation technique has only been evaluated with simulated data, it is crucial that the simulation process represent realistic conditions as closely as possible. Therefore, two independent simulations are employed in the research:

(1) An analytical, or numerical simulation was developed for the specific purpose of evaluating the distortion estimation process on the Georgia Tech CYBER computer.

(2) The Interactive Communications Simulator (ICS), an Air Force owned and operated system for performing research on digital communication systems, was used to independently verify the results of the local numerical simulation.

To this point, all discussions of the communication system have referenced a generalized MPSK system. Henceforth, all simulations will employ a QPSK system. The QPSK system is chosen primarily for its simplicity in that its inphase and quadrature information signals are binary. This allows a nearly independent treatment of the components of the complex baseband signal, since they resemble two independent BPSK signals. All simulation procedures can be directly extended to the M-level case, however.

The Simulation Process

Analytic Simulation

The primary reason for studying data transmission by simulation is the flexibility it affords in allowing a controlled investigation of a wide range of conditions that may occur in actual practice. Known values of transmission distortion can be inserted into the channel, and

105

measurements can be made to determine the system's effectiveness in estimating the type of distortion and its severity. Furthermore, Gaussian noise can be added to the channel so that system performance can be measured with a specified signal to noise ratio.

Unfortunately, the analytic approach requires a number of simplifying assumptions which may, under certain conditions, lead to misleading results. One crucial simplifying assumption is ideal carrier phase recovery and symbol timing. Realistic simulation of the errors caused by these factors can be quite complex, and therefore are avoided in the present research. They represent an area of study that would be more appropriately conducted before a hardware implementation of the distortion estimation process is accomplished.

The simulation attempts to duplicate mathmatically the action of the real system in operating on a signaling waveform. Figure 7.1 presents the entire simulation system in block diagram form. The operation of the transmission facility and propagation medium on each signaling pulse is simulated entirely in the time domain. Other popular simulation techniques described in the literature employ simulation in the frequency domain [22,34,59]. However, since the object of the research is to describe the operation of a time-domain system for estimating transmission distortion, a complete time domain simulation

106
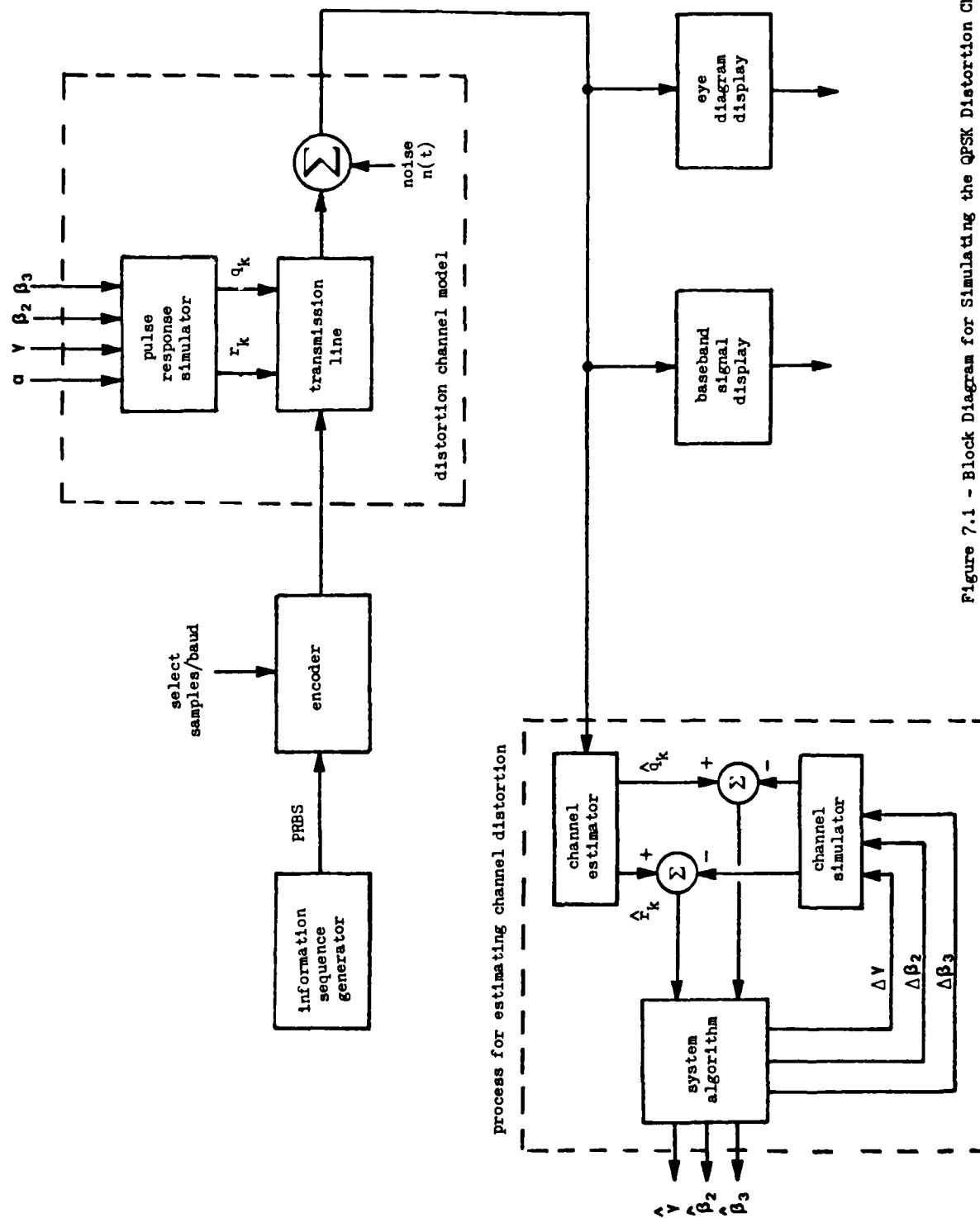
Figure 7.1 - Block Diagram for Simulating the QPSK Distortion Channel

was found to be more suitable. To accomplish the time
domain simulation throughout the system, each pulse is
defined by a sequence of sample values at a succession of
evenly spaced time points. The number of sample values per
baud can be selected to suit the requirements of a
particular simulation. To simulate the baseband output of
the receiver sampler, only one sample per baud is required
throughout the system. However, if graphical outputs are
required, multiple samples per baud are neccessary. The
graphical outputs take further advantage of the time domain
simulation by allowing the system designer a realistic look
at the signaling waveform at various points in the system.

The information sequence is generated as a
pseudorandom binary sequence (PRBS). The PRBS generator is
implemented in software as a seven stage maximal length
shift register with appropriate feedback taps to generate a
127 bit pseudorandom sequence [60]. The PRBS generator and
its resulting output autocorrelation function are shown in
Figure 7.2.

The encoder does nothing more than convert the PRBS
information sequence at R symbols/sec to two bit streams at
R/2 symbols/sec. At this point, the quadrature components
of the complex information sequence are input to the channel
distortion model. The channel distortion model allows user
selection of the type of signaling pulse to be employed
(i. e. raised cosine with selectable rolloff factor, α) as
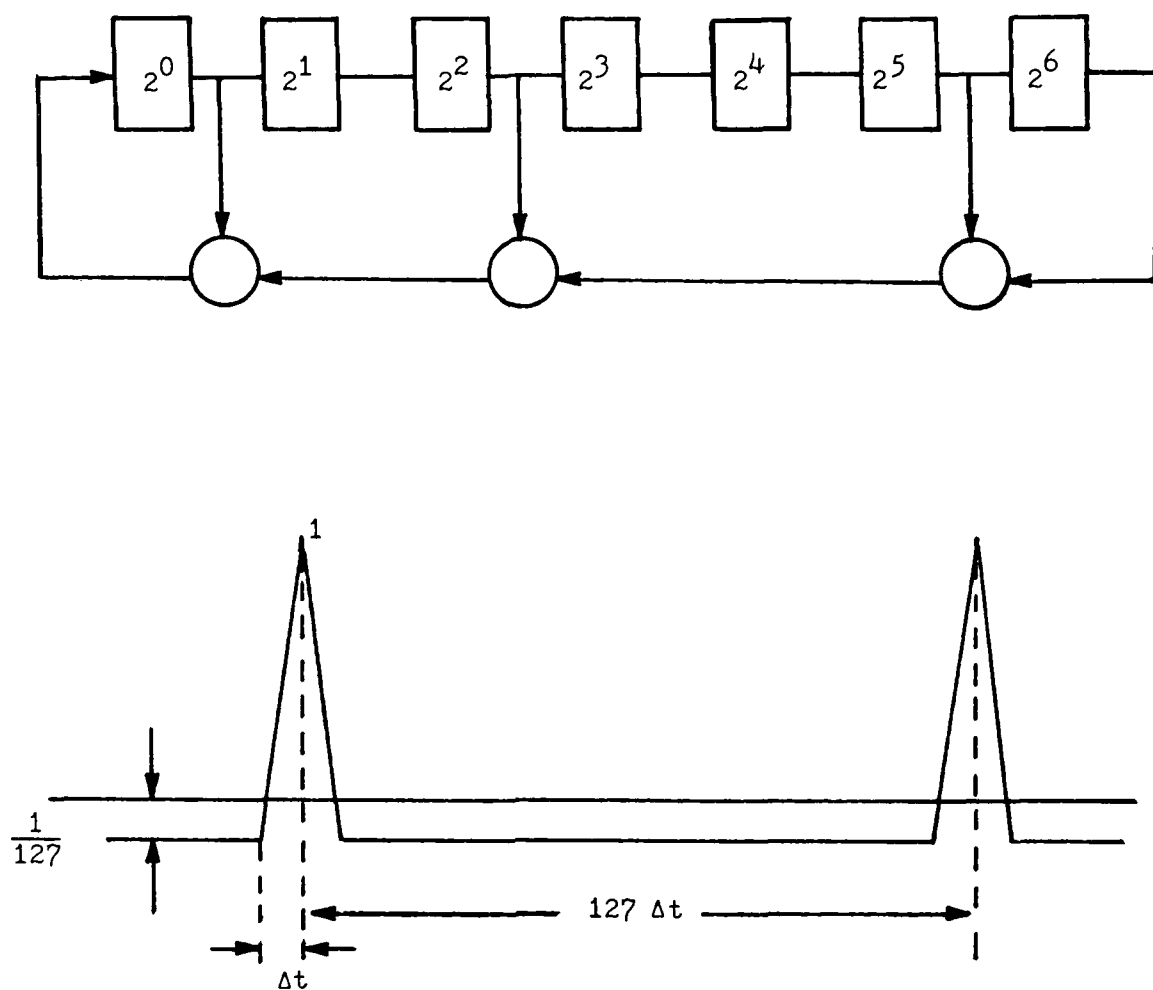
Figure 7.2 - The PRBS Information Sequence Generator
and its Autocorrelation Function

well as the type and amount of channel transmission distortion, and selection of the amount of additive noise. The transmission line is actually the lowpass complex discrete-channel model illustrated in Figure 3.5. The purpose of the pulse response simulator is to select the values of the inphase and quadrature tap gains, r_k and q_k, by converting frequency-domain specifications of both the channel pulse response and the channel transmission distortion to time-domain samples. The method by which this is accomplished is described below.

The inphase and quadrature components of the baseband channel pulse response were described by (3-3) and (3-4) in which $P(\omega)$ is the spectrum of the raised cosine pulse (as previously illustrated in Figure 2.5), which is

$$P(\omega) = \begin{cases} \dfrac{\pi}{2\Omega} \, , & |\omega| \leq \Omega(1 - a) \\[2em] \dfrac{\pi}{2\Omega}\cos^2\left\{\dfrac{\pi\omega}{4a\Omega} - \dfrac{(1 - a)}{4a}\right\} \, , & \Omega(1 - a) \leq |\omega| \leq \Omega(1 - a) \\[2em] 0, & \text{otherwise} \end{cases} \qquad (7\text{-}1)$$

where the baud interval is $T = \pi/\Omega$. By employing a change of variables in (3-3) and (3-4) with $x = \pi\omega/4\Omega$, the following forms result:

$$r(t) = \frac{2}{\pi} \int_{-\pi(1-\alpha)/4}^{\pi(1-\alpha)/4} B\left(\frac{4x}{T}\right) \cos\left[\left(\frac{4t}{T}\right)x - \psi''\left(\frac{4x}{T}\right)\right] dx$$

$$+ \frac{2}{\pi} \int_{\pi(1-\alpha)/4}^{\pi(1+\alpha)/4} \cos^2\left\{\frac{x}{\alpha} - \frac{\pi(1-\alpha)}{4\alpha}\right\} \left[B\left(\frac{4x}{T}\right)\cos\left\{\frac{4tx}{T} - \psi\left(\frac{4x}{T}\right)\right\}\right.$$

$$\left. + B\left(\frac{-4x}{T}\right)\cos\left\{\frac{4tx}{T} - \psi\left(\frac{-4x}{T}\right)\right\}\right] dx \qquad (7\text{-}2)$$

$$q(t) = \frac{2}{\pi} \int_{-\pi(1-\alpha)/4}^{\pi(1-\alpha)/4} B\left(\frac{4x}{T}\right) \sin\left[\left(\frac{4t}{T}\right)x - \psi\left(\frac{4x}{T}\right)\right] dx$$

$$+ \frac{2}{\pi} \int_{\pi(1-\alpha)/4}^{\pi(1+\alpha)/4} \cos^2\left\{\frac{x}{\alpha} - \frac{\pi(1-\alpha)}{4\alpha}\right\} \left[B\left(\frac{4x}{T}\right)\sin\left\{\frac{4tx}{T} - \psi\left(\frac{4x}{T}\right)\right\}\right.$$

$$\left. - B\left(\frac{-4x}{T}\right)\sin\left\{\frac{4tx}{T} - \psi\left(\frac{-4x}{T}\right)\right\}\right] dx \qquad (7\text{-}3)$$

The amplitude and phase distortion become

$$B\left(\frac{4x}{T}\right) = 1 + \frac{\gamma 4x}{T} = 1 + \gamma' x \qquad (7\text{-}4)$$

$$\psi\left(\frac{4x}{T}\right) = \beta_2\left(\frac{4x}{T}\right)^2 + \beta_3\left(\frac{4x}{T}\right)^3 \qquad (7\text{-}5)$$

$$= \beta_2' x^2 + \beta_3' x^3 \qquad (7\text{-}6)$$

Therefore, to initialize the channel distortion model, the

frequency-domain variables γ, β_2 and β_3 are selected. The resultant time-domain channel pulse response is set into the transmission line. As a convenience in notation and for discussion, the phase distortion parameters and the time variable are specified in terms of normalized time units with respect to a single baud interval. Therefore if, for example, $\beta_3 = 2.0$ baud intervals, then this can be interpreted as 208.3 microseconds of quadratic group delay distortion on a 9600 baud data signal or 41.67 microseconds of quadratic group delay distortion on a 48 Kilobaud data signal.

At the output of the transmission line, Gaussian noise is added to the signal to simulate any desired signal to noise ratio. At the ouput of the channel distortion model, the signal represents the received complex baseband signal sampled at some specified evenly spaced number of times per baud. At this point, the signal can be viewed in either of two formats:

(1) The baseband signal can be viewed graphically in its exact time-domain form. Any portion of the received waveform can be viewed at any scale factor. An example of the baseband signal appearing at the output of the channel simulator is shown in Figure 7.3. In Figure 7.3a, no distortion is present and the signaling waveform is a full raised cosine with $\alpha = 1.0$. The same waveform then experiences 2.5 baud intervals of quadratic group delay

112
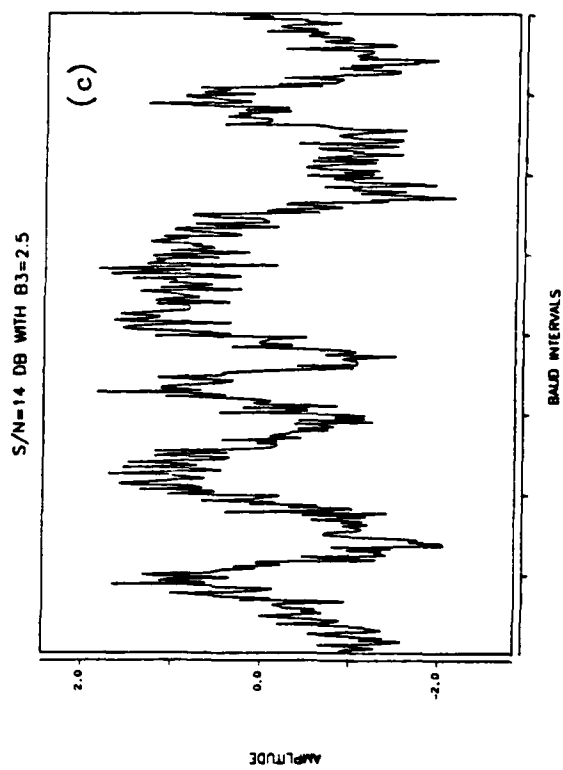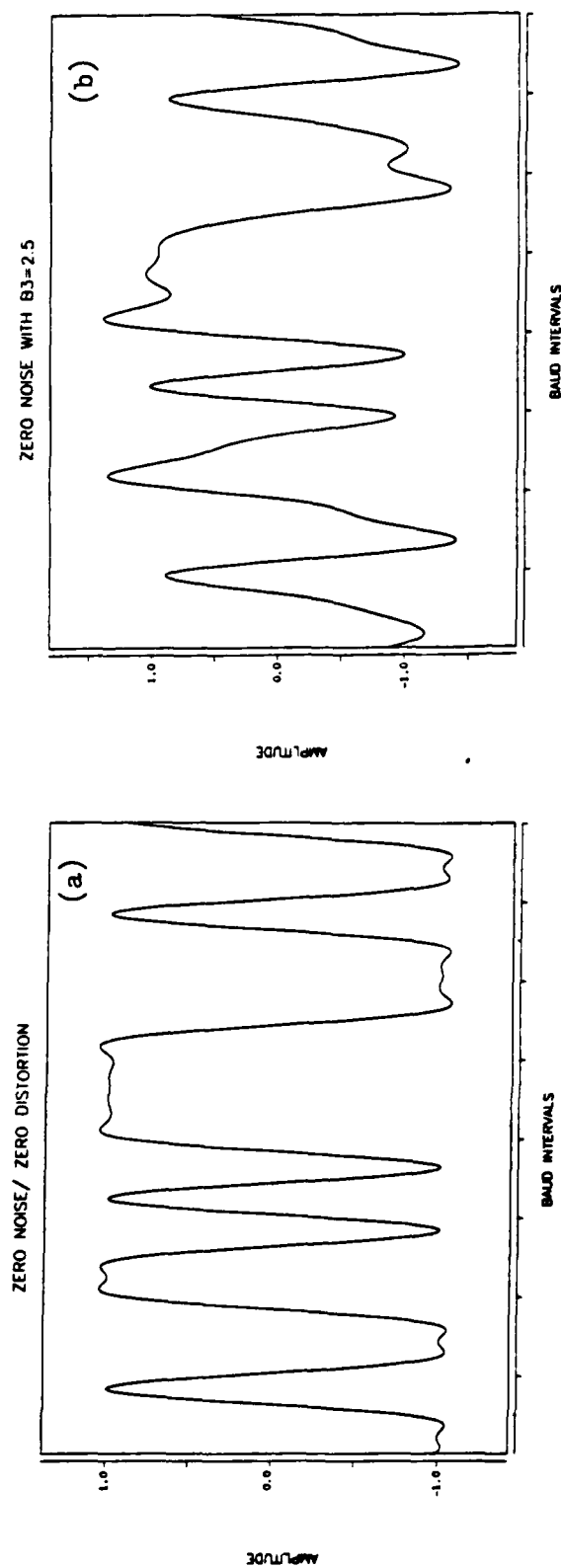
Figure 7.3 – Baseband Output of the Distortion Channel Model with (a) Zero Distortion, (b) Quadratic Dealy Distortion, and (c) Quadratic Delay Distortion with Noise

distortion (Figure 7.3b), and finally, noise is added so that the signal-to-noise ratio is 13 dB (Figure 7.3c).

(2) The baseband signal can be viewed graphically as an eye diagram. This is a particularly useful tool for assessing the degradation in expected·system performance for specif,c types of transmission distortion. The ratio of the eye aperture under distortion conditions to the aperture under ideal transmission conditions has been established as a useful criterion for measuring transmission quality [41,59]. Several examples of the eye diagram output are shown in Figure 7.4. It can be seen from Figure 7.4b that the presence of delay distortion results in a closing of the aperture.

By using the aperture of the eye diagram as a criterion, it is easy to determine the maximum allowable ampitude and delay distortion parameters. The degradataion in the eye opening versus delay distortion in baud intervals is shown in Figure 7.5a and 7.5c. A similar illustration for amplitude distortion is shown in Figure 7.5b. Obviously, $\gamma = 1.0$ is the maximum physically realizable limit for the amplitude distorion parameter. Therefore, the maximum tolerable amplitude distortion is not limited by signal degradation, but rather by physical considerations. These graphs were computed based upon a noiseless baseband signal with a pseudorandom periodic length of 127 bits.

The same baseband signal that can be viewed in the

114
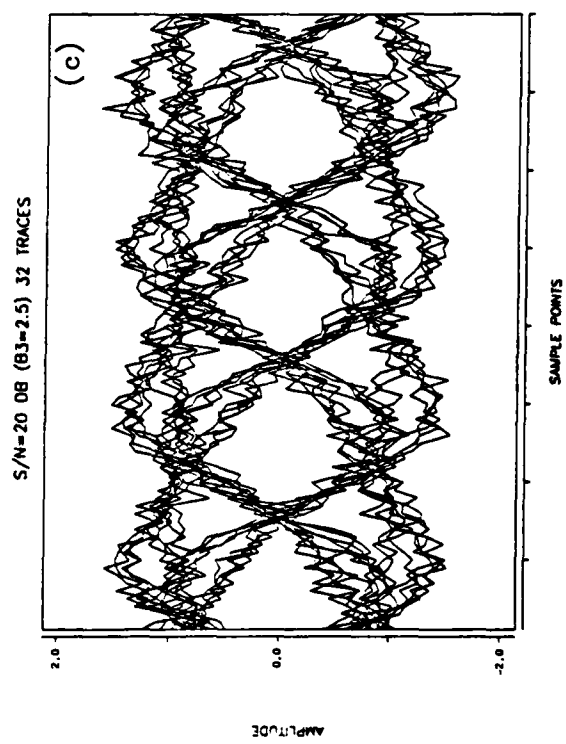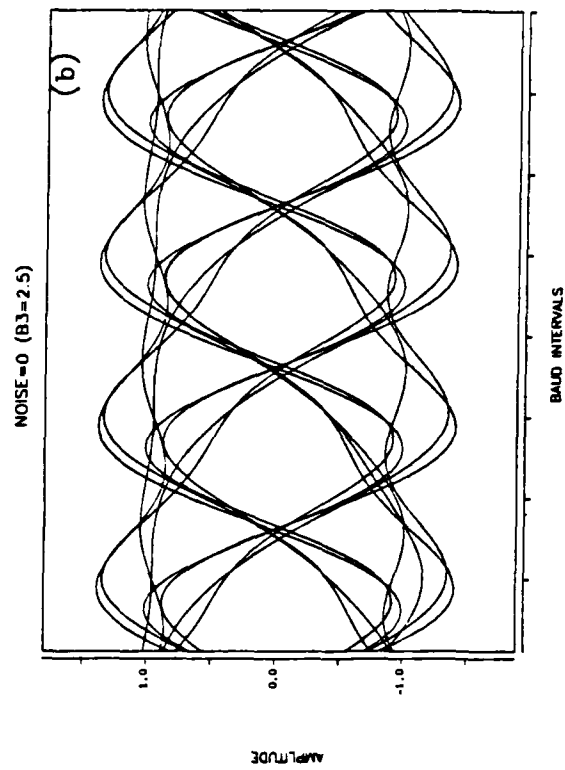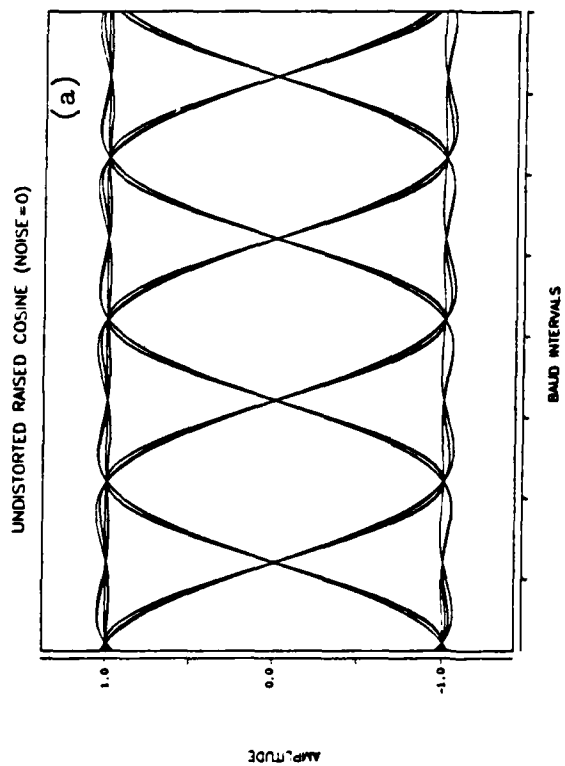
Figure 7.4 - Eye Diagram Output of the Distortion Channel Model with (a) Zero Distortion, (b) Quadratic Delay Distortion, and (c) Quadratic Delay Distortion with Noise
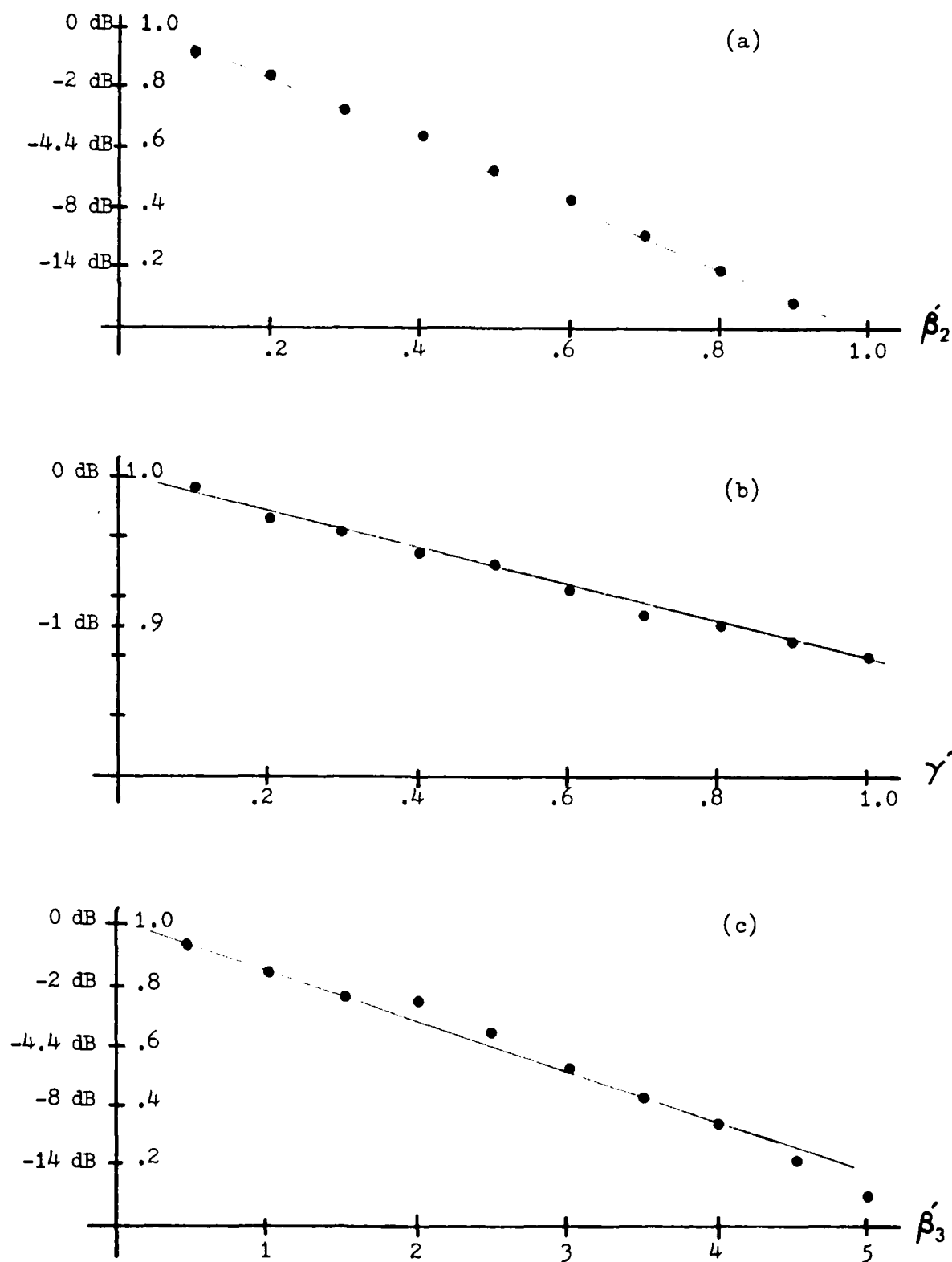
Figure 7.5 - Degradation in Eye Aperture due to Linear Distortion

time domain is input to the processor for estimating the channel transmission distortion. This processor first extracts the channel pulse response from the baseband signal sequence, and then estimates the type and amount of amplitude and group delay distortion present in the pulse response, as described in previous chapters. The performance of each of the components that make up the distortion estimation process are examined in the sections that follow.

The Interactive Communications Simulator

The Interactive Communications Simulator (ICS) is a modeling and simulation tool for the development and evaluation of advanced digital communication signal processing techniques [61,62]. The ICS modeling structure allows the user access to the various signal processing functions and environments in a typical digital communication link, i. e. source and link, source encoding and decoding, channel encoding and decoding, modulation and demodulation, transmitter and receiver, and propagation channel, as shown in Figure 7.6.

The ICS was designed for the U.S. Air Force at the Rome Air Development Center, Griffiss AFB, New York, by the Electrical and Systems Engineering Department at Rensselaer Polytechnic Institute. The ICS was designed to be a flexible, graphics oriented interactive hardware/software system consisting of a minicomputer acting as host to a fast
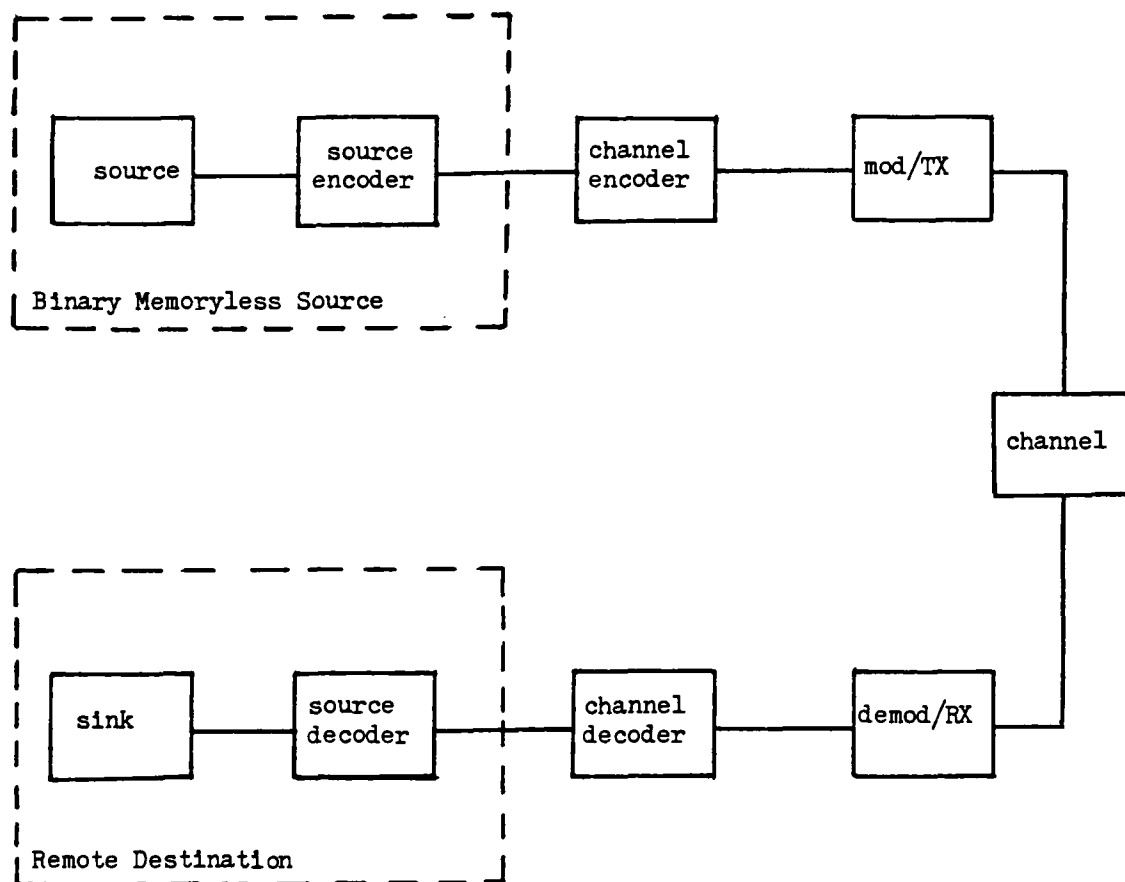
Figure 7.6 - Block Diagram of the Interactive Communications Simulator

peripheral array processor. It is currently resident at three locations:

(1) The system at RPI is being used both as a testbed for the development of improvements to the ICS and as a research tool for the Institute.

(2) The system at RADC is installed in the Digital Communications Experimental Facility, and is being employed to evaluate existing modem performance and to explore new modulation and coding concepts appropriate for military, commercial, and space applications.

(3) The system at the U.S. Air Force Academy is used primarily as a teaching and research tool. Currently, it is being used to evaluate several new on-line performance monitoring techniques, including the approach outlined in the present research.

Using the ICS, a wide variety of arbitrary point-to-point digital communication systems can be simulated from the basic modules shown in Figure 7.6. These modules include modems for a number of modulation stategies, receiver front end filtering, and various bit synchronization and phase tracking algorithms. In addition to additive white Gaussian noise channels, the simulator includes the ability to model impulsive noise channels as well as fading dispersive channels typical of HF or tropospheric scatter channels.

The simulation employed for the present research was

conducted at RADC during August-September 1983 and at the U.S. Air Force Academy during February 1984. In order for the simulation to be performed, it was necessary to modify the ICS so that the user could insert the desired amount and type of amplitude or group delay distortion into the channel. This modification was performed on the ICS resident at the Air Force Academy. It was decided that the easiest way to implement the required capability was to actually build the complex lowpass channel filter shown in Figure 3.5 into the transmitter module. In this manner, the discrete complex channel pulse response can be completely specified by the user. Since it is the pulse response that is user specified and not some predefined distortion parameter, the ICS retains the flexibility to investigate higher order distortion parameters and different signaling pulse shapes. All that needs to be known is the complex channel pulse response. Furthermore, by inserting the filter at the transmitter output, all the normal functions included in the channel module can still be used (i.e. AWGN and multipath fading).

After completing the modification, numerous types and values of amplitude and group delay distortion were inserted into the channel. The baseband data at the input to the receiver matched filter was recorded for each sequence of data containing some specified amount and type of distortion. The distortion estimator algorithm was then

allowed to perform all the essential operations on this data, such as identifying the complex channel pulse response and estimating the distortion parameters. These were then compared to the numerical analysis developed on the Georgia Tech CYBER computer. An extensive comparison based upon numerous samples verified the numerical analysis to be accurate and illustrated identical results when the distortion estimator was used with either system.

The primary usefulness of the ICS therefore was to verify that the local numerical simulation was accurate and appropriate for evaluating the distortion estimator. Since the ICS is not readily available for extensive use in gathering data to evaluate the performance of the distortion estimation process, the error analyses that follow were accomplished, via numerical simulation on the Georgia Tech CYBER computer as described in the previous section.

The Channel Estimator

The complex channel estimator shown in Figure 5.7 was evaluated by transmitting a 127 bit pseudorandom binary sequence through the channel distortion model under a variety of distortion conditions and noise levels. Initially, a comparison was made of the output from the channel estimator, $\hat{r}_k$ and $\hat{q}_k$, with the actual values of the complex channel pulse response, r_k and q_k, present in the distortion channel model. The results of this comparison,

in terms of the percentage of error between the estimated pulse response and the actual pulse response under zero noise conditions, are shown in Figure 7.7. When compared on a percentage basis for increasing levels of distortion, the error remains consistently below 2%; however, a nearly random variation in the error is observed. These variations were found to be highly dependent upon the input information sequence. This is expected, since each adaptive iteration made by the channel estimator is dependent upon five previous and future symbols. Therefore, if the information sequence is changed (by selecting a different PRBS length, for example), the error at any given value of distortion is likely to be different. However, it was found that regardless of the PRBS length selected, all error were consistently in the low percentage range as represented in Figure 7.7.

A more useful parameter for evaluating the performance of the channel estimator is the error signal resulting from comparison between the input baseband signal (x_k and y_k) and the output of the adaptive linear combiner ($\hat{x}_k$ and $\hat{y}_k$). By squaring the error on each adaptive iteration and averaging over a long time period, a useful mean squared error criterion results. It is this criterion that most analyses in the literature attempt to minimize [52,55]. Figure 7.8 shows several examples of the real component of the error signal plotted as a function of the
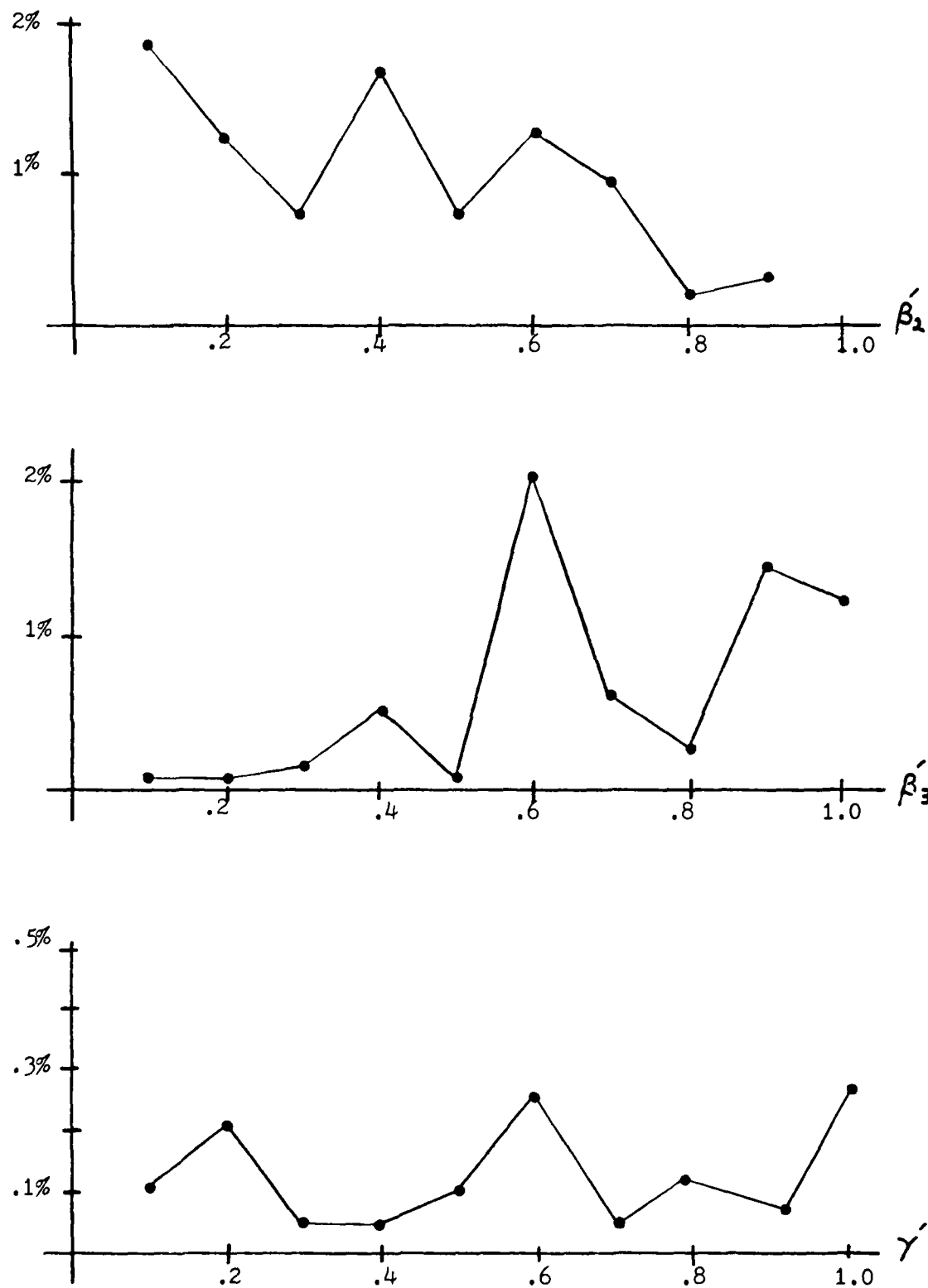
Figure 7.7 - Percent Error in Channel Estimation
under Zero Noise Conditions

number of symbols processed by the channel estimator. The
zero noise condition is illustrated in Figure 7.8a. In this
case, the channel estimator is seen to converge to an
extremely low error within 100 symbols. Figures 7.8b and
7.8c show the same estimation process performed under
increasing signal to noise ratios. It is obvious that the
Gaussian noise, which is added to the baseband signal in the
channel, has a significant effect on the error signal.
However, the adaptive process acts as a low pass filter to
the noise, so that its effect on the estimation process is
greatly minimized. In fact, when the channel estimator is
in its steady state, the process of subtracting the
estimated signal from the baseband signal serves to isolate
the additive Gaussian noise. This is verified by observing
Figure 7.8, where on each plot is indicated the average
error and its variance. The average error is nearly zero
and the variance is closely related to the noise power.

An important consideration in the design of the
channel estimator is the relationship between the speed of
adaptation and performance of the adaptive system. Widrow
[55] thoroughly investigated this problem and determined
that the gradient estimation process introduces noise into
the weight vector that is proportional to the speed of
adaptation and the number of weights. This noise causes a
misadjustment in the weight vector from that of the optimum
case as given in (5-30). The rate of convergence of the

124
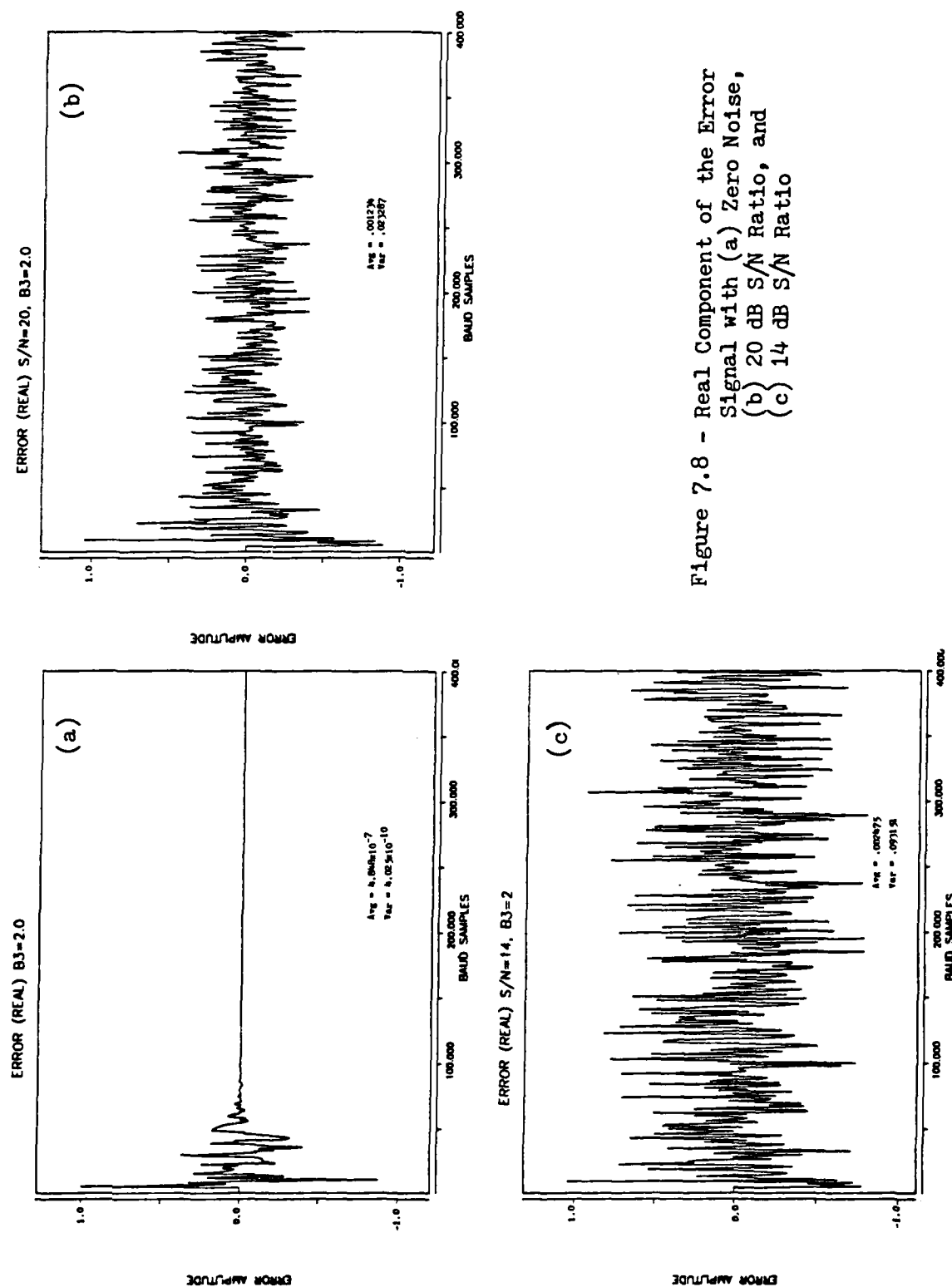
Figure 7.8 – Real Component of the Error Signal with (a) Zero Noise, (b) 20 dB S/N Ratio, and (c) 14 dB S/N Ratio

estimator is determined primarily by the convergence parameter, μ. This parameter scales the error signal which directs the adaptive process. In Figure 7.9 the number of iterative steps required for convergence is shown as a function of the value of μ. The range illustrated does indeed fall within the theoretical constraint given by (5-29). By proper selection of μ, the channel estimator can be made to converge well within 100 iterative steps. The size of the estimator (i. e. the number of taps) also has an important influence upon convergence time, however the tap size for the present situation is constrained by factors discussed in Chapter V.

The effect that the selection of μ has on the mean square error is shown in Figure 7.10. Here it is shown that the value of μ which allows fastest convergence may not be the ideal value for minimizing the mean squared error. In fact, the MSE increases with increasing μ and noise power. Previously, it was noted that under certain conditions the minimum theoretical MSE would be equal to the noise variance. The actual MSE, as shown in Figure 7.10, is a function of the minimum MSE and the misadjustment. The misadjustment factor, given as (5-30) can also be shown [55] to be dependent upon μ:

$$M = \mu \, \mathrm{Tr}\left\{W \; W^*\right\} \qquad (7\text{-}7)$$
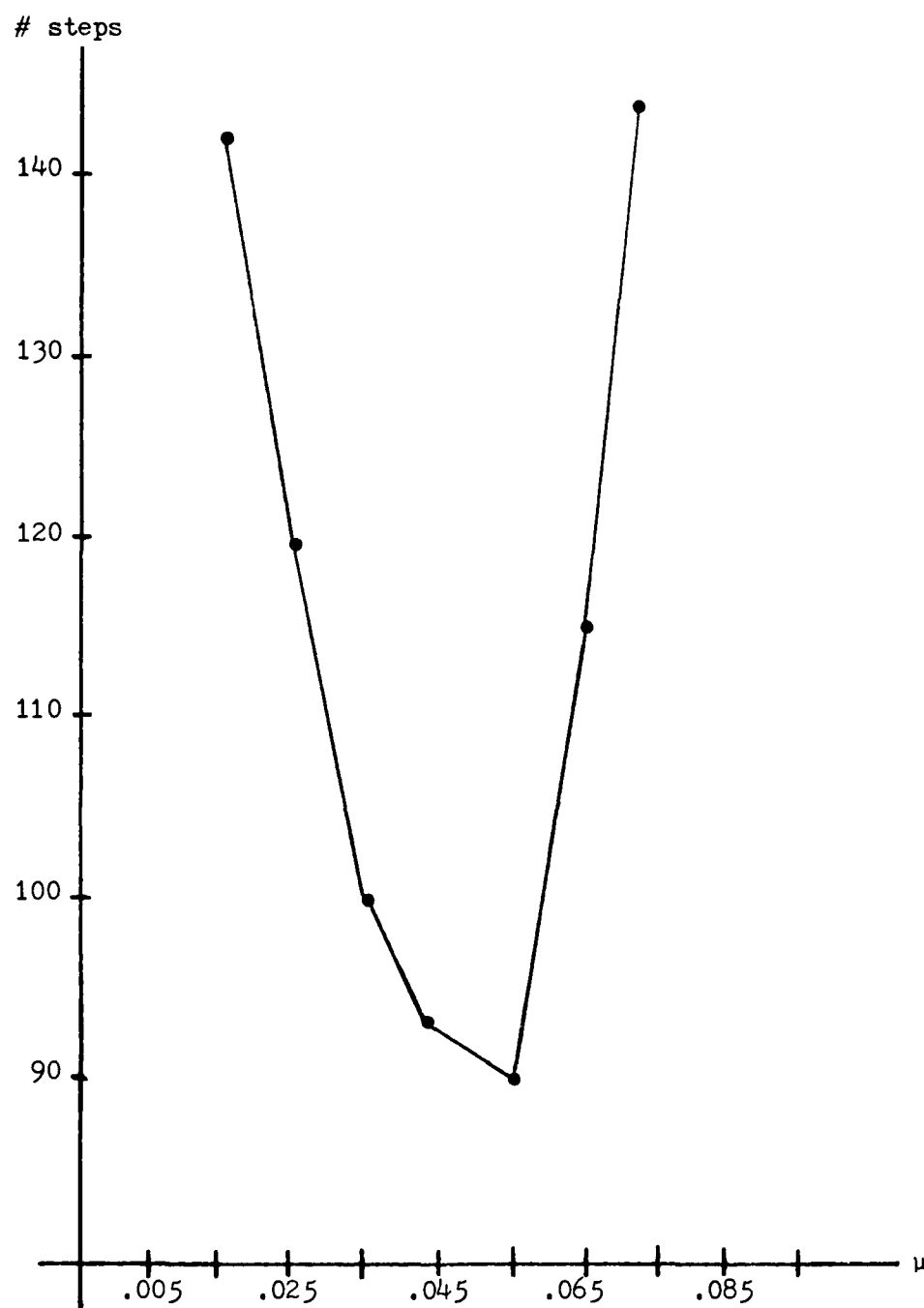
Figure 7.9 - Number of Iterations required for Convergence
for a Given Value of μ
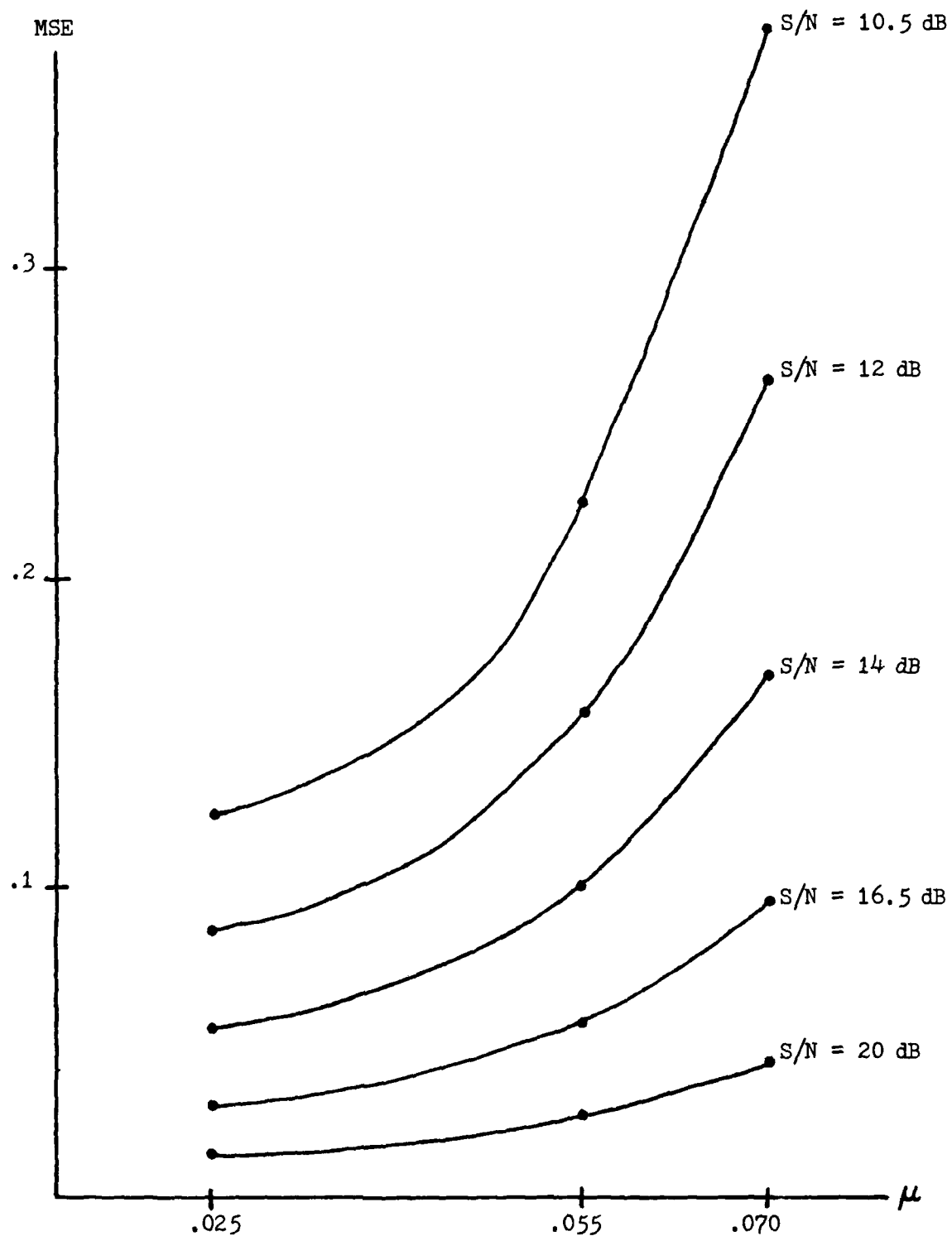
Figure 7.10 - Effect of Convergence Parameter Value on the
Channel Estimator Mean Squared Error

where "M" is a percentage, in which a value of M=0.10 means that the adaptive system has a MSE which is 10% greater than the minimum MSE. This formula works well only for values of misadjustment under 25%. By choosing μ = .025, the misadjustment becomes M=.149. This case is illustrated in Figure 7.11, which verifies that the actual 'ninimum MSE (computed from the measured MSE) is very nearly equal to the noise variance, as expected.

A qualitative assessment of the effectiveness of the channel estimator can be made based upon the preceeding graphs and measurements. In the zero noise condition, the estimator is extremely precise in estimating the discrete channel pulse response; and it behaves equally well regardless of the type or severity of distortion present in the channel (as long as the maximum values shown in Figure 7.5 are not exceeded). Extremely accurate performance of the channel estimator may be expected since it is very similar in structure to the discrete channel model shown in Figure 3.5. Essentially, the channel estimator recovers the impulse response of the discrete channel model.

Additive Gaussian noise has an important impact on operation of the estimator. In order to obtain useful channel estimates under noise conditions, it is necessary to average the output of the channel estimator over a fairly large number of symbols. In the research, the averaging was done over 5000 symbols. Figure 7.12 shows the impact of
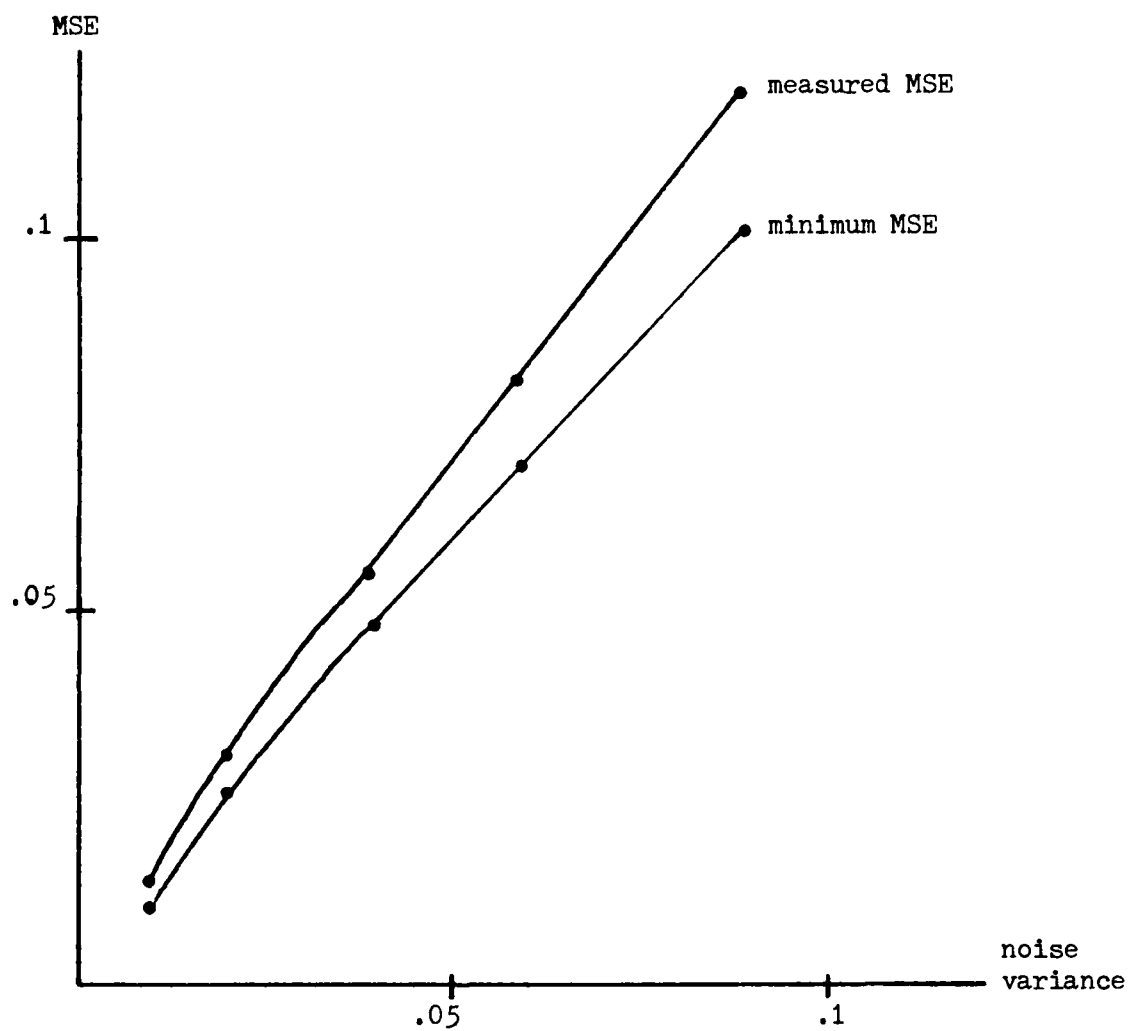
Figure 7.11 - The Effect of Misadjustment (M = .149) on the
Measured MSE (μ = .025)

additive Gaussian noise on the accuracy of the estimator. The error in this case is the MSE obtained by comparing the actual channel pulse response with the estimated channel pulse response (i. e. the MSE in the channel estimator weight vector). Note that, although estimator accuracy seems to be affected significantly, the actual MSE is quite low (in the 10^{-5} range), over a wide range of noise power.

The channel estimator is the first component in the distortion estimation process, and it is also the most crucial. Any inaccuracies in the final output of the channel distortion estimation process can be traced to the channel estimator, as shown later.

The Channel Simulator

As previously noted, the channel simulator attempts to mathmatically emulate the output of the channel estimator. This is accomplished via a prior knowledge of the structure of the signaling pulse as expressed in (6-2) through (6-5). The only unknown parameters in the channel simulator are the values of amplitude and group delay distortion, γ, β_2, and β_3 as given by (6-4) and (6-5). From (6-24), the error between the outputs from the channel simulator and the channel estimator which must be minimized is,

$$E = \sum_{k=-N}^{N} \left\{ r_k - r_k \right\}^2 + \left\{ q_k - q_k \right\}^2 \tag{7-8}$$
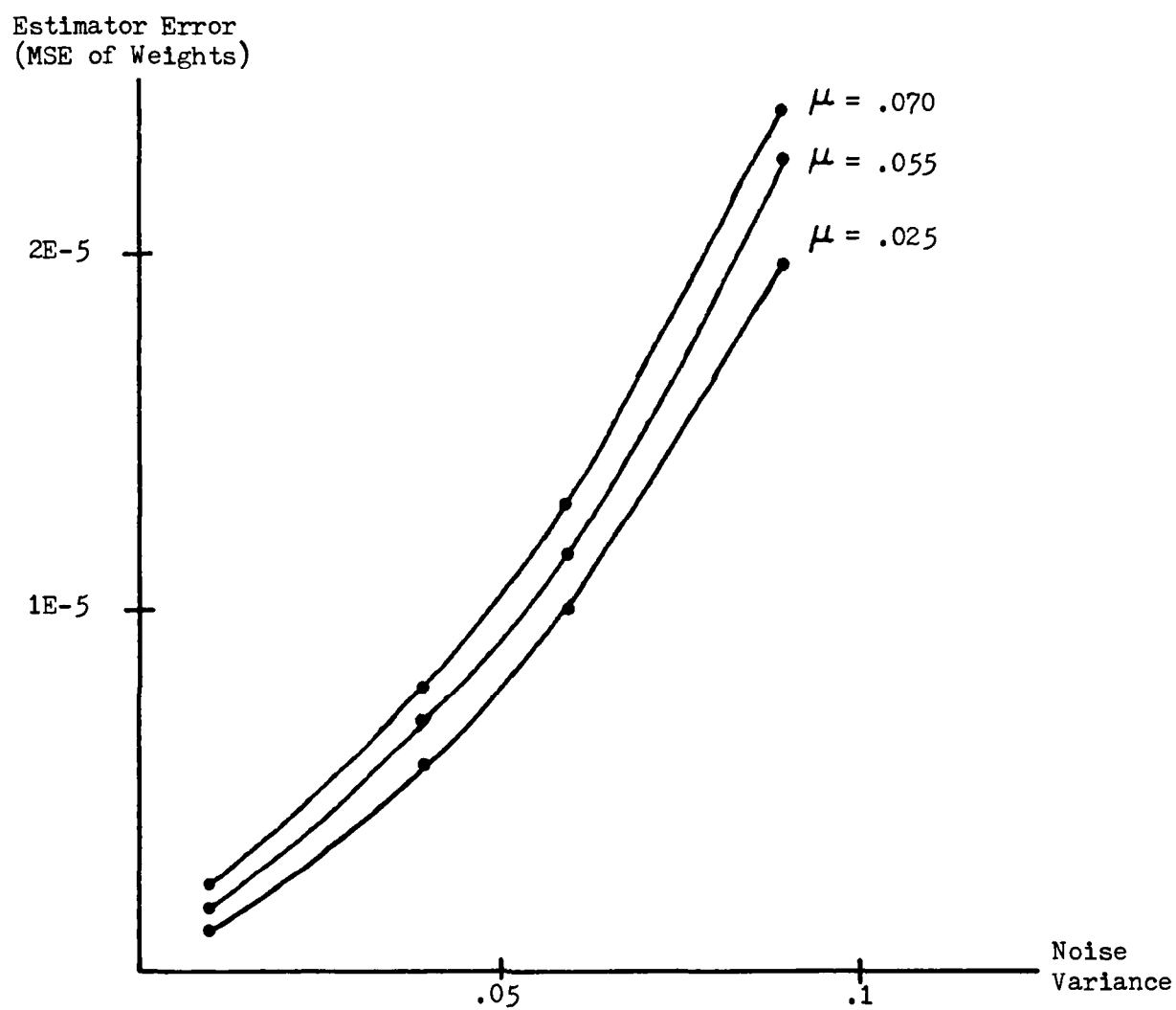
Figure 7.12 - Effect of Gaussian Noise on Channel Estimator
Accuracy

Note that in this case, $\hat{r}_k$ and $\hat{q}_k$ are fixed channel estimates, and the channel simulator adjusts $\tilde{r}_k$ and $\tilde{q}_k$ to match these as closely as possible. Therefore, the error is a quadratic function of the channel simulator output, which can be perceived as a concave hyperparaboloidal surface. In order for the system algorithm to successfully adjust the distortion parameters so that the channel simulator output exactly matches the channel estimator output, the error function must also be a quadratic function of the distortion parameters. To verify that this is the case, the error, as expressed by (7-8), was plotted as a function of a single distortion parameter. Figure 7-13 shows the results. Several values of γ, β_2, and β_3 were chosen for the channel estimator output, and the behavior of the channel simulator about that value of distortion is plotted. The abscissa is normalized to baud intervals in the case of delay distortion, and fractional amplitude in the case of amplitude distortion. It is apparent that γ yields the most consistent behavior over changing values of the distortion parameter. Note however, that the concave minima are very shallow compared to the phase distortion parameters. The linear delay distortion parameter, β_2 also exhibits very consistent behavior over the entire range of possible values. The quadratic group delay distortion parameter, β_3, appears to be more dependent upon the amount of distortion in the received signal than the other
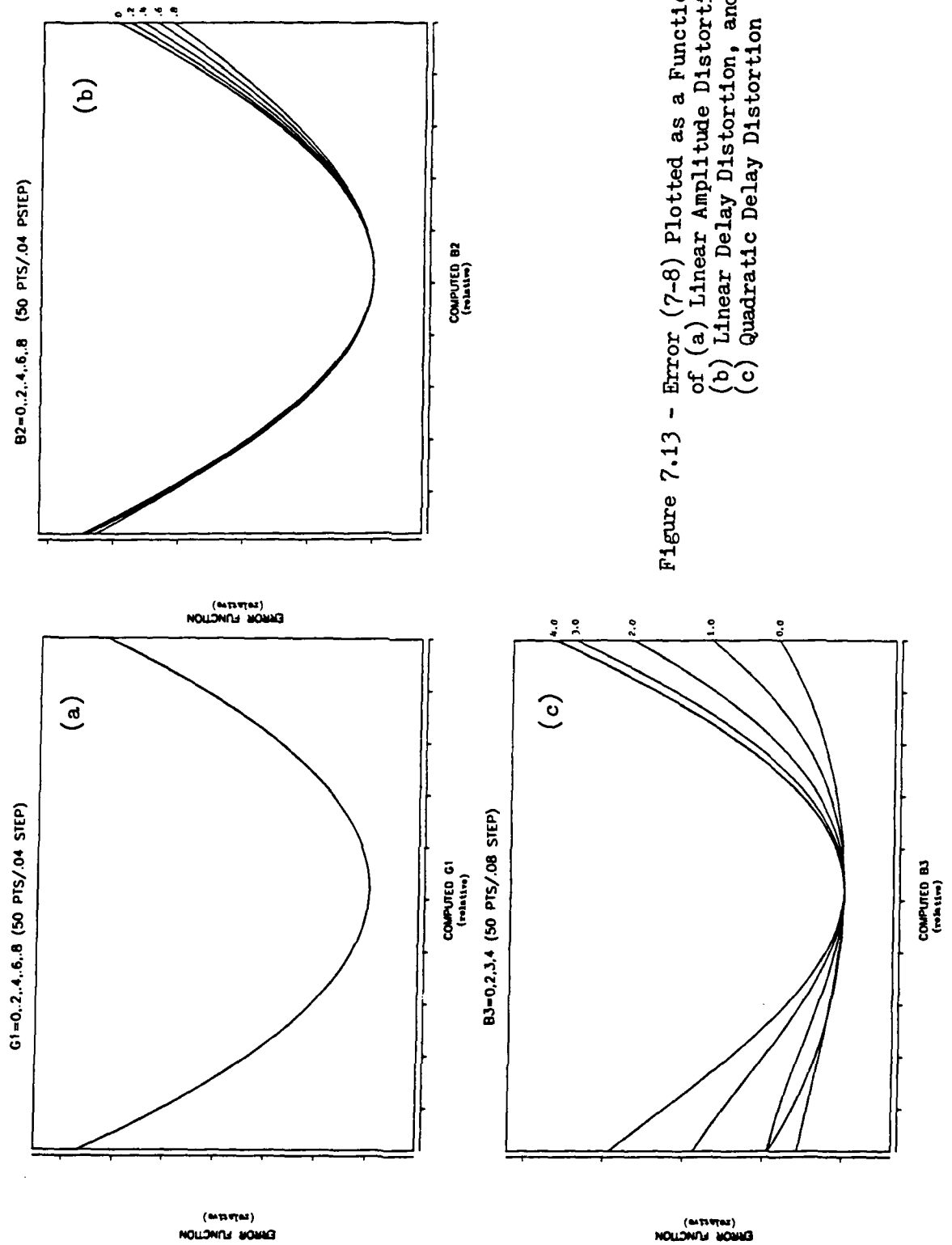
Figure 7.13 – Error (7-8) Plotted as a Function
of (a) Linear Amplitude Distortion,
(b) Linear Delay Distortion, and
(c) Quadratic Delay Distortion

paramters. In fact, it appears to have a progressively more difinitive concave minimum as the amount of distortion in the channel increases.

These measurements illustrate the simple convex nature of each distortion component. Since each component has only a single global min·mum, the optimization process incorporated into the system algorithm which minimizes (7-8) will be assured of accurate operation. An important issue to be resolved at this point is the effect of additive Gaussian noise in the channel on the minimization process. Figure 7.14 shows the behavior of the error function (7-8) under zero noise (solid line) and severe noise (10 dB S/N - dashed line) for each distortion component. The noise induced innaccuracies in the estimation of the discrete channel pulse response ($\hat{r}_k$ and $\hat{q}_k$) cause the minimum point of the error function to be skewed left or right (as in the case of β_2 or β_3) or to be raised slightly (as in the case of γ). Therefore, inaccuracies in the output of the distortion estimation process can be traced to a misalignment in the concave minima of the distortion components which result due to noise induced inaccuracies in the channel estimator.

The System Algorithm

The system algorithm seeks to minimize the difference between the estimated channel pulse response ($\hat{r}_k$ and $\hat{q}_k$) and
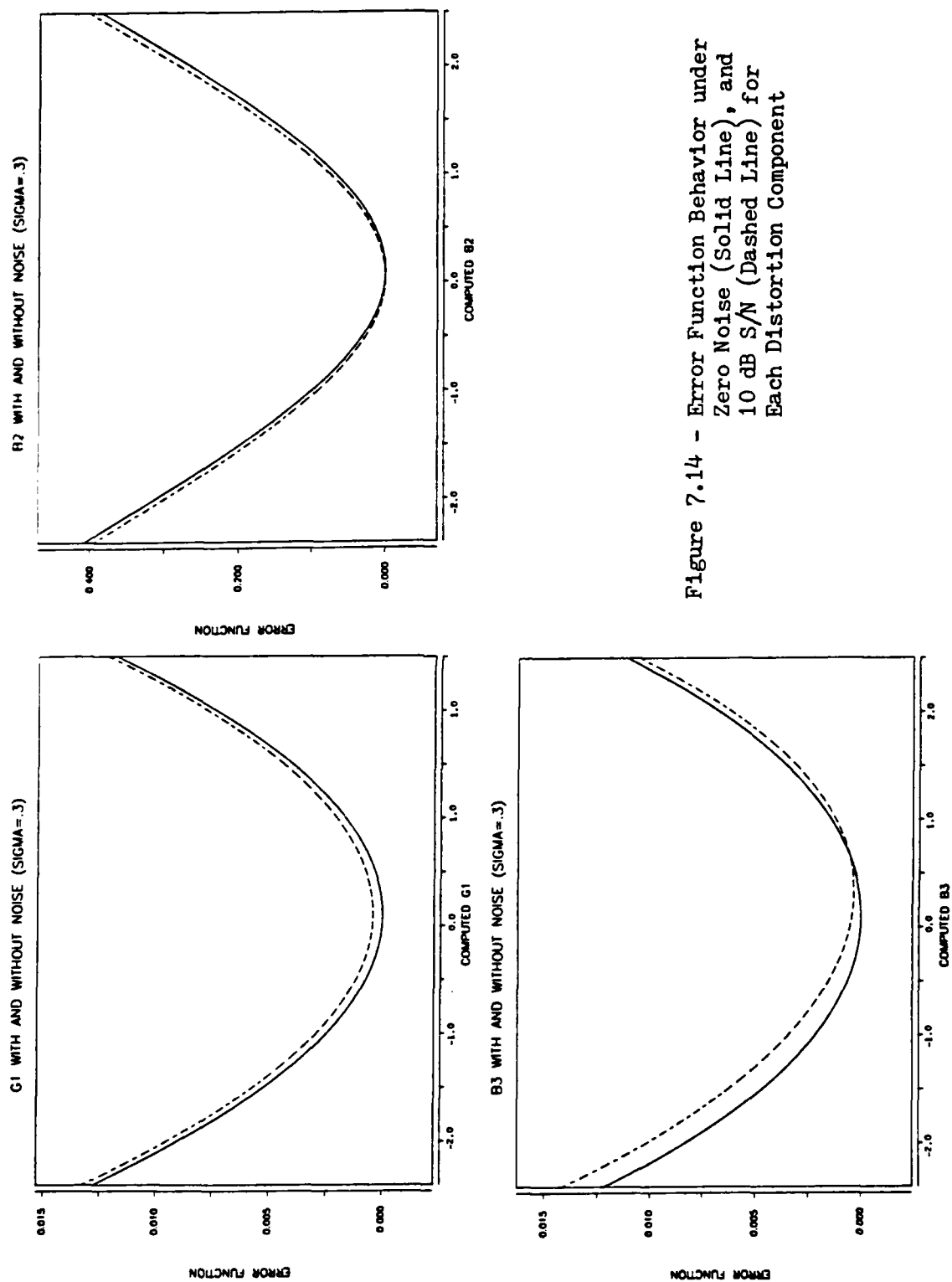
Figure 7.14 – Error Function Behavior under Zero Noise (Solid Line), and 10 dB S/N (Dashed Line) for Each Distortion Component

136

the simulated channel pulse response ($\tilde{r}_k$ and $\tilde{q}_k$) according to (6-24) by optimizing the channel distortion parameters γ, β_2 and β_3. The operation of the algorithm is outlined in Figure 6.1.

To determine the accuracy of the distortion estimation system, known values of amplitude and delay distortion were inserted into the pulse response simulator (Figure 7.1). These values were then converted to a time-domain pulse response for use in the transmission line. After the encoded information sequence was passed through the transmission line and noise added, the resultant baseband signal was processed by the channel estimator. The channel estimator functions to recover the impulse response of the transmission line. The system algorithm then processes the output from the channel estimator to produce an estimate of the distortion component values which were originally inserted into the pulse response simulator. The most important issue remaining is the accuracy with which this system is able to estimate and classify the actual distortion present on the channel.

Previously, it was noted that the primary source of error in the distortion estimation process was expected to be the noise induced inaccuracy within the channel estimator. Since the error signal, (6-24), exhibits a simple convex (or quadratic) behavior with respect to the distortion parameters, minimization of this error is

expected to be straightforward. Therefore, (6-24) can now be evaluated in terms of possible inaccuracies which occur in the channel estimate, such that,

$$\hat{r}_k = r_k + e_{r,k} \tag{7-9}$$

$$\hat{q}_k = q_k + e_{q,k} \tag{7-10}$$

where $e_{r,k}$ and $e_{q,k}$ represent the individual tap innacuracies which occur primarily due to additive channel noise and estimator misadjustment. Now (6-24) can be expressed as,

$$E = \sum_{k=-N}^{N} (r_k - \tilde{r}_k + e_{r,k})^2 + (q_k - \tilde{q}_k + e_{q,k})^2 \tag{7-11}$$

By assuming that (with $e_{r,k} = e_{q,k} = 0$) the error, E, can be reduced to zero (i. e. $\tilde{r}_k = r_k$ and $\tilde{q}_k = q_k$) a potential residual inaccuracy (or misadjustment) can be expressed as,

$$E = \sum_{k=-N}^{N} (e_{r,k})^2 + (e_{q,k})^2 \tag{7-12}$$

Unfortunately the effect that the specific values of $e_{r,k}$

and $e_{q,k}$ (which are time-domain parameters) have on the estimated channel distortion components γ, β_2 and β_3 (which are frequency-domain parameters) appears to be a nonlinear function of time and frequency due to the operation of the system algorithm. Even though the system algorithm is linear, it is required to take time-domain measurements from the channel estimator and pro/ide frequency-domain estimates of the channel distortion. From Figure 7-14 it is obvious that inaccuracies in the channel estimate actually cause a shift in the optimum value of each distortion component with respect to (6-24). The degree of this shift is a function of the 11 complex components of the channel estimator output. Determining the effect of the variation of 11 complex time-domain components on the three frequency-domain parameters was determined to be a problem of sufficient complexity to be beyond the scope of the present research.

Tables 7.1 through 7.7 illustrate the performance of the channel distortion estimator under differing signal to noise ratios and increasing values of each distortion parameter. The values on the left side of each table represent the actual distortion component values inserted into the distortion channel model; while the values on the right are the output estimates produced by the distortion estimation system.

Table 7.1 - Actual vs. Measured Parameter Values (Linear Amplitude Distortion Only)

ACTUAL (input)		ESTIMATED (output)			ERROR			S/N
γ'	β'	γ'	β'	β'	$\Delta\gamma'$	$\Delta\beta'$	$\Delta\beta'$	
.2	0	0.200	0.000	0.000	0.000	0.000	0.000	∞
.4	0	0.400	0.000	0.000	0.000	0.000	0.000	
.6	0	0.600	0.000	0.000	0.000	0.000	0.000	
.8	0	0.800	0.000	0.000	0.000	0.000	0.000	
.2	0	0.200	-.013	0.051	0.000	-.013	0.051	20 dB
.4	0	0.400	-.014	0.055	0.000	-.014	0.055	
.6	0	0.600	-.017	0.064	0.000	-.017	0.064	
.8	0	0.800	-.022	0.080	0.000	-.022	0.080	
.2	0	0.200	-.024	0.111	0.000	-.024	0.111	14 dB
.4	0	0.400	-.030	0.116	0.000	-.030	0.116	
.6	0	0.603	-.036	0.136	0.003	-.036	0.136	
.8	0	0.799	-.042	0.136	-.001	-.042	0.136	

Table 7.2 – Actual vs. Measured Parameter Values (Linear Delay Distortion Only)

ACTUAL (input)			ESTIMATED (output)			ERROR			S/N
γ'	β'_2	β'_3	γ'	β'_2	β'_3	$\Delta\gamma'$	$\Delta\beta'_2$	$\Delta\beta'_3$	
0	.2	0	0.000	0.200	0.000	0.000	0.000	0.000	
0	.4	0	0.000	0.400	0.000	0.000	0.000	0.000	∞
0	.6	0	0.000	0.600	0.000	0.000	0.000	0.000	
0	.8	0	0.000	0.800	0.000	0.000	0.000	0.000	
0	.2	0	-.001	0.190	0.038	-.001	-.010	0.038	
0	.4	0	-.008	0.389	0.039	-.008	-.011	0.039	20 dB
0	.6	0	0.009	0.590	0.005	0.009	-.010	0.005	
0	.8	0	0.018	0.788	-.025	0.018	-.012	-.025	
0	.2	0	-.006	0.181	0.081	-.006	-.019	0.081	
0	.4	0	-.007	0.378	0.059	-.007	-.022	0.059	14 dB
0	.6	0	0.003	0.575	0.028	0.003	-.025	0.028	
0	.8	0	-.008	0.713	0.009	-.008	-.087	0.009	

Table 7.3 – Actual vs. Measured Parameter Values (Quadratic Delay Distortion Only)

ACTUAL (input)			ESTIMATED (output)			ERROR			S/N
γ'	β'_2	β'_3	γ'	β'_2	β'_3	$\Delta\gamma'$	$\Delta\beta'_2$	$\Delta\beta'_3$	
0	0	.5	0.000	0.000	0.500	0.000	0.000	0.000	∞
0	0	1.0	0.000	0.000	1.000	0.000	0.000	0.000	
0	0	2.0	0.000	0.000	2.000	0.000	0.000	0.000	
0	0	3.0	0.000	0.000	3.000	0.000	0.000	0.000	
0	0	4.0	0.000	0.000	4.000	0.000	0.000	0.000	
0	0	.5	0.011	-.011	0.537	0.011	-.011	0.037	20 dB
0	0	1.0	0.017	-.014	1.014	0.017	-.014	0.014	
0	0	2.0	0.008	-.015	1.986	0.008	-.015	-.014	
0	0	3.0	-.003	-.010	2.982	-.003	-.010	-.018	
0	0	4.0	-.007	-.007	3.987	-.007	-.007	-.013	
0	0	.5	0.016	-.021	0.563	0.016	-.021	0.063	14 dB
0	0	1.0	0.023	-.026	1.026	0.023	-.026	0.026	
0	0	2.0	0.015	-.029	1.972	0.015	-.029	-.028	
0	0	3.0	-.005	-.020	2.962	-.005	-.020	-.038	
0	0	4.0	-.018	-.011	3.944	-.018	-.011	-.056	

Table 7.4 - Actual vs. Measured Parameter Values (Linear and Quadratic Delay Distortion Only)

ACTUAL (input)			ESTIMATED (output)			ERROR			
γ'	β'_2	β'_3	γ'	β'_2	β'_3	$\Delta\gamma'$	$\Delta\beta'_2$	$\Delta\beta'_3$	S/N
0	.2	1.0	0.000	0.200	1.000	0.000	0.000	0.000	
0	.4	2.0	0.000	0.400	2.000	0.000	0.000	0.000	∞
0	.6	3.0	0.000	0.600	3.000	0.000	0.000	0.000	
0	.8	4.0	0.000	0.800	4.000	0.000	0.000	0.000	
0	.2	1.0	0.042	0.181	0.999	0.042	-.019	-.001	
0	.4	2.0	0.024	0.377	1.988	0.024	-.023	-.012	20 dB
0	.6	3.0	0.001	0.585	2.988	0.001	-.015	-.012	
0	.8	4.0	-.012	0.790	3.988	-.012	-.010	-.012	
0	.2	1.0	0.082	0.164	1.000	0.082	-.036	0.000	
0	.4	2.0	0.051	0.352	1.979	0.051	-.048	-.021	14 dB
0	.6	3.0	-.010	0.563	2.964	-.010	-.037	-.036	
0	.8	4.0	-.045	0.740	3.911	-.045	-.060	-.089	

Table 7.5 - Actual vs. Measured Parameter Values (Linear Amplitude and Quadratic Delay)

ACTUAL (input)			ESTIMATED (output)			ERROR			S/N
γ'	β'_2	β'_3	γ'	β'_2	β'_3	$\Delta\gamma'$	$\Delta\beta'_2$	$\Delta\beta'_3$	
.2	0	1.0	0.200	0.000	1.000	0.000	0.000	0.000	∞
.4	0	2.0	0.400	0.000	2.000	0.000	0.000	0.000	
.6	0	3.0	0.600	0.000	3.000	0.000	0.000	0.000	
.8	0	4.0	0.800	0.000	4.000	0.000	0.000	0.000	
.2	0	1.0	0.235	-.016	1.009	0.035	-.016	0.009	20 dB
.4	0	2.0	0.425	-.020	1.994	0.025	-.020	-.006	
.6	0	3.0	0.610	-.018	2.995	0.010	-.018	-.005	
.8	0	4.0	0.734	-.036	3.882	-.066	-.036	-.118	
.2	0	1.0	0.259	-.029	1.017	0.059	-.029	0.017	14 dB
.4	0	2.0	0.446	-.037	1.981	0.046	-.037	-.019	
.6	0	3.0	0.605	-.028	2.964	0.005	-.028	-.036	
.8	0	4.0	0.686	0.002	3.743	-.114	0.002	-.257	

Table 7.6 - Actual vs. Measured Parameter Values (Linear Amplitude and Linear Delay Distortion)

ACTUAL (input)			ESTIMATED (output)			ERROR			S/N
γ'	β'_2	β'_3	γ'	β'_2	β'_3	$\Delta\gamma'$	$\Delta\beta'_2$	$\Delta\beta'_3$	
.2	.2	0	0.200	0.200	0.000	0.000	0.000	0.000	
.4	.4	0	0.400	0.400	0.000	0.000	0.000	0.000	∞
.6	.6	0	0.600	0.600	0.000	0.000	0.000	0.000	
.8	.8	0	0.800	0.800	0.000	0.000	0.000	0.000	
.2	.2	0	0.206	0.189	0.048	0.006	-.011	0.048	
.4	.4	0	0.412	0.388	0.033	0.012	-.012	0.033	20 dB
.6	.6	0	0.619	0.588	0.018	0.019	-.12	0.018	
.8	.8	0	0.816	0.783	0.016	0.016	-.017	0.016	
.2	.2	0	0.225	0.179	0.079	0.025	-.021	0.079	
.4	.4	0	0.417	0.376	0.078	0.017	-.024	0.078	14 dB
.6	.6	0	0.545	0.554	0.192	-.055	-.046	0.192	
.8	.8	0	0.752	0.704	0.114	-.048	-.096	0.114	

Table 7.7 - Actual vs. Measured Parameter Values (Linear Amplitude, Linear and Quadratic Delay)

ACTUAL (input)			ESTIMATED (output)			ERROR			S/N
γ'	β'_2	β'_3	γ'	β'_2	β'_3	$\Delta\gamma'$	$\Delta\beta'_2$	$\Delta\beta'_3$	
.2	.2	1.5	0.200	0.200	1.500	0.000	0.000	0.000	
.3	.3	2.0	0.300	0.300	2.000	0.000	0.000	0.000	∞
.4	.4	2.5	0.400	0.400	2.500	0.000	0.000	0.000	
.5	.5	3.0	0.500	0.500	3.000	0.000	0.000	0.000	
.2	.2	1.5	0.239	0.176	1.496	0.039	-.024	-.004	
.3	.3	2.0	0.324	0.279	1.996	0.024	-.021	-.004	20 dB
.4	.4	2.5	0.434	0.370	2.462	0.034	-.030	-.038	
.5	.5	3.0	0.496	0.476	2.981	-.004	-.024	-.019	
.2	.2	1.5	0.275	0.154	1.496	0.075	-.046	-.004	
.3	.3	2.0	0.351	0.254	1.991	0.051	-.046	-.009	14 dB
.4	.4	2.5	0.418	0.340	2.484	0.018	-.060	-.016	
.5	.5	3.0	0.468	0.471	2.961	-.032	-.029	-.039	

CHAPTER VIII

CONCLUSIONS AND RECOMMENDATIONS

Summary and Conclusions of the Research

The research reported in this thesis was directed at developing an on-line , time domain approach for measuring certain forms of amplitude and group delay distortion which are common to line-of-sight PSK channels. The primary contribution of the research is the systematic development of a time-domain technique which allows continuous monitoring of channel distortion while the communication system is processing a normal traffic load. This measurment technique is designed to be implemented as a test instrument for digital radios, so that little or no modifications to the radio will be required for its use. After connection to the digital radio, this system will provide periodically updated estimates of amplitude and group delay distortion on a dynamically time-variant channel.

In assessing the usefulness of the distortion estimation process, two issues are of primary importance - speed of operation and accuracy. The speed with which the channel distortion estimates are updated is largely dependent upon the capabilities of the processor which executes the system algorithm. The system algorithm is the

component of the distortion estimation process which requires the greatest amount of processing time. This is because the system algorithm must solve a 3-dimensional optimization of the distortion parameters and present the estimates to the system user. The channel estimator, on the other hand, was shown to converge in rel-tively few (less than 100) iterations. Therefore, on even the lowest speed data systems, numerous updated channel estimates can be made in less than one second.

With a large, general purpose computer such as the Georgia Tech CYBER, updated channel estimates can be provided every few seconds. Obviously, this is much faster operation than can be obtained with a portable, small scale processor. With a 16 bit minicomputer operating around the 10 MHz range, it is anticipated that updated estimates can be provided every minute or so.

The accuracy of the process, which was measured and analyzed in Chapter VII, was found to be largely dependent upon the accuracy of the channel estimator. Any error in estimating the discrete channel pulse response inevitably leads to error in the final estimates of the channel distortion parameters. The relationship between the error present in the channel estimate and the error present in the distortion parameter estimates could only partially be explained and quantified. The specific influences of noise induced inaccuracies in the channel estimate on the final

distortion parameter estimate appear to be nonlinear in nature, and highly dependent upon the form and severity of distortion present in the channel.

The tables at the end of Chapter VII provide the best insight into the accuracy to be expectd from the process. The largest inaccuracies occur when linear amplitude distortion is present in a noisy channel. In fact, the accuracy of any given estimate is more dependent upon the signal-to-noise ratio than upon the severity of distortion; but the linear amplitude distortion parameter appears to be more sensitive to noise than the other parameters. Examination of these tables verifies that the distortion estimation technique is indeed sufficiently accurate to be useful in any application in which knowledge of channel amplitude and group delay distortion is required.

Recommendations for Further Research

Several unresolved issues surfaced in the course of the research which were beyond the scope of the immediate research goals. The most important of these was the question of how the noise induced inaccuracies of the time-domain channel estimate affected the estimates of each of the frequency-domain distortion parameters. Further investigation of this relationship may yield valuable insight into understanding system errors. However, due to the apparent nonlinear behavior in this relationship, it

might not be possible to obtain a useful quantitative characterization.

The next logical step in the extension of the present research is to implement the distortion estimation technique in hardware/software and analyze its operation and effectiveness on a real system. If a complete hardware implementation is atempted, the limited accuracy simulator described by (6-22) and (6-23) will need to be examined further to determine the number of significant terms required in the series to produce an acceptable error. If a combination hardware/software implementation is attempted by using an external processor, then the accuracy attained will be a function of the processing time allowed to make the distortion estimates.

As an instrument, the distortion estimation technique has potential for expansion into a device which can measure a number of other important communication system parameters. In their conceptual description of a digital on-line instrument for testing high bit-rate digital radios, J. L. Hammond et. al. [28] proposed that the following on-line measurements could easiy be made:

(1) Measurement of total distortion power (noise power plus intersymbol interference power).

(2) Measurement of dynamic modulator phase error.

(3) Estimation of system symbol error rate.

(4) Evaluating channel equalization parameters.

A final important caveat concerning the ability of the distortion estimator to provide the degree of accuracy demonstrated in Chapter VII, as well as to make accurate measurements of the distortion power and modulator errors, is the problem of accurate symbol timing recovery. This will necessarily be an extremely important issue to be examined in the implementation of the distortion estimation technique, since timing requirements will be more stringent for the proposed technique than are normally required for symbol recovery.

BIBLIOGRAPHY

1.   Gulstad, K. "Vibrating Cable Relay," The Electrical Review, Vol. 42, August 1898.

2.   Nyquist, H. "Certain Topics in Telegraph Transmission Theory," AIEE Transactions, April 1928.

3.   Wheeler, H. A. "The Interpretation of Amplitude and Phase Distortion in Terms of Paired Echoes," Proceedings of the IRE, June 1939, pp. 359-385.

4.   Sunde E. D. "Theoretical Fundamentals of Pulse Transmission," Bell System Technical Journal, Vol. 33, May 1954, pp. 721-788.

5.   Sunde, E. D. "Pulse Transmission by AM, FM, and PM in the Presence of Phase Distortion," Bell System Technical Journal, Vol. 40, March 1961, pp. 353-422.

6.   Rudin, H. Jr. "Automatic Equalization using Transversal Filters," IEEE Spectrum, January 1967, pp. 53-59.

7.   Zadeh, L. A. "Frequency Analysis of Variable Networks," Proceedings of the IRE, Vol. 38, November 1950, pp. 1342-1345.

8.   Kailath, T. "Channel Characterization: Time Variant Dispersive Channels," Lectures on Communication System Theory by E. J. Baghdady, pp. 95-123, McGraw Hill, New York, 1961.

9.   Bello, P. A. "Characterization of Randomly Time-Variant Linear Channels," IEEE Transactions on Communications, Vol. 11, December 1963, pp. 360-393.

10. Greenstein, L. J. "A Multipath Fading Channel Model for Terrestrial Digital Radio Systems," IEEE Transactions on Communication, Vol. 26, No. 8, August 1978, pp. 1247-1250.

11. Ramaden, M. "Availability Predictions of 8-PSK Digital Microwave Systems during Multipath Propagation," IEEE Transactions on Communication, December 1979, Vol. 27, pp. 1862-1869.

12. Lundgren, C. W. and Rummler, W. D. "Digital Radio Outage Due to Selective Fading," Bell System Technical

Journal, Vol. 58, No. 5, May 1979.

13. Anderson, C. W.; Barber, S. G. and Patel, R. N. "The Effect of Selective Fading on Digital Radio," IEEE Transactions on Communication, December 1979, Vol. 27, pp. 1870-1879.

14. Greenstein, L. J. and Czekaj, B. "A Polynomial Model for Multipath Fading Channel Responses," Bell System Technical Journal, Vol. 59, No. 7, September 1980, pp. 1197-1225.

15. Greenstein, L. J. and Czekaj-Augum, B. "Performance Comparisons among Digital Radio Techniques Subjected to Multipath Fading," IEEE Transactions on Communication, Vol. 30, May 1982, p. 1184.

16. Greenstein, L. J. and Vitello, "Digital Radio Receiver Responses for Combating Frequency-Selective Fading," IEEE Transactions on Communication, Vol. 27, No. 4, April 1979, pp. 671-681.

17. Rummler, W. D. "A New Selective Fading Model: Application to Propagation Data," Bell System Technical Journal, Vol. 58, May-June 1979, pp. 1037-1071.

18. Rummler, W. D. "Extensions of the Multipath Fading Model," IEEE International Conference on Communications 1979, pp. 32.2.1-32.2.5.

19. Rummler, W. D. "A Comparison of Calculated and Observed Performance of Digital Radio in the Presence of Interference," IEEE Transactions on Communication, Vol. 30, No. 7, July 1982.

20. Giger, A. J. and Barnett, W. T. "Effects of Multipath Propagation on Digital Radio," IEEE International Conference on Communication 1981, pp. 46.7.1-46.7.5.

21. Fowler, A. D. and Gibby, R. A. "Assessment of the Effects of Delay Distortion in Data Systems," Communications and Electronics, Vol. 40, 1959, pp. 918-923.

22. Gibby R. A. "An Evaluation of AM Data System Performance by Computer Simulation," Bell System Technical Journal, Vol. 39, 1960, pp. 675-704.

23. Papoulis, A. The Fourier Integral and Its Applications. McGraw-Hill, New York, 1962.

24. Cross, T. G. "Intermodulation Noise in FM Systems Due

to Transmission Deviations and AM/PM Conversion," Bell System Technical Journal, Vol. 45, December 1966, pp. 1749-1773.

25.   Halford, D. and Gonzalez, A. "Transparent Metrology of Signal-to-Noise Ratio of Noisy Digital Signals," Draft Proposal, National Bureau of Standards, August 1981.

26.   The MITRE Corporation, "Theoretical Capabilities of the ACE Algorithm," Internal technical reported submitted to RADC, undated.

27.   Hammond, J. L. and Pidgeon, R. E. "Design of a Digital Link Transmission Analyzer," Scientific Atlanta unpublished technical report, 15 June 1979.

28.   Hammond, J. L.; Hodge, S. R. and Pidgeon, R. E. Jr. "A Digital On-line Instrument for Testing High Bit Rate Digital Radios," Scientific Atlanta unpublished technical report, 27 June 1979.

29.   Thomas, C. M.; Alexander, J. E. and Rahneberg, E. W. "A New Generation of Digital Microwave Radios for U. S. Military Telephone Networks," IEEE Transactions on Communication, Vol. 27, No. 12, December 1979, pp. 1916-1927.

30.   Proakis, J. G. Digital Communications. McGraw-Hill, New York, 1983.

31. Bayless, J. W.; Collins, A. A. and Pedersen, R. D. "The Specification and Design of Bandlimited Digital Radio Systems," IEEE Transactions on Communication, Vol. 27, No. 12, December 1979, pp. 1763-1770.

32.   Proakis,   J. G.   "Advances in Equalization for Intersymbol Interference," in Advances in Communication Systems, Vol. 4, A. J. Viterbi (ed.), Academic Press, New York, 1975.

33.   Schwartz,   M.;   Bennett,   W.   R. and Stein, S. Communication Systems and Techniques.   New   York, McGraw-Hill, 1966.

34.   Ramaden, M. "Practical Considerations in the Design of Minimum Bandwidth, 90 Mb, 8-PSK Digital Microwave System," Rockwell International Technical Bulletin #523-0602745-001A3R, 14 November 1977.

35.   Pedersen, R. D. and Bayless, J. W. "Efficient Pulse Shaping Using MSK or PSK Modulation," IEEE Transactions on

Communication, Vol. 27, NO. 6, June 1979.

36. Feher, K. _Digital Communications: Satellite/Earth Station Engineering_. Prentice-Hall Inc., Englewood Cliffs, New Jersey, 1983.

37. Savage, J. E. "Some Simple Self-Synchronizing Digital Data Scramblers," _Bell System Technical Journal_, February 1967, pp. 449-487.

38. Lucky, R. W. "A Functional Analysis Relating Delay Variation and ISI in Data Transmission," _Bell System Technical Journal_, Vol. 42 September 1963, pp. 2427.

39. Hartman, P. R. and Allen, E. W. "An Adaptive Equalizer for Correction of Multipath Distortion in a 90 Mb/S 8-PSK System," _IEEE International Conference on Communication 1979_, pp. 5.6.1-5.6.4.

40. Jakes, W. C. "An Aproximation Method to Estimate an Upper Bound on the Effects of Multipath Delay Distortion on Digital Transmission," _IEEE Transmission on Communication_, Vol. 27, No. 1, January 1979, pp. 76-81.

41. Lucky, R. W.; Salz, J. and Weldon, E. J., Jr. _Principles of Data Communication_. McGraw-Hill, New York, 1968.

42. Oetting, J. D. "A Comparison of Modulation Techniques for Digital Radio," _IEEE Transactions on Communication_, Vol. 27, No. 12, December 1979.

43. Barnett, W. T. "Multipath Fading Effects on Digital Radio," _IEEE Transactions on Communication_, Vol. 27, No. 12, December 1979.

44. Sunde E. D. _Communication System Theory_. John Wiley and Sons, New York, 1969.

45. Magee, F. R. and Proakis, J. G. "Adaptive Maximum-Liklihood Sequence Estimation for Digital Signaling in the Presence of Intersymbol Interference," _IEEE Transactions on Information Theory_, January 1973, pp. 120-124.

46. Landau, I. D. "A Summary of Model Reference Adaptive Techniques- Theory and Applications," _Automatica_, Vol. 10, 1974, pp. 353-395.

47. Mendel, J. M. "Gradient Error-Correction Identification Algorithms," _Information Science_, Vol. 1, 1968, pp. 23-42.

48. Sondhi and Berkley. "Silencing E .hoes on the Telephone Network," _Proceedings of the IEEE_, Vol. 68, No. 8, August 1980.

49. Forney, G. D., Jr. "Maximum-Liklihood Sequence Estimation of Digital Sequences in the Presence of Intersymbol Interference," _IEEE Transactions on Information Theory_, Vol. 18, May 1972, pp. 363-378.

50. Clark, A. P.; Kwong, C. P.; and McVerry, F. "Estimation of the Sampled Impulse Response of a Channel," _Signal Processing_, Vol. 2, No. 1, January 1980, pp. 39-53.

51. Proakis, J. G. "Channel Identification for High Speed Digital Communications," _IEEE Transactions on Automatic Control_, Vol. 19, No. 6, December 1974, pp. 916-922.

52. Widrow, B. and McCool, J. "A Comparison of Adaptive Algorithms Based on the Methods of Steepest Descent and Random Search," _IEEE Transactions on Antennas and Propagation_, Vol. 24, September 1976, pp. 615-637.

53. Widrow, B. and Hoff, M. Jr. "Adaptive Switching Circuits," in _IRE WESCON Conference Record_, Pt. 4, 1960, pp. 96-104.

54. Widrow, B. "Adaptive Filters I: Fundamentals," Stanford Electronic Labs, Stanford University Report SU-SEL-66-126, December 1966.

55. Widrow, B.; McCool, J.; Larimore, M.; and Johnson, C. "Stationary and Nonstationary Learning Characteristics of the LMS Adaptive Filter," _Proceedings of the IEEE_, Vol. 64, No. 8, August 1976, pp. 1151-1162.

56. Daniels, R. W. _An Introduction to Numerical Methods and Optimization Techniques_, North-Holland Publishing, New York, 1972.

57. Cooper and Steinberg, _Introduction to Methods of Optimization_, W. B. Saunders Company, New York, 1970.

58. Durling, Allen. _Computational Techniques: Analog, Digital and Hybrid Systems_, Intext Publishers, New York.

59. Rappeport, M. A. "Digital Computer Simulation of a Four Phase Data Transmission System," _Bell Systems Technical Journal_, May 1964, pp 927-964.

60. Peterson, W. and Weldon, E. Jr. _Error Correcting Codes_, The MIT Press, Cambridge, Mass., 1972.

61. Modestino, J. W.; Jung, K. Y.; Matis, K. R.; Vickers, A. L. "Design and Implementation of the Interactive Communications Simulator (ICS)," RADC-TR-81-37, April 1981, Rome Air Development Center, Griffiss AFB, N. Y.

62. Modestino, J. W. and Matis, K. R. "Interactive Simulation of Digital Communication Systems," IEEE Journal on Selected Areas in Communications, Vol. 2, No. 1, January 1984, pp. 51-76.

VITA

Glenn Eugene Prescott was born in Defuniak Springs, Florida on October 4, 1948. As a member of an Air Force family, he traveled extensively during his formative years living in Japan and Germany. In 1966 he graduated from F. W. Ballou High School in Washington D. C. and enlisted in the Air Force. In his early Air Force career, as a radar technician stationed in Washington and Maine, Sgt. Prescott accumulated enough college credits to apply for an Air Force education and commissioning program. He was accepted to the program and asigned to Georgia Tech, where he received the Bachelor of E. E. degree in 1974. Following graduation and commissioning, Lt. Prescott was trained as a Communications Officer and sent to Kansas City, where he received the Master of Science in E. E. from the University of Missouri in 1977. His experience as an engineer includes assignments with the Office of the Chief Scientist and the Office of Advanced Satellite Plans at the Air Force Communications Command. He is currently assigned to the faculty of the Air Force Institute of Technology, Wright-Patterson AFB., Ohio, as Assistant Professor. Capt. Prescott and his wife, Jacqueline Marie, were married in 1967. They have three children - Wendy (15), Beverly (10), and Kevin (6).

END

FILMED

12-84

DTIC